A review of the ecological affinities of marine organic microfossils from a Holocene record offshore of Adélie Land (East Antarctica)

Julian D. Hartman, Peter K. Bijl, and Francesca Sangiorgi

Marine Palynology and Paleoceanography, Department of Earth Sciences,
Utrecht University, P.O. Box 80.115, 3508 TC Utrecht, the Netherlands

Correspondence: Francesca Sangiorgi (f.sangiorgi@uu.nl)

Abstract. Integrated Ocean Drilling Program (IODP) Expedition 318 recovered a ~ 170 m long Holocene organic-rich sedimentary sequence at Site U1357. Located within the narrow but deep Adélie Basin close to the Antarctic margin, the site accumulated sediments at exceptionally high sedimentation rates, which resulted in extraordinary preservation of the organic sedimentary component. Here, we present an overview of 74 different mainly marine microfossil taxa and/or types found within the organic component of the sediment, which include the remains of unicellular and higher organisms from three eukaryotic kingdoms (Chromista, Plantae, and Animalia). These remains include phytoplanktonic (phototrophic dinoflagellates and prasinophytes) and very diverse zooplanktonic (heterotrophic dinoflagellates, tintinnids, copepods) organisms. We illustrate each marine microfossil taxon or type identified by providing morphological details and photographic images, which will help with their identification in future studies. We also review their ecological preferences to aid future (palaeo)ecological and (palaeo)environmental studies. The planktonic assemblage shows a high degree of endemism related to the strong influence of the sea-ice system over Site U1357. In addition, we found the remains of various species of detritus feeders and bottom-dwelling scavengers (benthic foraminifers and annelid worms) indicative of high export productivity at Site U1357. This study shows the potential of organic microfossil remains for reconstructing past environmental conditions, such as sea-ice cover and (export) productivity.

1 Introduction

Site U1357 was drilled as part of the Integrated Ocean Drilling Program (IODP) Expedition 318 and is located in the Adélie Basin downwind and downcurrent from the Mertz Glacier Polynya. Polynyas are seasonal openings within the sea ice formed through the vertical mixing of warmer subsurface waters or through advection from the coast by wind or currents (Arrigo et al., 1998a; Arrigo and van Dijken, 2003; Morales Maqueda et al., 2004). These polynyas overlying the Antarctic shelf fuel increased primary productivity through nutrient release and sustain entire ecosystems including marine mammals and birds (Stirling, 1997; Arrigo and van Dijken, 2003). The Mertz Glacier Polynya is one of the larger and more productive coastal polynyas of the Antarctic margin (Arrigo and van Dijken, 2003). Annu-

ally, the Mertz Glacier Polynya is open between December and March, which allows for blooms of primary productivity (on average over the bloom period 0.31 ± 0.26 g C m^{-2} d^{-1}) and therefore increased particle fluxes to the sea floor (Arrigo and van Dijken, 2003). Over the Holocene, this process has accumulated 172 m of diatomaceous ooze. In addition to the diatoms, the sediments from Site U1357 contain abundant microfossil remains left behind by a large variety of phytoplankton species and their predators. Although organic microplankton remains are less commonly used for reconstructing past environmental conditions (e.g. sea ice, temperature, productivity) in the Southern Ocean because not all organic remains are able to withstand lithification processes and/or oxygen degradation, the organic microplankton remains of Site U1357 are exceptionally well preserved. The high organic carbon content of these sediments includes

not only dinoflagellate cysts, but also less commonly preserved material such as tintinnid loricae. In addition, the remains of higher animal taxa, foraminifers, chlorophytes, and ciliates were mentioned (Expedition 318 Scientists, 2011). The whole organic microfossil abundance and diversity of the unique sediments from Site U1357 has the potential of increasing our knowledge on Holocene environmental changes within a polynya-controlled environment close to the Antarctic margin than the generally less diverse dinoflagellate cyst assemblages south of the sea-ice edge.

Future changes in sea-ice concentration due to global warming will likely affect Southern Ocean primary productivity, but how the seasonal sea-ice concentrations will change under current global warming and how this will affect primary productivity is still highly uncertain (Deppeler and Davidson, 2017). With respect to coastal polynyas there is even higher uncertainty on how climate change will affect them because the expected increased temperatures and increased precipitation have counteracting effects on polynya size (Marsland et al., 2007). In this regard, there is a growing need for high-resolution sedimentary archives from close to the Antarctic margin, which straddle past warmer time intervals, and accurate proxies that can be used to reconstruct past sea surface conditions (e.g. sea-ice concentrations, sea surface temperature, and productivity). However, before we can interpret the diverse and highly abundant organic microfossil assemblages from the polynya sediments from Site U1357 and other Antarctic coastal records in terms of palaeoenvironmental changes, an accurate review of their ecological preferences is required. To this end, we have compiled an overview of the palynomorphs that we encountered in IODP Hole U1357B and reviewed the palaeoenvironmental affinities of known marine organic microfossils.

2 Material

Site U1357 was triple cored to ensure maximum recovery of the sequence. Hole U1357B was drilled at a depth of 1017 m below sea level and recovered about 172 m of the sedimentary succession (Expedition 318 Scientists, 2011). The lithology of Hole U1357B consists of dark black sediment, the surface of which oxidizes post-recovery into an alternation of centimetre-scale lighter and darker green layers of diatomaceous ooze, with a diatom content of 80 %–99 % (Expedition 318 Scientists, 2011). Throughout the core the total organic carbon (TOC) has been consistently high with values between 1 and 2 wt % (Expedition 318 Scientists, 2011). For this review a total of 34 samples, taken throughout the 172 m of recovery, were examined for their palynological content. Samples were obtained from both dark- and light-coloured laminae covering the entire Holocene record to anticipate potential differences in the palynological assemblage between lamina types and shifts in the palynological composition through time. In a follow-up paper (Hartman et al.,

2018c) we will discuss the changes in palynological content through time for palaeoenvironmental interpretations.

3 Methods

3.1 Palynological processing

For palynological processing, samples were freeze-dried, weighted, and ground manually in a mortar. For quantitative analyses a tablet of *Lycopodium clavatum* spores was added, and the sediment was wetted with an Agepon dilution (1 : 200). To remove carbonates and silicates, the samples were treated with 30 % cold HCl and 38 % cold HF, respectively. Subsequently, samples were shaken for 2 h at 250 rpm, after which the samples were diluted with tap water and left to settle for 24 h. After decantation, 30 % HCl was added to remove fluoride gels, tap water was added, and the samples were centrifuged, after which the samples were decanted again. The material was treated once more with 38 % HF and all subsequent steps. The organic residue was sieved using a 10 μm mesh sieve and clumps were fragmented using ultrasound. Heavy minerals were removed by pouring the residue from the sieve into an evaporating dish floating in an ultrasonic bath and decanting this back into the sieve after 5 min. No oxidation was applied. The fraction > 10 μm was concentrated to ∼ 1 mL of glycerine–water and a fraction thereof was mounted on a microscope slide using glycerine jelly. Samples are stored in the microscope slide collection of the Laboratory of Palaeobotany and Palynology at Utrecht University.

3.2 Microscope photography

Images were taken at either 400×, 630×, or 1000× magnification using a Leica DM2500 LED microscope with a mounted Leica MC170 HD camera. In some cases the live *z*-stacking tool Live Image Builder (LIB) within the Leica Application Suite software 4.0 was used. *Z*-stacking constructs a two-dimensional (2-D) image from a 3-D object by combining the areas in focus from multiple images, which is ideal for 3-D microscopic objects.

3.3 Taxonomic framework

Because we have encountered palynomorphs derived from taxa within various eukaryote kingdoms, we have chosen to structure this review of organic microfossils according to the most recent systematic classifications of these taxa. The classification we use is based on the publications of Ruggiero et al. (2015) for the Chromista, on a lower taxonomic level Fensome et al. (1993) and the online classification Dinoflaj3 (Williams et al., 2017) for the dinoflagellate cysts, and Agatha and Strüder-Kypke (2012, 2013) for the tintinnids. For the classification of chlorophytes we rely on several molecular phylogenetic and classification studies (Nakayama

et al., 1998; Guillou et al., 2004; Marin and Melkonian, 2010; Tragin et al., 2016). In cases in which we were able to identify the remains of higher organisms at class level at least, they have been structured according to known classifications as well: Marley et al. (2011) for the tardigrades and Fauchald (1977) and Struck et al. (2006) for the eunicid polychaete worms. Acritarchs are classified according to Downie et al. (1963). Remaining unidentified organic microfossils and reworked palynomorphs are listed at the end of our review.

4 Background and terminology

Because this review comprises the remains from a very broad array of organic microplankton, we first provide background information for the larger microplankton groups. First, relevant descriptive terminology for each of the palynomorph types is given to aid the morphological descriptions of each species in the Results section. Second, we explain on a superordinate level the relationship between the microfossils in the sediments and their species living in the water column from which they originate and how we can interpret these in terms of environmental conditions. Species-specific ecological preferences are discussed in the Results section in more detail.

4.1 Dinoflagellates and their cysts

4.1.1 Descriptive terminology

Dinoflagellate cysts are produced as part of a dinoflagellate's life cycle. Dinoflagellate cysts are characterized by a cingulum and sulcus, the shallow depressions that mark the position of the two flagella of the dinoflagellate, and an archaeopyle, the hole through which the living dinoflagellate escapes its cyst (Evitt, 1985). Dinoflagellate cysts can be produced by thecate (armoured) and athecate (naked) dinoflagellates. In the case of thecate dinoflagellates the tabulation of the cyst (paratabulation) reflects the tabulation (plate arrangement) of the theca, which is unique for each species (Evitt, 1985). In these cysts, the archaeopyle is often formed through the loss of a distinct set of paraplates, which is used for classification (Fensome et al., 1993). Furthermore, dinoflagellate cysts can possess a wide variety of wall ornamentations that either reflect the tabulation of the theca of the motile cell or do not correspond to this tabulation at all (Evitt, 1985). The larger morphological diversity of dinoflagellate cysts versus motile dinoflagellates as well as their stratigraphic application has led to a taxonomic classification for cysts separate from the classification of the biological species (Evitt, 1985). Because the biological species is unknown for many dinoflagellate cysts, we also apply the classification of dinoflagellate cysts and primarily list the dinoflagellate cyst taxa below unless the dinoflagellate cyst has none, in which case we use "Cyst of (*biological taxon*)".

4.1.2 Fossil–plankton–ecosystem relationships

In the Southern Ocean, dinoflagellates form one of the largest microplankton group after diatoms and *Phaeocystis*, blooming in late summer in response to the sea-ice decline and phytoplankton (i.e. diatom) blooms (Garrison and Buck, 1989; Andreoli et al., 1995; Clarke and Leakey, 1996; Assmy et al., 2014). The taxonomic diversity includes species with various life strategies including heterotrophic and phototrophic life styles, parasitism, symbiosis, and phagotrophy (Evitt, 1985). Among heterotrophic dinoflagellates, a wide variety of feeding strategies is applied to a large variation of prey, including prey that is larger than the dinoflagellates themselves (Jacobson, 1999). Therefore, they can be important for top-down control of phytoplankton blooms (Bjørnsen and Kuparinen, 1991). However, because only a minority of dinoflagellates produces cysts which can be preserved in the sediments (Evitt, 1985), the cysts found in Hole U1357B are not representative of the total dinoflagellate abundance and diversity in the surface waters. The cysts of dinoflagellates have, however, proven to be powerful tools for reconstructing past sea surface-water conditions because their distribution in the surface sediments has been linked to specific surface-water environmental conditions, such as temperature and productivity (e.g. Pross and Brinkhuis, 2005; Esper and Zonneveld, 2007). Although dinoflagellate cyst assemblages do not show much species diversity in most Holocene ice-proximal Southern Ocean records (Harland et al., 1999; Howe et al., 2002; Esper and Zonneveld, 2007) or within recent sediments (Marret and De Vernal, 1997; Harland et al., 1998; Wrenn et al., 1998; Harland and Pudsey, 1999; Marret et al., 2001; Esper and Zonneveld, 2002, 2007; Pieńkowski et al., 2013b; Prebble et al., 2013), the distribution of dinoflagellate cysts in the sediments has been linked to the Southern Ocean fronts and the sea-ice extent (Marret and De Vernal, 1997; Harland et al., 1998; Esper and Zonneveld, 2002, 2007; Prebble et al., 2013). As they become generally very scarce south of the maximum sea-ice edge (Marret and De Vernal, 1997; Harland et al., 1998), dinoflagellate cyst abundances have been useful for inferring the position of the maximum sea-ice edge throughout the Quaternary (Harland et al., 1999; Howe et al., 2002). South of the Subantarctic Front, the dinoflagellate cyst assemblage in the surface sediments is dominated by heterotrophic species (Marret and De Vernal, 1997; Harland et al., 1998; Esper and Zonneveld, 2002, 2007; Prebble et al., 2013). This means that prey availability likely determines their distribution in the surface sediments. For example, it has been shown that the dominance of a certain heterotrophic dinoflagellate species in the water column is in part controlled by the size of the available prey, as certain prey is too large for some types of feeding strategies that dinoflagellates apply (Assmy et al., 2014).

While dinoflagellate cysts are usually found in surface sediments, the cyst of the photosynthetic dinoflagellate *Polarella glacialis* is abundant in the sea ice and underlying

waters (Montresor et al., 1999, 2003, and references therein), but it has seldom been found in surface sediments (Ichinomiya et al., 2008; Heikkilä et al., 2014). Instead, its biogeographic distribution is based on reports from fast ice along the Antarctic coast (Thomson et al., 2006) and DNA extraction from water column and sediment samples (Rengefors et al., 2008; Boere et al., 2009).

4.2 Tintinnid loricae

4.2.1 Descriptive terminology

Unlike other spirotrich ciliates, tintinnids are the only group that produces a shell, the so-called lorica. These loricae have an oral opening at the anterior end through which adoral membranelles (used for swimming and feeding) of the ciliate protrude when the tintinnid is in its extended state (Agatha et al., 2013). In most cases the lorica is larger than the cell proper so that it is able to retract within the lorica for protection (Agatha et al., 2013). The posterior end of the lorica can have various forms (a.o. conical, globular, or tubular) and the anterior collar can possess openings (fenestrae). The vast majority of tintinnids build a transparent lorica, known as a hyaline lorica (Agatha et al., 2013). However, a selection of tintinnid genera agglomerates mineral or biogenic particles to their lorica to form a so-called hard lorica, or a lorica with a hard bowl if the particles only stick to the posterior end (Agatha et al., 2013). Palynological treatment with hydrochloric and hydrofluoric acid will dissolve the siliceous and carbonate microfossils (e.g. diatom frustules and coccoliths) of the tintinnids with hard lorica. However, most of the underlying organic shells of hard loricae and hyaline loricae are able to withstand these acid treatments (Agatha and Simon, 2012). The lorica is probably built from crystalline proteins (Agatha and Simon, 2012; Agatha et al., 2013), which also makes it resistant to a certain degree of diagenesis. For this reason, tintinnids can be used as environmental proxies in palynological studies. This is, however, not common practice. Tintinnids have been used in Antarctic palaeoenvironmental reconstructions before (Ace Lake, Antarctica), although no palynological treatment was applied here (Cromer et al., 2005).

Because the shape of the lorica is species specific, identification can be achieved at species level based on the lorica only. However, there is an increasing awareness of considerable morphological plasticity within species, which is related to the life cycle stages of the ciliate (Boltovskoy et al., 1990; Wasik, 1998; Agatha et al., 2013; Dolan et al., 2013). The intraspecific morphological varieties of several Antarctic species were recently confirmed by a genetic study (Kim et al., 2013).

4.2.2 Fossil–plankton–ecosystem relationships

Within the Southern Ocean there is a large diversity of endemic and more widespread species (Dolan et al., 2012).

The geographic distribution of Southern Ocean tintinnids, based on plankton studies, shows that there is a relation between the distribution of tintinnids and the Southern Ocean fronts (Dolan et al., 2012). In general, however, tintinnids are only a minority component of the microzooplankton in the Southern Ocean compared to, for example, heterotrophic dinoflagellates (Dolan et al., 2012). Tintinnids feed on a wide variety of prey ranging from picozooplankton to microzooplankton size, including diatoms, dinoflagellates, and chlorophytes (Montagnes, 2013). Remains of the latter two taxonomic groups in particular have also been found in Hole U1357B. Furthermore, it has been shown that species endemic to the Antarctic coastal waters become relatively more abundant when the phytoplankton community is dominated by *Phaeocystis* (Dolan et al., 2013). It is, however, uncertain whether a predator–prey relationship is involved here, as spirotrich ciliates in general are known to have difficulty preying on *Phaeocystis* colonies and only feed on individual cells (Dolan et al., 2013). The range of organisms that feed on tintinnids is also extensive, but reported predators of the tintinnids endemic to the Antarctic are limited to copepods, small malacostracans (e.g. krill), and ostracods (Stoecker, 2013).

4.3 Foraminifer linings

4.3.1 Descriptive terminology

Mainly benthic foraminifera produce a foraminiferal lining between their cytoplasm and their calcareous or arenaceous shell (de Vernal, 2009). However, planktonic species produce an inner lining as well (Hemleben et al., 1977), some of which may be preserved in the sediments (Arai and Koutsoukos, 1998). Our focus here lies on the linings of benthic foraminifera, which remain after the calcareous or arenaceous shell has been dissolved. Dissolution can occur in the sediment pore waters or after palynological processing. Foraminiferal linings are composed of a complex mixture of polysaccharide and protein macromolecules with some chitin derivatives and even traces of lignin derivatives (Ní Fhlaithearta et al., 2013), which makes most linings resistant to lithification processes and palynological acid treatments. However, not all foraminiferal linings survive lithification and acid treatment. It has been suggested for calcareous benthic foraminifera that the thickness, and therefore its preservation potential, is linked to the thickness of the calcareous test and therefore the capacity of the foraminifer to bind magnesium (Ní Fhlaithearta et al., 2013). At Site U1357, calcareous tests of benthic foraminifera have been recorded (Expedition 318 Scientists, 2011). Similar to the tests, the foraminiferal linings occur in various forms and can be recognized as a series of spherical or half-moon-shaped, reddish brown chambers arranged in a spiral form (trochospiral or planispiral), as a bunch of grapes (triserial), or as a bead necklace (uniserial).

4.3.2 Fossil–organism–ecosystem relationships

Because benthic foraminiferal linings are preserved better than the calcareous shell, which may dissolve in the sediment pore waters, they have been considered a better representation of benthic (palaeo)productivity than the calcareous shells (de Vernal, 2009). Benthic productivity is controlled mainly by the availability of free oxygen in the bottom waters and the nutrient supply from the surface waters (Jorissen et al., 1995; Thomas et al., 1995), which links the productivity at the sea floor to surface-water productivity. It has been suggested that the abundance of epifaunal versus infaunal species is directly related to the amount of organic material that reaches the sea floor (Thomas et al., 1995). However, high abundances of epifaunal species could also reflect a well-ventilated bottom-water environment with pulsed high primary productivity in the surface waters (Jorissen et al., 1995; Thomas et al., 1995; Costello and Bauch, 1997). Conversely, high abundances of infaunal species could reflect regions with high surface-water productivity and a sustained flux of organic matter to the sea floor, which consumes oxygen and could result in low oxygen concentrations in the bottom waters (Thomas et al., 1995). Although it is not always possible to determine the foraminifer species from the benthic foraminifer linings, uniserial or triserial forms are generally infaunal, while trochospiral forms are more commonly epifaunal (Corliss, 1991).

4.4 Prasinophyte phycomata

4.4.1 Descriptive terminology

Phycomata are the reproductive cysts formed during the asexual reproduction of scaled green algae (prasinophytes). Although many prasinopytes produce cysts (e.g. Daugbjerg, 2000; Moro et al., 2002; Moestrup et al., 2003), these appear to be mostly polysaccharide in nature and are therefore not preserved in the sediments (O'Kelly, 2007). However, within the order of Pyramimonadales, one of the most basal clades of green algae (Nakayama et al., 1998; Guillou et al., 2004; Suda et al., 2013), the family of Halosphaeraceae make a multilayered phycoma (resting spore) of which at least one of the layers is made from sporopollenin, which makes them fossilizable (Colbath and Grenfell, 1995). Originally the phycomata of prasinophytes found in the fossil record were classified as acritarchs until the resemblance was noticed between the former acritarchs *Cymatiosphaera* and *Pterospermella* and the phycomata of species of *Pterosperma* (Martin, 1993). Various types of prasinophyte phycomata are known from palynological records (Martin, 1993; Colbath and Grenfell, 1995; Mudie et al., 2011). Because many of them were originally formally described from sedimentary deposits, these phycomata have their own taxon (Colbath and Grenfell, 1995). The surface wall of prasinophyte phycomata can be smooth or ornamented, including the presence of pores and (equatorial) wings or ridges, which are termed alae (Parke et al., 1978; Colbath and Grenfell, 1995).

4.4.2 Fossil–plankton–ecosystem relationships

Prasinophytes are predominantly marine plankton (Parke et al., 1978; O'Kelly, 2007). In addition, studies based on pigment signatures of Antarctic seawater show that prasinophyte abundances in general increase during periods of decreased stratification (Rozema et al., 2017) with the highest prasinophyte pigments found offshore below the mixed layer depth (Hashihama et al., 2008; Kozlowski et al., 2011). Because stratification along the Antarctic coast is directly related to the presence of sea ice and/or meltwater runoff from the continent, increased amounts of prasinophytes should instead reflect more open ocean conditions (Rozema et al., 2017). However, some prasinophytes occur in fresh and brackish water environments, and fossil phycomata of prasinophytes have mainly been found in association with inshore shallow lagoonal and deltaic environments (Mudie et al., 2010). Also in the Arctic, pigment signatures show that the highest prasinophyte concentrations are located in cool, nitrogen-depleted, meltwater-influenced surface waters (Fujiwara et al., 2014). It is possible that these Arctic prasinophytes are different species than those living offshore of Antarctica and therefore have different environmental preferences, but species-specific ecological preferences for phycomate prasinophytes (i.e. Halosphaeraceae) are not available. Species-specific biogeographic information has been mainly obtained from phytoplankton checklists (Moita and Vilarinho, 1999; Hällfors, 2004; Guilloux et al., 2013; Medvedeva and Nikulina, 2014; Veen et al., 2015; Cărăuş, 2017) and the online Global Biodiversity Information Facility (GBIF; https://www.gbif-uat.org/, last access: 23 September 2018) and is therefore rather patchy. Ecological inferences based on the presence of prasinophyte phycomata should therefore be made carefully, in particular because ecologically the Pyramimonadales (including Halosphaeraceae) only represent a minor component of the green algae (Tragin et al., 2016). It is known, however, that several species within Pyramimonadales have been associated with sea-ice-dominated environments of the Antarctic (Daugbjerg, 2000; Moro et al., 2002). This is also evident from the fossil record in which fossil prasinophyte phycomata have been found in sediment cores and surface sediments from the shelves of the Ross Sea, Prydz Bay, and the Antarctic Peninsula (Hannah et al., 1998; Wrenn et al., 1998; Hannah, 2006; Warny et al., 2006, 2009; Warny, 2009; Clowes et al., 2016). In sea-ice-dominated environments, fossil prasinophyte phycomata have been associated with the sea-ice edge and increased stratification after sea-ice retreat (Mudie et al., 1992; Wrenn et al., 1998; Hannah, 2006). Pyramimonadales are considered important spring bloomers around Antarctica (Varela et al., 2002) and Greenland (Harðardóttir et al., 2014) and might be important in maintaining the heterotrophic microbial community dur-

ing the winter (Harðardóttir et al., 2014). Although prasinophytes are predominantly autotrophic, mixotrophy has also been reported as a means to survive the cold light-limited Antarctic winters (Bell and Laybourn-Parry, 2003).

4.5 Scolecodonts

4.5.1 Descriptive terminology

While annelids are soft-bodied organisms and generally do not fossilize, the hardened jaw parts of eunicid annelids are commonly found in fossil assemblages dating back to the late Cambrian (Struck et al., 2006). In this context they are commonly known as "scolecodonts" (Struck et al., 2006). The eunicid jaw apparatus consists of mandibles and rows of maxillary pieces with or without carrier (Fauchald, 1977; Struck et al., 2006). Jaw morphologies are quite similar between taxa, but in general three major types are distinguished based on the number of maxillae and the shape of the carrier: ctenognath, prionognath, and labidognath (Struck et al., 2006).

4.5.2 Fossil–plankton–ecosystem relationships

Scolecodonts have been reported from Cretaceous, Oligocene, and Miocene Antarctic drill holes or outcrops (Szaniawski and Wrona, 1987; Hannah et al., 2000; Amenábar et al., 2014; Warny et al., 2016), but never as such from Antarctic or Southern Ocean Holocene deposits. Considering that scolecodonts are the remains of benthic organisms, their presence is indicative of oxygenated bottom-water conditions. Still, when part of the palynological assemblage, scolecodonts are generally not used for palaeoenvironmental interpretation because eunicid mandible parts are often difficult to relate to extant taxa and difficult to distinguish from the sclerotized mouthparts of cladocerans and chaetognaths (Mudie et al., 2011). Possible scolecodonts are discussed in Sect. 5.7 "Palynomorphs of unknown affinity". The characteristics of eunicid jaw apparatuses have, however, been extensively compared at family level and their phylogenetic relationships have been discussed (Fauchald, 1977; Struck et al., 2006). We are therefore fairly certain that the eucinid jaws found in the samples of Hole U1357B are of the ctenognath type (relatively large basal maxillae and symmetrical rows of numerous anterior denticles in longitudinal series without carriers) and therefore belong to the family of Dorvilleidae (Struck et al., 2006).

The knowledge of Antarctic or Southern Ocean dorvilleids is limited, but recently the experimental deployment of whale bones off the coast of Deception Island (South Shetland Islands) has led to the discovery of some new dorvilleid species; these include *Parougia diapason* (Taboada et al., 2015), *Ophryotrocha clava*, and *Ophryotrocha orensanzi* (Taboada et al., 2013).

4.6 Arthropod remains

4.6.1 Descriptive terminology

Some of the remains in the samples of Hole U1357B were identified as derived from copepods, but for other thick-walled, yellow, chitinous remains the true biological affinity is unknown. These palynomorphs are possibly derived from crustacean exoskeletons as their appearance resembles that of known copepod remains. We discuss these in Sect. 5.7 "Palynomorphs of unknown affinity". The palynomorphs that were identified as belonging to copepods are listed under the subclass Copepoda in the Results section. Among these remains are chitinous body parts, but also copepod eggs and spermatophores.

Copepod egg sizes can range between 60 and 300 µm (Koga, 1968; van Waveren, 1992; Belmonte, 1998) and can be a common component in palynological assemblages (van Waveren, 1992; Mudie et al., 2010, 2011; Candel et al., 2013). In general copepods produce two types of eggs: quiescent subitaneous eggs, which are produced under unfavourable environmental conditions and hatch open within a few weeks when conditions improve, and diapause eggs, which are produced when copepod production is highest and during population decline and will not open until after a gene-controlled refractory phase is over (Marcus, 1996; Castellani and Lucas, 2003; Katajisto, 2003; Hansen et al., 2010; Berasategui et al., 2012). These diapause eggs are able to remain viable for several decades (Marcus, 1996). Both subitaneous and diapause eggs can be smooth or ornamented, but diapause eggs possess a thicker egg envelope consisting of multiple layers (Santella and Ianora, 1990; Marcus, 1996). Various ornamentation types of subitaneous and diapause eggs have been described, ranging from smooth to reticulate, covered with short, long, and/or branched spines, or with a equatorial wing (Koga, 1968; Santella and Ianora, 1990; Belmonte, 1992, 1998; van Waveren, 1992; Hansen et al., 2010). It has been suggested that such surface ornamentation provides protection against carnivores or serves as a floating device (Koga, 1968; Dumont et al., 2002). Some eggs might appear smooth under the light microscope but when viewed under a scanning electron microscope are rough or finely tuberculated (Belmonte, 1998; Berasategui et al., 2012). The morphology of the eggs is not known for all of the Southern Ocean species, and studies on copepod reproduction generally report the amount of copepod egg (and also spermatophore) observations and do not describe their morphology (e.g. Swadling, 1998; Loots et al., 2009).

4.6.2 Fossil–organism–ecosystem relationships

In palynological studies, fragments of chitinous body parts of arthropods are common components of the non-pollen palynomorph assemblage (Mudie et al., 2011). Marine arthropods (i.e. crustaceans) include the Antarctic krill *Euphausia superba* and amphipods, but in particular copepods as they

can comprise more than 75 % of the Southern Ocean standing biomass (Atkinson et al., 2012). Copepods are important grazers in the Southern Ocean, feeding predominantly on large-range diatom species (Pasternak and Schnack-Schiel, 2001). However, some species supplement their diets by a certain degree of carnivory, preying on dinoflagellates, small crustaceans, and protozoans during early spring when phytoplankton is still scarce (Atkinson, 1998; Pasternak and Schnack-Schiel, 2001). The production of faecal pellets by copepods is an important mechanism for the export productivity of organic material to the sea floor (Harris, 2001), also in coastal high-latitude water (Fabiano et al., 1997; Smith Jr. et al., 2011), and therefore has likely contributed to the high sedimentation rates in the Adélie Basin. Today, only three species of copepods are found in the sea ice and water column close to our study site in the Adélie Basin: *Drescheriella glacialis*, *Stephos longipes*, and *Paralabidocera antarctica*, the latter of which was the most abundant (Loots et al., 2009).

Taxonomy on the species level is not possible on the exoskeleton parts found in Hole U1357B because these are fragmentary. However, using the online database "Diversity and Geographic Distribution of Marine Planktonic Copepods" of Razouls et al. (2005–2017) we have been able to identify several copepod exoskeleton parts. In particular, mandibular gnathobases can potentially provide information on the different copepod taxa from which we find the remains in the samples of Hole U1357B. Mandibular gnathobases are the basal parts of the copepod mandibles and are used for crushing and mincing food (Michels and Gorb, 2015). Mandibular gnathobases consist of a chitinous exoskeleton with sockets on which opal teeth (crown- or cap-like structures) are located (Michels and Gorb, 2015). Palynological processing of the material from Hole U1357B will have dissolved these opal teeth, making identification on the species level more difficult. It also means that the sizes, both absolute and relative, of the preserved chitinous tooth sockets do not necessarily represent the original sizes of the teeth that have been dissolved from these sockets. In future studies, it might be possible to quantify copepod diversity if e.g. eggs and mandibular gnathobases can be identified on the genus or species level. Changes in the diversity of copepod species in the sediments could be related to the sea-ice extent (Swadling, 1998; Loots et al., 2009; Kramer et al., 2011). Because of the difficulties with assigning copepod remains to particular genera or species, a geographic distribution and environmental interpretation are generally not provided for the copepod remains.

4.7 Acritarchs

4.7.1 Descriptive terminology

Acritarchs are hollow, organic-walled, and have a wide range of morphologies and surface-wall ornamentations (Mar-

tin, 1993). Surface-wall ornamentations can include ridges (septa) or processes (Martin, 1993). Most of the acritarchs described here have a single circular opening or pylome. By convention a single circular opening is said to be apical and a pylome is defined as a (sub)circular opening whose periphery is distinct before excystment (Martin, 1993). The pylome is closed off by a lid, the operculum (Martin, 1993).

4.7.2 Fossil–plankton–ecosystem relationships

Acritarchs are the remains of a variety unicellular biological affinity (red and green algae), although their exact origin is uncertain. Under the group Acritarcha we discuss known acritarchs that have a genus and species name. Other palynomorphs (including hollow organic-walled specimens) with unknown biological affinity are listed in Sect. 5.7 "Palynomorphs of unknown affinity". The geographic distribution of acritarch species is primarily based on palynological studies of recent marine surface sediments.

4.8 Reworked material

Pollen, spores, and some dinoflagellate cysts recovered from Hole U1357B are considered part of the reworked assemblage as they clearly reflect input from older strata. The eutardigrade egg found in Hole U1357B is also probably derived from the Antarctic mainland. Modern-day biogeographic information and ecological preferences for these species are therefore not relevant for this study and generally not provided here. However, qualitatively, increased abundances of reworked material could be related to increased iceberg discharge, ice-shelf collapse, or submarine slope instability, since early Cenozoic and Cretaceous strata do surface on the Antarctic continental shelf in the region (Expedition 318 Scientists, 2011).

5 Results

5.1 Dinoflagellate cysts

Kingdom CHROMISTA Cavalier-Smith 1981

Subkingdom HAROSA Cavalier-Smith 2010

Infrakingdom HALVARIA Cavalier-Smith 2010

Superphylum ALVEOLATA Cavalier-Smith 1991

Phylum MIOZOA Cavalier-Smith 1987

Division DINOFLAGELLATA (Bütschli, 1885) Fensome et al. 1993

Subdivision DINOKARYOTA Fensome et al. 1993

Class DINOPHYCEAE Pascher 1914

Subclass GYMNODINIPHYCIDAE Fensome et al. 1993

Order GYMNODINIALES Apstein 1909

Suborder GYMNODINIINEAE Fensome et al. 1993

Family GYMNODINIACEAE Lankester 1885

Genus *Gymnodinium* Stein 1878

Cyst of *Gymnodinium microreticulatum* Bolch et al. 1999 (Plate 2, figs. 9–16)

Morphology and identification: These are spherical brown-coloured microreticulate cysts with chasmic archaeopyles. Sometimes only half-cysts are found when the chasmic archaeopyle has ruptured the cyst in two. Only four modern dinoflagellate species are known to produce these kind of fossilizable cysts and they all belong to the naked (unarmoured) dinoflagellate genus *Gymnodinium*, namely *Gymnodinium catenatum* Graham (cyst described by Anderson et al., 1988), *Gymnodinium nolleri* Ellegaard & Moestrup 1999, *Gymnodinium microreticulatum*, and *Gymnodinium trapeziforme* Attaran-Fariman & Bolch 2007 in Attaran-Fariman et al. (2007). *G. trapeziforme* is, however, not spherical like the specimens found in the samples of Hole U1357B, but subrectangular (Attaran-Fariman et al., 2007). The cysts of the other three species are spherical and look very similar under the light microscope, but they can be distinguished primarily by their colour and size (Bolch et al., 1999). Cysts of *G. microreticulatum* are the smallest of the three species (17–28 µm) and have a pale brown or purplish brown colour versus the reddish brown of *G. nolleri* and *G. catenatum*. There is, however, some overlap between the size ranges of *G. nolleri* and *G. microreticulatum* (Bolch et al., 1999; Ribeiro et al., 2012b). Still, *G. nolleri* possesses fewer rows of relatively larger paravesicles in the paracingular area (Ribeiro et al., 2012b). In addition, the chasmic archaeopyle *G. microreticulatum* runs along the parasulcus and not along the paracingulum as is the case for the other two species (Bolch et al., 1999). However, paracingular ruptures could be present due to damage during sedimentation (Bolch et al., 1999). Based on the size and pale brown colour of the microreticulate cysts encountered in the samples of Hole U1357B we assign these cysts to *G. microreticulatum*. We have not been able to distinguish a paracingulum due to the small size of the paravesicles, but as *G. nolleri* possesses a paracingulum with better-recognizable larger vesicles this also suggests that our specimens are *G. microreticulatum*.

Biological taxon: *Gymnodinium microreticulatum*.

Dimensions: Cyst diameters range between 28 and 36 µm (average: 31 µm, $n = 8$).

Geographic distribution: The distribution of microreticulate *Gymnodinium* cysts in coastal marine sediments is rather patchy and is probably influenced by ship ballast water (Hallegraeff, 1998; Bolch and Reynolds, 2002). The highest abundances of cysts of *G. microreticulatum* have been found in surface sediments of southern Australia and Tasmania, but also in Uruguay, Hong Kong, the Chinese coast, the Russian east coast, and Portugal (Amorim et al., 2001; Bolch and Reynolds, 2002; Orlova et al., 2004; Ribeiro et al., 2012b, 2016).

The fossil record: Palynological records of cyst-forming *Gymnodinium* species are sparse. To our knowledge records are only available from the Kattegat (south-western Scandinavia) (Thorsen et al., 1995; Fjellså and Nordberg, 1996), the Adriatic Sea (Sangiorgi and Donders, 2004), and the Portuguese margin (Ribeiro et al., 2012b, 2016). There are therefore no published records of *G. microreticulatum* in the Southern Ocean. However, there is one account that states that *G. microreticulatum* has only been introduced in southern Australian waters within the past 50 years (McMinn, 2002).

Ecological preferences and environmental interpretation: The large distribution area renders this species a generalist: the associated broad temperature and salinity range makes it difficult to infer ecological preferences. Culture experiments have only been performed with a temperature range of 17–25 °C and 26–35 g L^{-1} (Bolch et al., 1999). However, its occurrence in samples of Hole U1357B suggests it is able to live under much cooler temperature conditions. All three spherical cyst-forming *Gymnodinium* species are autotrophic, and increased abundances of the three species have been associated with an increased influence of warmer waters and surface-water stratification (Ribeiro et al., 2016). Notably, however, cysts of *Gymnodinium* cf. *catenatum* have also been found in northern high latitudes along the Russian east coast (Orlova et al., 2004), thereby confirming the ability of spherical cyst-forming *Gymnodinium* species to live in relatively colder waters.

Order SUESSIALES Fensome et al. 1993

Family SUESSIACEAE Fensome et al. 1993

Genus *Polarella* Montresor, Procaccini & Stoecker 1999

Cysts of *Polarella glacialis* Montresor, Procaccini & Stoecker 1999 (Plate 2, figs. 21–23)

Morphology and identification: This is a small, ovoidal, transparent cyst with more than 40 solid, spiny processes. The cyst wall is relatively thick. Most specimens have been found with cell content. Paratabulation is not visible on the cyst underneath the light microscope, but it is known from scanning electron microscope images that each spiny process reflects a paraplate (Montresor et al., 1999). This species was described from the brine in upper sea ice at McMurdo Sound, Ross Sea, and is the first account of a

free-living species in the order Suessiales, which before its official description only included fossil taxa and symbionts (Montresor et al., 1999).

Biological taxon: *Polarella glacialis*.

Dimensions: The cyst length is $14 \pm 1\,\mu m$ ($n = 3$).

Geographic distribution: The occurrence of its cysts in fast ice of the Weddell Sea (Buck et al., 1992), Ross Sea (Stoecker et al., 1997; Montresor et al., 1999; Andreoli et al., 2000), and Prydz Bay areas (Thomson et al., 2004, 2006), but also in water samples from Prydz Bay (Rengefors et al., 2008) and the Arctic (Montresor et al., 2003, and references therein), indicate an Antarctic circumpolar and bipolar distribution for *Polarella glacialis*. There are only a few accounts of cysts of *P. glacialis* in surface sediments: from the Hudson Bay area (Heikkilä et al., 2014) and off the coast near Syowa station, Queen Maud Land, Antarctica (Ichinomiya et al., 2008), and the Ross Sea (Francesca Sangiorgi, unpublished data).

The fossil record: Cysts (and fossil 18S rDNA) of *P. glacialis* have rarely been found in surface sediments and never below the upper few centimetres of sediment cores (Ichinomiya et al., 2008; Boere et al., 2009; Heikkilä et al., 2014), which may be because the cyst lacks dinosporin, allowing for long-term preservation (Montresor et al., 1999). The fact that we find cysts of *P. glacialis* several metres deep underlines the exceptional preservation of organic matter in Hole U1357B.

Ecological preferences and environmental interpretation: In Hole U1357B *Polarella glacialis* is one of the three autotrophic dinoflagellate species (the others being *G. microreticulatum* and *Impagidinium pallidum*) that were found in situ. It has been shown that the highest concentrations of *P. glacialis* occur in the upper ice layers of fast ice, but are generally poorly represented in pack ice (Stoecker et al., 1997; Andreoli et al., 2000; Thomson et al., 2006). Mass excystment of *P. glacialis* occurs at $-6\,°C$ and $100\,psu$ in austral spring (around early November) after which the number of cells increases until early December (Stoecker et al., 1997; Thomson et al., 2006). Sexual reproduction takes place at around $-2\,°C$ and $37\,psu$ followed by encystment (Thomson et al., 2006). Large amounts of these cysts are released into the water column through brine rejection in late spring (Thomson et al., 2006). Considering the low preservational potential, the presence of *P. glacialis* is indicative of the nearby fast ice extending from the Antarctic coast, but should be interpreted as a preservation signal as the disappearance of *P. glacialis* from the sedimentary record does not necessarily mean the fast ice has retreated.

Subclass PERIDINIPHYCIDAE Fensome et al. 1993

Order GONYAULACALES Taylor 1980

Suborder GONYAULACINEAE (autonym)

Family GONYAULACACEAE Lindemann 1928

Subfamily GONYAULACOIDEAE Fensome et al. 1993

Genus *Impagidinium* Stover & Evitt 1978

Impagidinium pallidum Bujak 1984 (Plate 1, figs. 29–35)

Morphology and identification: This species possesses very high septa (up to $15\,\mu m$) compared to the cyst diameter. Unlike other *Impagidinium* species these septa are not placed on a central body, but together form a thin-walled envelop with polygonal fields. The cyst is very transparent and can therefore be easily overlooked. However, in the samples of U1357B it is commonly found with a spherical body with cell content inside the transparent cyst.

Biological taxon: Cyst of *Gonyaulax* sp. indet. (Head, 1996; Zonneveld et al., 2013).

Dimensions: The cyst lengths range between 59 and $102\,\mu m$ (average: $77\,\mu m$, $n = 5$) and the diameter of the central spherical body is $39 \pm 10\,\mu m$ ($n = 3$).

Geographic distribution: The highest relative abundances of *I. pallidum* are observed in areas influenced by the melt-back of seasonal sea ice in both the Arctic and the Antarctic (Mudie, 1992; Marret and De Vernal, 1997; De Vernal et al., 2001; Kunz-Pirrung et al., 2001; Esper and Zonneveld, 2007; Bonnet et al., 2010; Pieńkowski et al., 2013b; Zonneveld et al., 2013). In the Southern Ocean, it is generally restricted to waters south of the Subtropical Front (Marret and De Vernal, 1997; Crouch et al., 2010; Verleye and Louwye, 2010; Prebble et al., 2013), but remarkably very low amounts of *I. pallidum* have been found in surface samples of the south-east Atlantic Ocean (Esper and Zonneveld, 2002). In the Arctic, highest abundances of *I. pallidum* cysts are found in sediments of the deeper parts of the Arctic basins underlying the pack-ice margin (Mudie, 1992; Mudie and Harland, 1996). However, specimens of *I. pallidum* have been found in the Mediterranean and equatorial east Atlantic (Zonneveld et al., 2013).

The fossil record: *I. pallidum* is a particularly long-ranging species. Notably, it was first described from North Pacific sediments with ages ranging from the late Eocene to Pleistocene (Bujak, 1984). Also in the Southern Ocean, occurrences of *I. pallidum* date back as far as the Oligocene (Stocchi et al., 2013; Bijl et al., 2018). Temperatures close
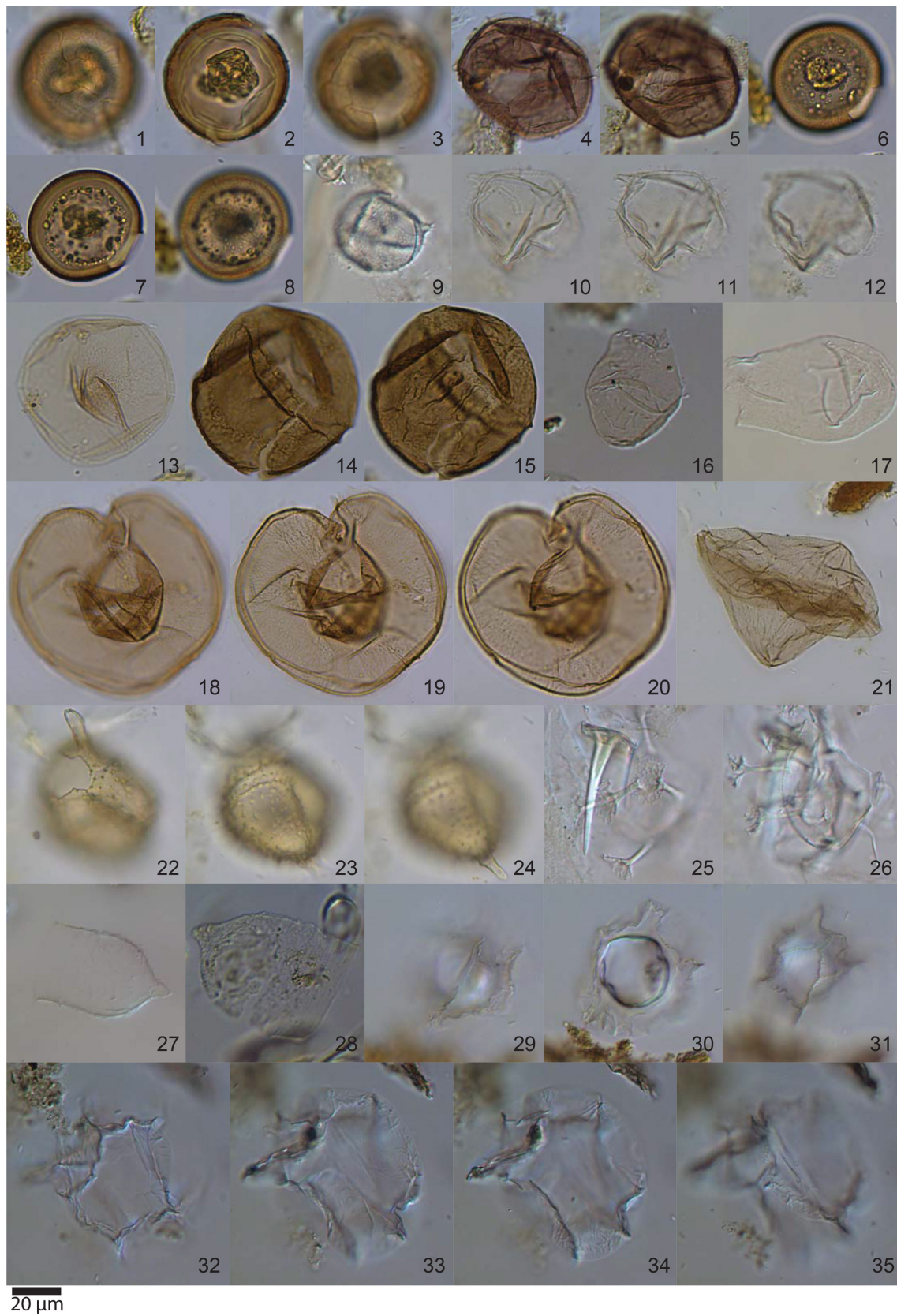
20 μm

Plate 1.

Plate 1. (1) *Cryodinium meridianum* with cell content and faint septa, U1357B-16H-1W 63–65 cm, slide 1, E.F.: E17.2, upper focus. **(2)** *Cryodinium meridianum* with cell content and faint septa, U1357B-16H-1W 63–65 cm, slide 1, E.F.: E17.2, mid focus. **(3)** *Cryodinium meridianum* with cell content and faint septa, U1357B-16H-1W 63–65 cm, slide 1, E.F.: E17.2, lower focus. **(4)** *Cryodinium meridianum* flattened with clear septa, U1357B-8H-3W 54–56 cm, slide 1, E.F.: U28.4, upper focus. **(5)** *Cryodinium meridianum* flattened with clear septa, U1357B-8H-3W 54–56 cm, slide 1, E.F.: U28.4, lower focus. **(6)** *Cryodinium* sp. 1 with cell content, U1357B-16H-1W 63–65 cm, slide 1, E.F.: O18.2, upper focus. **(7)** *Cryodinium* sp. 1 with cell content, U1357B-16H-1W 63–65 cm, slide 1, E.F.: O18.2, mid focus. **(8)** *Cryodinium* sp. 1 with cell content, U1357B-16H-1W 63–65 cm, slide 1, E.F.: O18.2, lower focus. **(9)** *Vozzhennikovia aperture*, oblique antapical view, U1357B-3H-7W 10–12 cm, slide 1, E.F.: J23.4, lower focus. **(10)** *Spinidinium colemanni*, oblique dorsal view, U1357B-2H-4W 111–113 cm, slide 1, E.F.: E20.2, upper focus. **(11)** *Spinidinium colemanni*, oblique dorsal view, U1357B-2H-4W 111–113 cm, slide 1, E.F.: E20.2, mid focus. **(12)** *Spinidinium colemanni*, oblique dorsal view, U1357B-2H-4W 111–113 cm, slide 1, E.F.: E20.2, lower focus. **(13)** *Selenopemphix antarctica*, (ant)apical view, U1357B-18H-4W 2–3 cm, slide 1, E.F.: D35.2, upper focus. **(14)** *Nucicla umbiliphora*, dorsal side up, U1357B-6H-4W 86–88 cm, slide 1, E.F.: K24.1, upper focus. **(15)** *Nucicla umbiliphora*, dorsal side up, U1357B-6H-4W 86–88 cm, slide 1, E.F.: K24.1, lower focus. **(16)** Dictyocystid lorica sac, U1357B-16H-1W 63–65 cm, slide 1, E.F.: G21.4. **(17)** Dictyocystid lorica sac, U1357B-17H-1W 18–20 cm, slide 1, E.F.: E25.1. **(18)** *Selenopemphix* sp. 1 sensu Esper & Zonneveld 2007, antapical side up, U1357B-6H-4W 86–88 cm, slide 1, E.F.: T30.4, upper focus. **(19)** *Selenopemphix* sp. 1 sensu Esper & Zonneveld 2007, antapical side up, U1357B-6H-4W 86–88 cm, slide 1, E.F.: T30.4, mid focus. **(20)** *Selenopemphix* sp. 1 sensu Esper & Zonneveld 2007, antapical side up, U1357B-6H-4W 86–88 cm, slide 1, E.F.: T30.4, lower focus. **(21)** *Selenopemphix* sp. 1 sensu Esper & Zonneveld 2007, lateral view, U1357B-19H-2W 39–41 cm, slide 1, E.F.: J29.4, LIB image. **(22)** *Vozzhenikovia netrona*, oblique apical view, U1357B-19H-2W 39–41 cm, slide 1, E.F.: F24.1, upper focus. **(23)** *Vozzhenikovia netrona*, oblique apical view, U1357B-19H-2W 39–41 cm, slide 1, E.F.: F24.1, lower focus. **(24)** *Vozzhenikovia netrona*, oblique apical view, U1357B-19H-2W 39–41 cm, slide 1, E.F.: F24.1, lower focus on the antapical horn. **(25)** *Enneadocysta dictyostila*, lateral view, U1357B-6H-6W 123–125 cm, slide 1, E.F.: J28.3, upper focus on the ragged clypeate processes. **(26)** *Enneadocysta dictyostila*, lateral view, U1357B-6H-6W 123–125 cm, slide 1, E.F.: J28.3, mid focus. **(27)** *Codonellopsis glacialis*, U1357B-1H-2W 40–42 cm, slide 1, E.F.: K24.1, LIB image. **(28)** *Codonellopsis glacialis*, U1357B-5H-7W 5–7 cm, slide 1, E.F.: N31.3. **(29)** *Impagidinium pallidum* with internal spherical body, U1357B-17H-5W 97–99 cm, slide 1, E.F.: H32.4, upper focus. **(30)** *Impagidinium pallidum* with internal spherical body, U1357B-17H-5W 97–99 cm, slide 1, E.F.: H32.4, mid focus. **(31)** *Impagidinium pallidum* with internal spherical body, U1357B-17H-5W 97–99 cm, slide 1, E.F.: H32.4, lower focus. **(32)** *Impagidinium pallidum*, U1357B-18H-4W 2–3 cm, slide 1, E.F.: K33.1, upper focus. **(33)** *Impagidinium pallidum*, U1357B-18H-4W 2–3 cm, slide 1, E.F.: K33.1, mid focus on upper right septa. **(34)** *Impagidinium pallidum*, U1357B-18H-4W 2–3 cm, slide 1, E.F.: K33.1, mid focus on lower septa. **(35)** *Impagidinium pallidum*, U1357B-18H-4W 2–3 cm, slide 1, E.F.: K33.1, lower focus.

to the Antarctic margin at that time were much warmer than today (Petersen and Schrag, 2015; Hartman et al., 2018) and it has been suggested that it was still able to tolerate much warmer temperatures during Pliocene–Pleistocene times, which could explain its modern bipolar distribution (De Schepper et al., 2011). This is also supported by accounts of *I. pallidum* from Oligocene to Pliocene strata from the Mediterranean area (Versteegh and Zonneveld, 1994; Zevenboom et al., 1994). In more recent Quaternary records of the Southern Ocean, the highest abundances of *I. pallidum* have been found during the interglacial stages south of the Subantarctic Front (SAF) (Esper and Zonneveld, 2007). North of the SAF the highest abundances are found during the glacial stages (Marret et al., 2001).

Ecological preferences and environmental interpretation: This is one of the three autotrophic dinoflagellate cyst species encountered in the samples of Hole U1357B. In both the Arctic and the Antarctic cysts are associated with temperatures between −1.7 and 5.4 °C (Mudie, 1992; Marret and De Vernal, 1997; De Vernal et al., 1997; Esper and Zonneveld, 2007; Zonneveld et al., 2013). In palynological records it is therefore also generally treated as a cold-water species (De Vernal et al., 2001; Brinkhuis et al., 2003), although it seems to have been more tolerant to warmer

temperatures in the past (Versteegh and Zonneveld, 1994; Sangiorgi et al., 2018). Its affinity for the pack-ice margin in the Arctic could mean an affinity for seasonal melt-back and the associated stratification and nutrient release (Mudie, 1992; Mudie and Harland, 1996). Also around Antarctica it is most abundant in nutrient-rich waters south of the APF and the seasonal sea-ice zone (Marret and De Vernal, 1997; Marret et al., 2001; Esper and Zonneveld, 2007).

Order PERIDINIALES Haeckel 1894

Suborder PERIDINIINEAE Fensome et al. 1993

Family PROTOPERIDINIACEAE (Bujak and Davies in Fensome et al. 1998) (Fensome et al. 1998)

Subfamily PROTOPERIDINIOIDEAE Bujak and Davies 1983

Genus *Cryodinium* Esper et Zonneveld 2002

Cryodinium meridianum Esper et Zonneveld 2002 (Plate 1, figs. 1–5)

Morphology and identification: *Cryodinium meridianum* is a brown, spherical, scabrate dinoflagellate cyst with septa (ridges) reflecting the paratabulation (Esper and Zonneveld, 2002). As in the original description of the species, the

height of the septa of the specimens in Hole U1357B is highly variable and can be very faint in the specimens of Hole U1357B. The combination of scabration and low septa is very characteristic and allows for identification even if the archaeopyle, which is formed through the loss of two intercalary plates (Esper and Zonneveld, 2002), is not very clear. Some specimens in the samples of Hole U1357B still contain cell content.

Biological taxon: Cyst of unknown dinoflagellate (Esper and Zonneveld, 2002).

Dimensions: Cyst diameters range between 40 and 56 μm (average: 46 μm, $n = 13$).

Geographic distribution: This species has been first described from surface sediments as endemic between the Antarctic Polar Front (APF) and the Weddell Sea Gyre with its highest abundances most distal from the coastline (Esper and Zonneveld, 2002). In later studies it has been reported from surface samples and Quaternary records from the South Atlantic (Esper and Zonneveld, 2007), the Prydz Bay area (Storkey, 2006; Boere et al., 2009), the south-eastern Pacific (Zonneveld et al., 2013), and most recently from the northern South China Sea (Li et al., 2017).

The fossil record: In the Atlantic sector of the Southern Ocean, low abundances of *C. meridianum* have been recorded during Marine Isotope Stage 2 and 3 just north of the modern-day Antarctic Polar Front (Esper and Zonneveld, 2007).

Ecological affinities and interpretation: Infrared analyses of modern cysts suggest that the brown protoperidinioid dinoflagellate cysts have a cyst wall chemistry that is distinctly different from the cyst wall chemistry of transparent autotrophic gonyaulacoid cysts, but similar to cyst of the distantly related heterotrophic gymnodinioid *Polykrikos* spp. (Ellegaard et al., 2013). It is therefore likely that the chemical composition of the cyst wall is determined by lifestyle (Ellegaard et al., 2013). This is also the reason why modern brown dinoflagellate cysts are generally considered heterotrophic. In the original description of *C. meridianum*, it is also considered as such and associated with the high phytoplankton concentrations within the Polar Frontal Zone (PFZ) and the Antarctic Zone (AZ) (Esper and Zonneveld, 2002). Because of this exclusive distribution within the PFZ and the AZ it is restricted to waters with a maximum summer temperature of 13.7 °C (Zonneveld et al., 2013). Recently, however, *C. meridianum* has been reported from the northern South China Sea, where it is oddly listed as an autotrophic species by Li et al. (2017). The species is, however, not discussed by Li et al. (2017) and no pictures of the species are provided, rendering the validity of its occurrence in the South China Sea difficult to prove.

Cryodinium sp. 1 (Plate 1, figs. 6–8)

Morphology and identification: In addition to *Cryodinium meridianum*, we regularly encountered cysts similar to *C. meridianum*, but which lack the septa. Still, these cysts have the typical scabration and 2I archaeopyle of *C. meridianum*.

Biological taxon: Cyst of unknown dinoflagellate.

Dimensions: They are of equal size as *C. meridianum* (48 ± 1 μm, $n = 3$).

Geographic distribution: There are no previous reports of this species from modern-day surface sediments. This is a new species, which will be formally described elsewhere.

The fossil record: Although there are no previous reports of granulated round brown cysts with a 2I archaeopyle, granulated round brown cysts (archaeopyle unknown) have been reported from Quaternary cores from the southern Atlantic Ocean as *Protoperidinium* sp. 1 (Esper and Zonneveld, 2007). These cysts are particularly abundant during Marine Isotope Stage 2 just north of the modern-day Antarctic Polar Front (APF) and also during marine isotope interglacial stages south of the modern-day APF (Esper and Zonneveld, 2007).

Ecological preferences and environmental interpretation: It is possible that these cysts belong to the same biological species as *C. meridianum* but that the cyst morphology is controlled by environmental conditions. There are other examples of morphological variations in cysts due to changes in environmental parameters. For instance, *Lingulodinium* and *Operculodinium* cyst process lengths have been related to changes in salinity (de Vernal et al., 1989; Mertens et al., 2009).

Genus *Echinidinium* Zonneveld 1997 ex Head, Harland & Matthiessen 2001

Echinidinium sleipnerensis Head, Riding, Eidvin & Chadwick 2004 (Plate 2, figs. 1–8)

Morphology and identification: In most of the core samples of Hole U1357B brown dinoflagellate cysts with numerous solid and/or apiculocavate processes can be found. Multiple round brown spiny dinoflagellate cyst taxa have been described, which can be distinguished based on the shape and hollowness of their processes and the granulation of the central body (Radi et al., 2013). Identification by archaeopyle type is often difficult, as the archaeopyle is rarely observed and/or not known for certain species. Based on the absence of granulation in all specimens encountered in Hole U1357B and some specimens exhibiting an archaeopyle that resembles a therophylic slit, we have
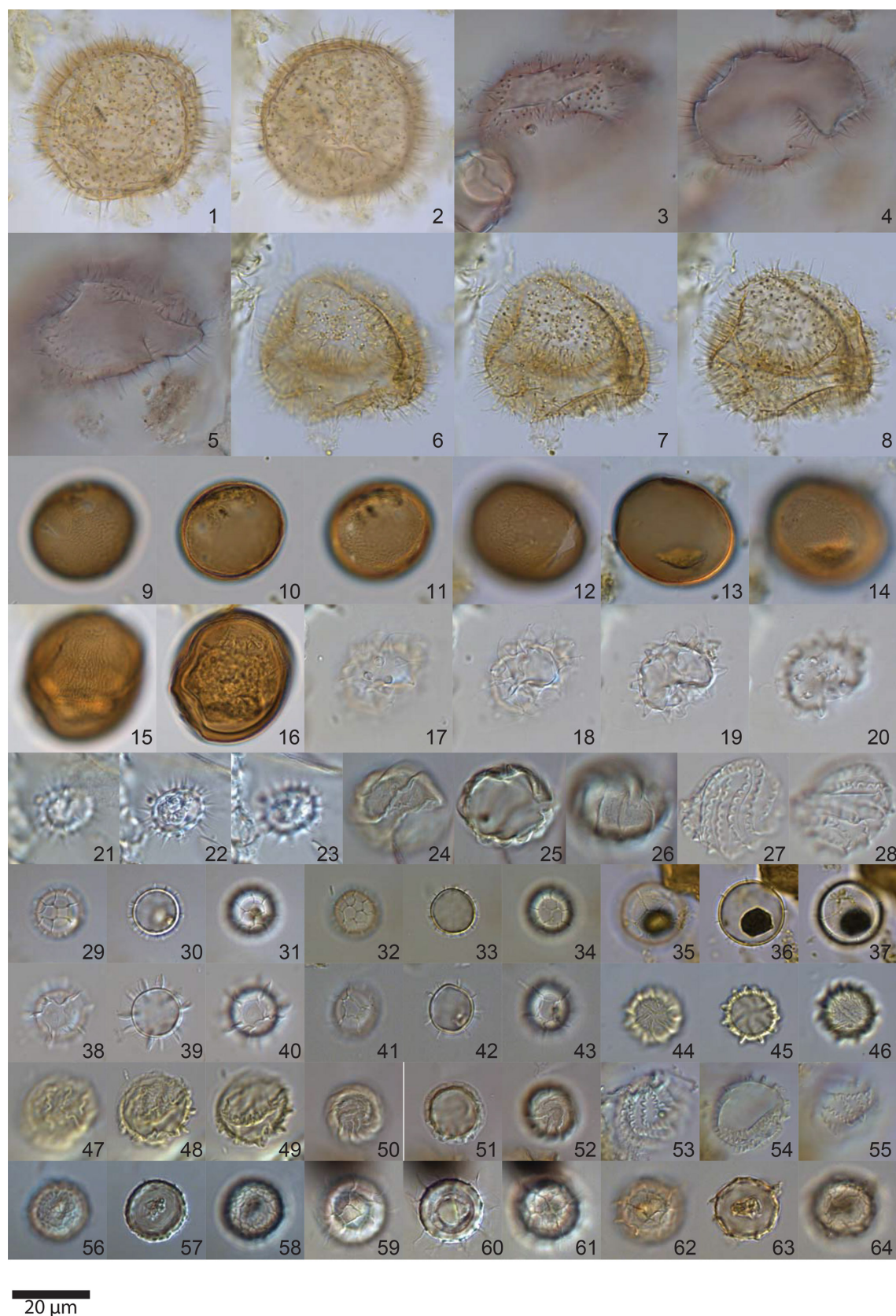
Plate 2.

20 µm

Plate 2. (1) *Echinidinium sleipnerensis*, U1357B-7H-3W 49–50 cm, slide 1, E.F.: V24.2, upper focus. (2) *Echinidinium sleipnerensis*, U1357B-7H-3W 49–50 cm, slide 1, E.F.: V24.2, lower focus. (3) *Echinidinium sleipnerensis*, U1357B-2H-3W 72–74 cm, slide 1, E.F.: R34.1, upper focus. (4) *Echinidinium sleipnerensis*, U1357B-2H-3W 72–74 cm, slide 1, E.F.: R34.1, mid focus. (5) *Echinidinium sleipnerensis*, U1357B-2H-3W 72–74 cm, slide 1, E.F.: R34.1, lower focus. (6) *Echinidinium sleipnerensis*, U1357B-13H-1W 108–110 cm, slide 1, E.F.: D28.3, upper focus on processes. (7) *Echinidinium sleipnerensis*, U1357B-13H-1W 108–110 cm, slide 1, E.F.: D28.3, upper focus on archaeopyle. (8) *Echinidinium sleipnerensis*, U1357B-13H-1W 108–110 cm, slide 1, E.F.: D28.3, lower focus. (9) *Gymnodinium microreticulatum*, U1357B-1H-1W 11–13 cm, slide 1, E.F.: G30.1, upper focus. (10) *Gymnodinium microreticulatum*, U1357B-1H-1W 11–13 cm, slide 1, E.F.: G30.1, mid focus. (11) *Gymnodinium microreticulatum*, U1357B-1H-1W 11–13 cm, slide 1, E.F.: G30.1, lower focus. (12) *Gymnodinium microreticulatum* with visible archaeopyle or rupture, U1357B-8H-3W 54–56 cm, slide 1, E.F.: G26.4, upper focus. (13) *Gymnodinium microreticulatum*, U1357B-8H-3W 54–56 cm, slide 1, E.F.: G26.4, mid focus. (14) *Gymnodinium microreticulatum*, U1357B-8H-3W 54–56 cm, slide 1, E.F.: G26.4, lower focus. (15) *Gymnodinium microreticulatum*, U1357B-17H-1W 18–20 cm, slide 1, E.F.: V24.1, upper focus. (16) *Gymnodinium microreticulatum*, U1357B-17H-1W 18–20 cm, slide 1, E.F.: V24.1, mid focus. (17) Macrobiotoid tardigrade egg, U1357B-3H-5W 28–30 cm, slide 1, E.F.: M22.4, upper focus on the tips of the conical projections. (18) Macrobiotoid tardigrade egg, U1357B-3H-5W 28–30 cm, slide 1, E.F.: M22.4, upper focus on the sides of the conical projections. (19) Macrobiotoid tardigrade egg, U1357B-3H-5W 28–30 cm, slide 1, E.F.: M22.4, mid focus. (20) Macrobiotoid tardigrade egg, U1357B-3H-5W 28–30 cm, slide 1, E.F.: M22.4, lower focus. (21) *Polarella glacialis*, U1357B-1H-2W 40–42 cm, slide 1, E.F.: J34.4, upper focus. (22) *Polarella glacialis*, U1357B-1H-2W 40–42 cm, slide 1, E.F.: J34.4, mid focus. (23) *Polarella glacialis*, U1357B-1H-2W 40–42 cm, slide 1, E.F.: J34.4, lower focus. (24) *Pterosperma parallelum*, large with straight alae, U1357B-3H-1W 97–99 cm, slide 1, E.F.: M36.1, upper focus. (25) *Pterosperma parallelum*, large with straight alae, U1357B-3H-1W 97–99 cm, slide 1, E.F.: M36.1, mid focus. (26) *Pterosperma parallelum*, large with straight alae, U1357B-3H-1W 97–99 cm, slide 1, E.F.: M36.1, lower focus. (27) *Pterosperma* cf. *parallelum*, U1357B-10H-7W 15–17 cm, slide 1, E.F.: G15.2, upper focus. (28) *Pterosperma* cf. *parallelum*, U1357B-10H-7W 15–17 cm, slide 1, E.F.: G15.2, lower focus. (29) *Pterosperma cristatum*, U1357B-17H-1W 117–119 cm, slide 1, E.F.: D21.4, upper focus. (30) *Pterosperma cristatum*, U1357B-17H-1W 117–119 cm, slide 1, E.F.: D21.4, mid focus. (31) *Pterosperma cristatum*, U1357B-17H-1W 117–119 cm, slide 1, E.F.: D21.4, lower focus. (32) *Pterosperma cristatum*, U1357B-17H-5W 97–99 cm, slide 1, E.F.: L24.3 upper focus. (33) *Pterosperma cristatum*, U1357B-17H-5W 97–99 cm, slide 1, E.F.: L24.3 mid focus. (34) *Pterosperma cristatum*, U1357B-17H-5W 97–99 cm, slide 1, E.F.: L24.3 lower focus. (35) *Pterosperma polygonum*, U1357B-8H-3W 54–56 cm, slide 1, E.F.: J15.2, upper focus. (36) *Pterosperma polygonum*, U1357B-8H-3W 54–56 cm, slide 1, E.F.: J15.2, mid focus. (37) *Pterosperma polygonum*, U1357B-8H-3W 54–56 cm, slide 1, E.F.: J15.2, lower focus. (38) *Pterosperma marginatum*, U1357B-10H-1W 58–60 cm, slide 1, E.F.: G15.4, upper focus. (39) *Pterosperma marginatum*, U1357B-10H-1W 58–60 cm, slide 1, E.F.: G15.4, mid focus. (40) *Pterosperma marginatum*, U1357B-10H-1W 58–60 cm, slide 1, E.F.: G15.4, lower focus. (41) *Pterosperma cristatum* or early developmental stage of *Pterosperma marginatum*, U1357B-17H-5W 97–99 cm, slide 1, E.F.: E25.3, upper focus. (42) *Pterosperma cristatum* or early developmental stage of *Pterosperma marginatum*, U1357B-17H-5W 97–99 cm, slide 1, E.F.: E25.3, mid focus. (43) *Pterosperma cristatum* or early developmental stage of *Pterosperma marginatum*, U1357B-17H-5W 97–99 cm, slide 1, E.F.: E25.3, lower focus. (44) *Pterosperma parallelum*, small with straight alae, U1357B-3W-1H 97–99 cm, slide 1, E.F.: H35.4, upper focus. (45) *Pterosperma parallelum*, small with straight alae, U1357B-3W-1H 97–99 cm, slide 1, E.F.: H35.4, upper focus. (46) *Pterosperma parallelum*, small with straight alae, U1357B-3W-1H 97–99 cm, slide 1, E.F.: H35.4, upper focus. (47) *Pterosperma parallelum*, large with undulating alae, U1357B-3H-1W 97–99 cm, slide 1, E.F.: J35.2, upper focus. (48) *Pterosperma parallelum*, large with undulating alae, U1357B-3H-1W 97–99 cm, slide 1, E.F.: J35.2, mid focus. (49) *Pterosperma parallelum*, large with undulating alae, U1357B-3H-1W 97–99 cm, slide 1, E.F.: J35.2, lower focus. (50) *Pterosperma parallelum*, small with relatively thick alae, U1357B-3H-1W 97–99 cm, slide 1, E.F.: J36.4, upper focus. (51) *Pterosperma parallelum*, small with relatively thick alae, U1357B-3H-1W 97–99 cm, slide 1, E.F.: J36.4, mid focus. (52) *Pterosperma parallelum*, small with relatively thick alae, U1357B-3H-1W 97–99 cm, slide 1, E.F.: J36.4, lower focus. (53) *Pterosperma* cf. *parallelum*, U1357B-8H-3W 54–56 cm, slide 1, E.F.: J24.1, upper focus. (54) *Pterosperma* cf. *parallelum*, U1357B-8H-3W 54–56 cm, slide 1, E.F.: J24.1, mid focus. (55) *Pterosperma* cf. *parallelum*, U1357B-8H-3W 54–56 cm, slide 1, E.F.: J24.1, lower focus. (56) *Pterosperma* aff. *reticulatum*, U1357B-16H-1W 63–65 cm, slide 1, E.F.: E23.3, upper focus. (57) *Pterosperma* aff. *reticulatum*, U1357B-16H-1W 63–65 cm, slide 1, E.F.: E23.3, mid focus. (58) *Pterosperma* aff. *reticulatum*, U1357B-16H-1W 63–65 cm, slide 1, E.F.: E23.3, lower focus. (59) *Cymatiosphaera* sp. 1, U1357B-3H-1W 97–99 cm, slide 1, E.F.: G29.4, upper focus. (60) *Cymatiosphaera* sp. 1, U1357B-3H-1W 97–99 cm, slide 1, E.F.: G29.4, mid focus. (61) *Cymatiosphaera* sp. 1, U1357B-3H-1W 97–99 cm, slide 1, E.F.: G29.4, lower focus. (62) *Cymatiosphaera* sp. 1 with degraded alae, U1357B-17H-1W 117–119 cm, slide 1, E.F.: L25.3, upper focus. (63) *Cymatiosphaera* sp. 1 with degraded alae, U1357B-17H-1W 117–119 cm, slide 1, E.F.: L25.3, mid focus. (64) *Cymatiosphaera* sp. 1 with degraded alae, U1357B-17H-1W 117–119 cm, slide 1, E.F.: L25.3, lower focus.

identified the round brown spiny cysts of Hole U1357B as *Echinidinium sleipnerensis* (Head et al., 2004; Radi et al., 2013).

Biological taxon: Cyst of unknown dinoflagellate. However, like all other modern-day round brown spiny cysts the motile cell is likely protoperidinioid and heterotrophic (Radi et al., 2013; Ellegaard et al., 2013)

Dimensions: Cysts are between 29 and 46 µm in diameter (average: 41 µm, $n = 8$).

Geographic distribution: No record of *E. sleipnerensis* has been published since its formal description by Head et al. (2004), except for a single mentioning as 0.003 % of the total dinoflagellate cyst abundance in a surface sediment survey of a Tunisian lagoon (Fertouna-Bellakhal et al., 2014). Because the archaeopyle of brown spiny cysts is generally difficult to distinguish, it is possible that earlier finds of *E. sleipnerensis* were misidentified (Radi et al., 2013). For example, *Islandinium minutum* cysts look very similar to *E. sleipnerensis*, but instead possess an apical archaeopyle and granulation (Head et al., 2001; Radi et al., 2013). In sediments around Antarctica, *Islandinium minutum* has been found in the fjords of Prydz Bay (Boere et al., 2009) and on both sides of the Antarctic Peninsula (as possibly *Algidasphaeridium minutum* in Harland et al., 1999; Harland and Pudsey, 1999). Although the archaeopyle in the specimens from Prydz Bay is well distinguishable, other reports of *Islandinium minutum* could be misidentified *E. sleipnerensis*.

The fossil record: The original description of *E. sleipnerensis* is based on samples from Upper Pliocene sediments of the northern North Sea (Head et al., 2004). Apart from that there is no other record of this species.

Ecological preferences and environmental interpretation: Because *E. sleipnerensis* has not been recorded in any surface sediment samples apart from a Tunisian lagoon (Fertouna-Bellakhal et al., 2014), its ecological preferences are unclear. However, brown spiny cysts are generally found in sediments underlying high-productivity surface waters (Zonneveld et al., 2013). In the Southern Ocean, the cysts identified as *I. minutum* have been associated with locations where sea-ice cover is longer than 3 months per year (Harland and Pudsey, 1999).

Genus *Nucicla* Hartman et al. (2018)

Nucicla umbiliphora Hartman et al. (2018)
(Plate 1, figs. 14–15)

Morphology and identification: This species was first depicted as Dinocyst sp. A in Wrenn et al. (1998) and has recently been formally described (Hartman et al., 2018).

In the U1357B record fragments of this species have been more often found than whole cysts. This could be due to the large 3I archaeopyle that favours rupture. Because of its unique 3I archaeopyle, relatively large hypocyst, and surface ornamentation (Hartman et al., 2018) the fragmentary remains were also easily identified.

Biological taxon: Cyst of unknown dinoflagellate.

Dimensions: Its size measured along the cingulum is 60 ± 8 µm ($n = 3$).

Geographic distribution: Prior to its formal description *N. umbiliphora* was found in surface samples from the Prydz Bay area (Storkey, 2006; Boere et al., 2009). In addition to that Hartman et al. (2018) reported its occurrence in surface sediments from the Ross Sea and the East Antarctic coastal margin, including Hole U1357B.

The fossil record: *N. umbiliphora* has been reported from multiple Quaternary records in the Ross Sea (Wrenn et al., 1998; Warny et al., 2006; Hartman et al., 2018). The oldest sample with a known age containing *N. umbiliphora* was obtained from Marine Isotope Stage 5e in the Ross Sea (Hartman et al., 2018).

Ecological preferences and environmental interpretation: This species appears to be endemic to the shallow marginal ice zone (MIZ): the (East) Antarctic shelf and the Ross Sea (Hartman et al., 2018).

Genus *Selenopemphix* (Benedek 1972) Head 1993

Selenopemphix antarctica Marret et De Vernal 1997 (Plate 1, fig. 13)

Morphology and identification: This is a brown, scabrate cyst that is polarly compressed, which is why under the light microscope they are typically in polar view (Marret and De Vernal, 1997). In polar view they possess a circular outline. Furthermore, it possesses one apical and two antapical horns and an intercalary archaeopyle, although this is not always visible (Marret and De Vernal, 1997).

Biological taxon: Cyst of unknown dinoflagellate (Zonneveld et al., 2013).

Dimensions: The diameter of the cyst in (ant)apical view ranges between 52 and 68 µm (average: 60 µm, $n = 8$).

Geographic distribution: *Selenopemphix antarctica* is restricted to and common in the sediments underlying the cool marine waters south of the Subantarctic Front (SAF) and dominant south of the Antarctic Polar Front (APF) (Marret and De Vernal, 1997; Harland and Pudsey, 1999;

Esper and Zonneveld, 2002, 2007; Crouch et al., 2010).

The fossil record: In Quaternary records south of the modern-day SAF, this species is generally one of the most dominant during both glacial and interglacial stages (Harland et al., 1999; Marret et al., 2001; Howe et al., 2002; Esper and Zonneveld, 2007). Dinoflagellate cysts that are morphologically very similar to *S. antarctica* have been recorded as far back as the Oligocene (Houben et al., 2013; Bijl et al., 2018).

Ecological preferences and environmental interpretation: High abundances of *S. antarctica* are generally associated with sea surface summer temperatures (SSSTs) below 5 °C, relatively low sea surface summer salinity (SSSS) (34–35 psu), and high chlorophyll *a* waters, and it is not found in oligotrophic regions (Marret and Zonneveld, 2003; Prebble et al., 2013). It is the dominant dinoflagellate cyst species in Antarctic waters that are influenced by seasonal sea-ice cover and has therefore been used as an indicator for the presence of seasonal sea ice in the past (Marret and De Vernal, 1997; Harland et al., 1999; Marret et al., 2001; Howe et al., 2002; Houben et al., 2013). As this is probably a heterotrophic species, its high abundances in the sediments underlying these sea-ice-dominated waters can be explained by the high primary (mainly diatom) productivity in the Antarctic summer when upwelling at the Antarctic Divergence enhances nutrient availability (Harland and Pudsey, 1999; Harland et al., 1999).

Selenopemphix sp. 1 sensu Esper & Zonneveld (2007) (Plate 1, figs. 18–21)

Morphology and identification: Although similar to *Selenopemphix antarctica*, *Selenopemphix* sp. 1 sensu Esper & Zonneveld (2007) is much larger and has a deep sulcus and a pronounced conical apical complex (Esper and Zonneveld, 2007). Nevertheless, this species is sometimes combined with *S. antarctica* as they have very similar morphology (Esper and Zonneveld, 2007; Prebble et al., 2013). In Harland et al. (1998) specimens of *Selenopemphix* sp. 1 are depicted as *S. antarctica*.

Biological taxon: Cyst of unknown dinoflagellate.

Dimensions: The diameter of the cyst in (ant)apical view ranges between 82 and 98 µm (average: 88 µm, $n = 4$).

Geographic distribution: The full geographic distribution of *Selenopemphix* sp. 1 is unknown because apart from its original description from the South Atlantic Ocean by Esper and Zonneveld (2007) both older (Harland et al., 1998) and newer studies (Prebble et al., 2013) did not differentiate between *Selenopemphix* sp. 1 and *S. antarctica*. Nevertheless, it is expected that the geographic distribution is similarly restricted to the Southern Ocean south of the Subantarctic Front, as is *Selenopemphix antarctica*.

The fossil record: From Quaternary sedimentary records of the South Atlantic it is clear that *Selenopemphix* sp. 1 is more abundant during interglacial stages south of the Antarctic Polar Front (APF), while it is more abundant during glacial stages north of the APF (Esper and Zonneveld, 2007). No other records of *Selenopemphix* sp. 1 exist.

Ecological preferences and environmental interpretation: It has been suggested that *Selenopemphix* sp. 1 is a larger species endmember of *S. antarctica* that only forms under ideal environmental conditions, although it is unclear what ideal environmental conditions (Esper and Zonneveld, 2007). Assuming that a larger cyst is also produced by a larger motile dinoflagellate, such dinoflagellates will have a lower surface-to-volume ratio. Dinoflagellates with a lower surface-to-volume ratio are known to sink faster and swim slower (Kamykowski et al., 1992). It is therefore possible that specific oceanographic conditions or an increased availability of prey, such that slower swimming does not limit the chance to capture prey, allows for larger dinoflagellate sizes. The larger cell size of *Selenopemphix* sp. 1 could also be related to temperature. For a Holocene core obtained from Disko Bay, Greenland, it has been shown that the dinoflagellate cysts obtained from the colder time interval were significantly larger than the dinoflagellate cysts obtained from the warmer time interval (Mousing et al., 2017). Alternatively, being larger could be a defense against predators that can only consume a restricted prey size, such as tintinnids (Dolan and Pierce, 2013).

5.2 Tintinnid loricae and lorica sacs

Phylum CILIOPHORA Doflein 1901

Class SPIROTRICHEA Bütschli 1889

Subclass CHOREOTRICHIA Small & Lynn 1985

Order TINTINNIDA Kofoid & Campbell 1929

Family DICTYOCYSTIDAE Haeckel 1873

Palynomorph: Dictyocystid lorica sac (Plate 1, figs. 16–17)

Morphology and identification: This palynomorph is one of the most abundant in Hole U1357B. They are bulb-shaped, transparent, hyaline vesicles. On the microscope slide they are pressed flat, but folds in their wall suggest they originally had a more 3-D form. Their size and shape resemble that of tintinnid loricae such as *Codonellopsis pusilla*, but without the scars of now-dissolved diatom frustules. Unlike the loricae of tintinnids, the oral opening of the vesicle looks torn or ragged and very thin-walled instead of a continuous rim. We believe that these vesicles are the lorica sacs of Dictyocystid tintinnids. The lorica sac is a non-ornamented membrane that lines the lorica wall

(Agatha, 2010; Agatha and Strüder-Kypke, 2013). At the oral opening it merges into a foldable closing apparatus that closes off the lorica opening in disturbed or contracted tintinnids (Agatha, 2010; Agatha and Strüder-Kypke, 2013). In contrast to the lorica sac the foldable closing apparatus is ornamented with furrows and/or ribs (Agatha, 2010). The membrane of the closing apparatus is just 0.1–0.2 μm thick (Agatha, 2010), and it is therefore not surprising that the closing apparatuses of the palynological remains of the lorica sacs of Hole U1357B are damaged either due to the sedimentation process or palynological processing.

Biological taxon: Recent phylogenetic analyses based on small subunit rRNA (Strüder-Kypke and Lynn, 2008) and the recognition of a shared morphological character, i.e. the lorica sac (Agatha, 2010), have resulted in the combination of the tintinnid families Codonellidae, Codonellopsidae, and Dictyocystidae into the oldest of these families, the Dictyocystidae (Agatha and Strüder-Kypke, 2012). Genera for which a lorica sac was observed are *Codonella*, *Codonellopsis*, *Dictyocysta*, and *Codonaria*. Of the genera that possess a lorica sac only *Codonellopsis* is an abundant genus endemic to the Southern Ocean (Dolan et al., 2012). Known Southern Ocean endemic species are *Codonellopsis gaussi*, *Codonellopsis glacialis*, and *Codonellopsis balechi* (Alder and Boltovskoy, 1991; Clarke and Leakey, 1996; Wasik et al., 1996; Wasik, 1998; Fonda Umani et al., 2005; Dolan et al., 2012, 2013). However, no lorica sac was observed in *C. gaussi* and it might therefore not belong to the Dictyocystidae (Kim et al., 2013). For the other two species the presence of a lorica sac has not been studied in detail, but if the lorica sac does indeed belong to one of these species, it more closely resembles the more bowl-shaped species *C. balechi*. No loricae of *C. balechi* have been found, but the preservation potential of the loricae of *C. balechi* might be lower than the lorica sacs. Alternatively, the lorica sacs could belong to *Codonellopsis*, *Dictyocysta*, or *Codonella* that have a widespread distribution but are also frequently encountered in the Southern Ocean (for a full overview see Dolan et al., 2012). Of these widespread species, *Codonella amphorella*, *Codonella aspera*, *Dictyocysta elegans*, and *Dictyocysta lepida* are known to possess a foldable closing apparatus and lorica sac (Agatha, 2010). Furthermore, *Codonellopsis pusilla* is particularly abundant in the PFZ (Dolan et al., 2012; Malinverno et al., 2016), and the loricae of *C. pusilla* have been found in some of the samples in Hole U1357B. However, for this species the closing apparatus and lorica sac have not been studied in detail. Also in this case it could be that the loricae of *C. pusilla* have less preservation potential than the lorica sacs.

Dimensions: The lorica sacs are 60 ± 11 μm in length (*n* = 4).

Geographic distribution: Lorica sacs have not been

reported in palynological studies before. However, identical forms have been reported from Prydz Bay as *Sphaeromorph* by Storkey (2006; pl. 2, fig. 7).

The fossil record: Tintinnid lorica sacs have not been reported from sedimentary records before.

Ecological preferences and environmental interpretation: Considering that most genera and species occurring in the Southern Ocean that possess a lorica sac have a more widespread distribution, we interpret higher abundances of lorica sacs in the sediments as reflecting an influence of more northerly sourced waters, in particular if the sacs belong to *C. pusilla*, which is known to be very abundant in the Polar Front Zone (Dolan et al., 2012; Malinverno et al., 2016).

Genus *Codonellopsis* Jörgensen 1924

Lorica of *Codonellopsis pusilla* (Cleve) Jörgensen 1924 (Plate 3, figs. 1–2)

Morphology and identification: This species has a globular posterior bowl on its lorica and an anterior hyaline part of the lorica that is characterized by a row of circular fenestrae. On the hyaline remains of the lorica the scars of diatom frustules can be recognized on the posterior end. The genus *Codonellopsis* generally builds a hard bowl at the posterior end of its lorica by agglutinating mineral particles, diatoms, and radiolaria (Petz et al., 1995; Wasik, 1998; Agatha et al., 2013). However, in *Codonellopsis pusilla* this hard bowl is typically built from coccoliths (Malinverno et al., 2016). On the other hand, photographs of *C. pusilla* in Dolan et al. (2012) and Dolan et al. (2013) show that its lorica can also contain diatoms.

Biological taxon: *Codonellopsis pusilla*.

Dimensions: The length of the lorica is 46 ± 2 μm (*n* = 4).

Geographic distribution: This is a widespread species originally described from the North Atlantic Ocean (Cleve, 1899). In the Southern Ocean, *Codonellopsis pusilla* can be found predominantly in the Polar Front Zone (PFZ) (Malinverno et al., 2016) and can be as common as the Antarctic endemic genera *Cymatocylis* and *Laackmanniella* (Dolan et al., 2012).

The fossil record: No fossil record of *C. pusilla* exists so far, as even published records of relatively young sedimentary core material containing tintinnid remains do not distinguish between individual species (see e.g. Roncaglia, 2004b; Cromer et al., 2005).

Ecological preferences and environmental interpretation: Because of its high abundances in the PFZ, increased

20 μm

Plate 3.

Plate 3. (1) *Codonellopsis pusilla*, U1357B-9H-4W 79–81 cm, slide 1, E.F.: G26.4, upper focus. **(2)** *Codonellopsis pusilla*, U1357B-9H-4W 79–81 cm, slide 1, E.F.: G26.4, lower focus. **(3)** *Coxliella* form lorica, U1357B-2H-2W 6–8 cm, slide 1, E.F.: J30.1, upper focus. **(4)** *Coxliella* form lorica, U1357B-2H-2W 6–8 cm, slide 1, E.F.: J30.1, lower focus. **(5)** Trochospiral foraminifer lining, U1357B-17H-5W 97–99 cm, slide 1, E.F.: E26.3. **(6)** Triserial foraminifer lining, U1357B-17H-5W 97–99 cm, slide 1, E.F.: H21.2. **(7)** *Laackmanniella naviculaefera*, U1357B-1H-2W 40–42 cm, slide 1, E.F.: K24.2, upper focus. **(8)** *Laackmanniella naviculaefera*, U1357B-1H-2W 40–42 cm, slide 1, E.F.: K24.2, mid focus. **(9)** *Laackmanniella naviculaefera*, U1357B-1H-2W 40–42 cm, slide 1, E.F.: K24.2, lower focus. **(10)** *Laackmanniella naviculaefera*, U1357B-10H-1W 58–60 cm, slide 1, E.F.: K24.2, LIB image. **(11)** *Cymatocylis convallaria* sensu stricto, U1357B-7H-5W 4–6 cm, slide 1, E.F.: W26.2, LIB image. **(12)** P-type maxillary apparatus of *Ophryotrocha orensanzi*, U1357B-4H-3W 61–63 cm, slide 1, E.F.: G21.4, LIB image. **(13)** Lorica (possibly) type 1, U1357B-2H-4W 111–113 cm, slide 1, E.F.: L17.3.3, upper focus. **(14)** Lorica (possibly) type 1, U1357B-2H-4W 111–113 cm, slide 1, E.F.: L17.3.3, mid focus. **(15)** Anterior denticle of maxillary apparatus of *Ophryotrocha*, U1357B-5H-7W 5–7 cm, slide 1, E.F.: H35.3. **(16)** Anterior denticle of maxillary apparatus of *Ophryotrocha*, U1357B-16H-4W 64–65 cm, slide 1, E.F.: L20.3. **(17)** Copepod mandibular gnathobase 2, U1357B-3H-3W 8–10 cm, slide 1, E.F.: Q29.4. **(18)** Pollen of *Nothofagus*, U1357B-17H-1W 18–20 cm, slide 1, E.F.: F22.1, LIB image. **(19)** Pollen of Podocarpaceae, U1357B-7H-5W 4–6 cm, slide 1, E.F.: K11.2, LIB image. **(20)** Forceps of a P-type maxillary apparatus of *Ophryotrocha orensanzi*, U1357B-9H-1W 112–114 cm, slide 1, E.F.: G22.4, LIB image. **(21)** Copepod mandibular gnathobase 1, U1357B-3H-3W 8–10 cm, slide 1, E.F.: V24.1. **(22)** Forceps of K-type maxillary apparatus of *Ophryotrocha*, U1357B-16H-1W 63–65 cm, slide 1, E.F.: P26.1, LIB image. **(23)** Forceps of K-type maxillary apparatus of *Ophryotrocha*, U1357B-16H-4W 64–65 cm, slide 1, E.F.: G21.4, LIB image. **(24)** Copepod spermatophore (Type AB-33), U1357B-17H-5W 97–99 cm, slide 1, E.F.: G30.2, upper focus on the distal end of the tube-like neck. **(25)** Copepod spermatophore (Type AB-33), U1357B-17H-5W 97–99 cm, slide 1, E.F.: G30.2, upper focus on the proximal part of the tube-like neck. **(26)** Copepod spermatophore (Type AB-33), U1357B-17H-5W 97–99 cm, slide 1, E.F.: G30.2, mid focus. **(27)** Copepod spermatophore (Type AB-33), U1357B-17H-5W 97–99 cm, slide 1, E.F.: G30.2, lower focus. **(28)** Copepod spermatophore (Type AB-33), U1357B-17H-1W 117–119 cm, slide 1, E.F.: D27.2. **(29)** Copepod thoracopod, U1357B-16H-4W 64–65 cm, slide 1, E.F.: H21.4, LIB image. **(30)** *Leiosphaeridia* sp. 2, U1357B-9H-1W 112–114 cm, slide 1, E.F.: K19.4, upper focus. **(31)** *Leiosphaeridia* sp. 2, U1357B-9H-1W 112–114 cm, slide 1, E.F.: K19.4, mid focus. **(32)** *Leiosphaeridia* sp. 2 with an apparent second membrane, U1357B-16H-1W 63–65 cm, slide 1, E.F.: E21.3, upper focus. **(33)** *Leiosphaeridia* sp. 2 with an apparent second membrane, U1357B-16H-1W 63–65 cm, slide 1, E.F.: E21.3, mid focus. **(34)** *Leiosphaeridia* sp. 2 with an apparent second membrane, U1357B-16H-1W 63–65 cm, slide 1, E.F.: E21.3, lower focus.

abundances of *C. pusilla* in samples of Hole U1357B could suggest an increased influence of northerly sourced waters.

Lorica of *Codonellopsis glacialis* Laackmann 1907 (Plate 1, figs. 27–28)

Morphology and identification: *Codonellopsis glacialis* has a straight short lorica. The palynological remains show the scars of diatoms that were attached to the posterior end of the lorica. Furthermore, it has a posterior acuminate tip. Fragments that consist of the hyaline anterior and miss part of the agglutinated bowl could have been mistakenly identified as *Laackmanniella naviculaefera*.

Biological taxon: Multiple authors have suggested that *Codonellopsis glacialis* is synonymous to *Codonellopsis gaussi* Laackmann 1907 based on the presence of transitional forms and the position of the kineties (ciliary rows), but genetic studies have yet to confirm this (Balech, 1958b, 1973; Alder, 1999; Kim et al., 2013). In comparison to *C. glacialis*, the lorica of *C. gaussi* sensu stricto is longer (140–180 µm; see junior synonym *Leprotintinnus gaussi* in Laackmann, 1910) and is characterized by a much expanded posterior bowl and a posterior acuminate tip. However, only whole specimens of *C. glacialis* were found in Hole U1357B with no (fragments of) expanded bowls of *C. gaussi*.

Dimensions: Specimens in Hole U1357B are 60 ± 6 µm long ($n = 3$), which is relatively short compared to the range of 60–125 µm in the original description (see junior synonym *Leprotintinnus glacialis* in Laackmann, 1910).

Geographic distribution: Both *C. glacialis* and *C. gaussi* are endemic to the Southern Ocean (Dolan et al., 2012; Dolan and Pierce, 2013).

The fossil record: No fossil record of *C. glacialis* exists, as even published records of relatively young sedimentary core material containing tintinnid remains do not distinguish between individual species (see e.g. Roncaglia, 2004b; Cromer et al., 2005).

Ecological preferences and environmental interpretation: *C. glacialis* and *C. gaussi* have both been associated with the sea-ice edge (Garrison and Buck, 1989). Petz et al. (1995) have also found *C. glacialis* within grease ice (sea ice of < 1 cm thickness), comprising 50 % of the total ciliate community. A preferred seawater temperature range was given by Petz et al. (1995) of −1.8 to 0.0 °C.

Incertae sedis *Laackmanniella* Kofoid & Campbell 1929

Laackmanniella naviculaefera (Laackmann 1907) Kofoid & Campbell 1929 (Plate 3, figs. 7–10)

Morphology and identification: Like *Codonellopsis*, *Laackmanniella* agglutinates mineral particles and diatoms to its lorica (Petz et al., 1995; Wasik et al., 1996; Agatha et al., 2013), the scars of which are visible on the hyaline palynological remains. This species is often considered also including *Laackmanniella prolongata*, which is suggested to be a morphological variety and therefore synonymous (Petz, 2005; Dolan et al., 2012; Kim et al., 2013, and references therein). *L. naviculaefera* differs from *L. prolongata* by having a shorter lorica (138 versus 308 μm) (Laackmann, 1907) and a slightly bulging bowl. In Hole U1357B often fragments consisting of both a long hyaline spiraling anterior and part of an agglutinated posterior bowl are found. Although the anterior part of the lorica of *Codonellopsis gaussi* is similar to that of *L. naviculaefera*, it is more likely that the remains in Hole U1357B belong to *L. naviculaefera* because the typical lorica of *C. gaussi* with large posterior bulge was never found.

Biological taxon: After the formation of the families Codonellidae, Codonellopsidae, and Dictyocystidae into the family Dictyocystidae, the genus *Laackmanniella* (formerly part of Codonellopsidae) was left as affiliated insertae sedis because it was unknown whether *Laackmanniella* possessed a lorica sac and the associated folded closing apparatus (Agatha and Strüder-Kypke, 2012). In a later phylogenetic study based on small subunit rDNA by Kim et al. (2013) it is mentioned that no lorica sac was observed in either *Codonellopsis gaussi* or *Laackmanniella prolongata* (*Laackmanniella naviculaefera*) and that they are very closely related. The validity of the genus *Laackmanniella* has therefore been questioned and it has been suggested that *C. gaussi* and *L. prolongata* should be united into one genus outside of Dictyocystidae (Kim et al., 2013).

Dimensions: The specimens encountered in Hole U1357B are often not intact, but the most complete specimens are 122 ± 3 μm long ($n = 3$), which is consistent with the description of *L. naviculaefera* by Laackmann (1907) and the specimens depicted by Wasik (1998), Dolan et al. (2012), and Dolan et al. (2013).

Geographic distribution: *Laackmanniella* (and its possible senior synonym *C. gaussi*) are endemic to the Antarctic and Subantarctic waters and most dominant south of the Polar Front (Dolan et al., 2012). Notably, *L. naviculaefera* was already described from the waters off Adélie Land in the 1950s (Balech, 1958a)

The fossil record: No fossil record of *L. naviculaefera*

exists, as even published records of relatively young sedimentary core material containing tintinnid remains do not distinguish between individual species (see e.g. Roncaglia, 2004b; Cromer et al., 2005).

Ecological preferences and environmental interpretation: A seawater temperature range was given for *L. naviculaefera* by Petz et al. (1995) of -0.8 to -0.5 °C and it is particularly dominant in inshore high-productivity environments associated with the retreat of the sea-ice edge and upwelling of modified Circumpolar Deep Water (Garrison and Buck, 1989; Garzio and Steinberg, 2013). It has been shown that *L. naviculaefera* actively selects the diatoms it incorporates into its lorica (Wasik et al., 1996), and it has been suggested that it adheres to the diatom frustules after ingesting their protoplasts (Gowing and Garrison, 1992). But living diatom frustules have also been found on loricae of *L. naviculaefera*, although it is uncertain whether these diatoms have been actively selected by the tintinnid or whether the diatoms have used the lorica as an ideal substrate for attachment (Armbrecht et al., 2017). A preference for a high-productivity environment and a diatom-based diet are consistent with the high sedimentation rates of diatom ooze in Hole U1357B.

Family PTYCHOCYLIDIDAE Kofoid & Campbell 1929

Genus *Cymatocylis* Laackmann 1910

Cymatocylis convallaria Laackmann 1910 (Plate 3, fig. 11; Plate 4, figs. 1–2, 5; Plate 6, figs. 1–4)

Morphology and identification: These are relatively large transparent loricae with an oral opening that is ornamented with acuminating tips along its rim. The surface of the anterior part of the lorica has a honeycomb structure. The posterior ends in a tip, which is either blunt or long and acuminate. Many samples of Hole U1357B contain high amounts of these hyaline acuminating horns and only a few specimens are found whole. These all belong to the various formae of tintinnid *Cymatocylis convallaria*. Because the larger formae of *C. convallaria* in Hole U1357B are often broken, the individual formae of *C. convallaria* can therefore not be quantified. However, formae with a long, narrow antapical horn (i.e. forma *cylindrica* and forma *calyciformis*) can be distinguished from (the posterior ends of) the formae without (i.e. forma *affinis* and forma *drygalskii*). Specimens of *C. convallaria* sensu stricto and forma *affinis* are generally preserved whole.

Biological taxon: Originally, multiple species of *Cymatocylis* were differentiated based on the length of the apical horn of the lorica versus the total lorica length (Laackmann, 1910). It was concluded later that the species
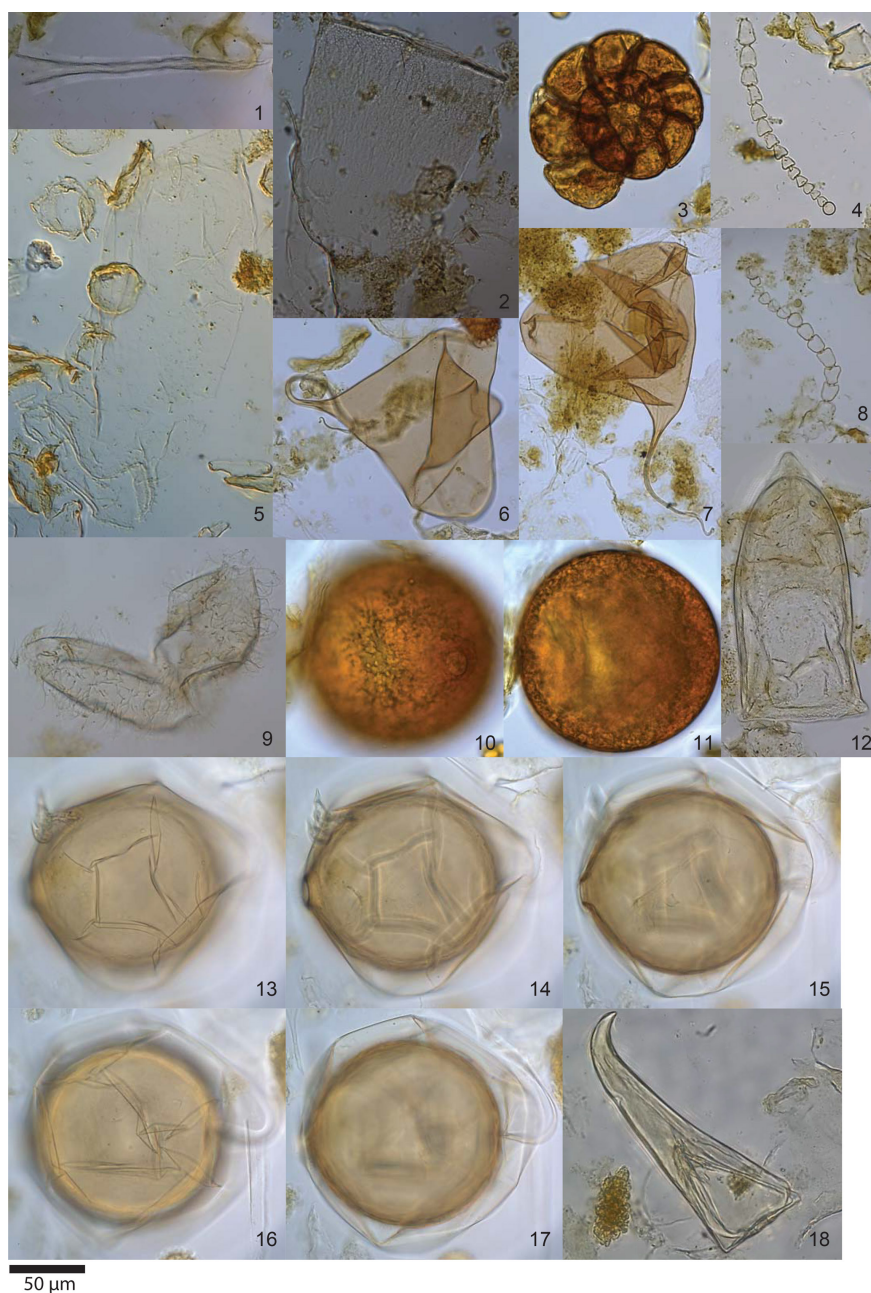
50 µm

Plate 4. (1) *Cymatocylis convallaria* forma *calyciformis* or *cylindrica* apical lorica horn, U1357B-3H-1W 97–99 cm, slide 1, E.F.: K36.4, LIB image. **(2)** *Cymatocylis convallaria* forma *calyciformis*, detail of the anterior part of Plate 6, fig. 1, U1357B-8H-3W 54–56 cm, slide 1, E.F.: K20.1, upper focus. **(3)** Trochospiral foraminiferal lining, U1357B-6H-4W 86–88 cm, slide 1, E.F.: V27.2. **(4)** Uniserial foraminiferal lining, U1357B-2H-2W 6–8 cm, slide 1, E.F.: K30.1, LIB image. **(5)** *Cymatocylis convallaria* forma *cylindrica*, detail of the anterior part of Plate 6, fig. 3, U1357B-6H-6W 123–125 cm, slide 1, E.F.: K24.1, LIB image. **(6)** Copepod (possibly) spermatophore (Type AB-22), U1357B-7H-5W 4–6 cm, slide 1, E.F.: J21.3. **(7)** Copepod (possibly) spermatophore (Type AB-22), U1357B-14H-5W 48–49 cm, slide 1, E.F.: H19.2. **(8)** Uniserial foraminifer lining, U1357B-7H-5W 4–6 cm, slide 1, E.F.: D16.3. **(9)** Copepod egg that has split open, U1357B-2H-6W 6–8 cm, slide 1, E.F.: K34.1, upper focus. **(10)** *Palaeostomocystis sphaerica* with content, pylome visible on the right, U1357B-5H-7W 5–7 cm, slide 1, E.F.: Q21.1, upper focus. **(11)** *Palaeostomocystis sphaerica* with content, U1357B-5H-7W 5–7 cm, slide 1, E.F.: Q21.1, mid focus. **(12)** Type AB-27c, bullet-shaped, U1357B-2H-6W 6–8 cm, slide 1, E.F.: O32.4, LIB image. **(13)** *Palaeostomocystis sphaerica* with outer envelope with tail, U1357B-1H-2W 40–42 cm, slide 1, E.F.: U23.3, upper focus on envelope. **(14)** *Palaeostomocystis sphaerica* with outer envelope with tail, U1357B-1H-2W 40–42 cm, slide 1, E.F.: U23.3, upper focus on cyst. **(15)** *Palaeostomocystis sphaerica* with outer envelope with tail, U1357B-1H-2W 40–42 cm, slide 1, E.F.: U23.3, mid focus. **(16)** *Palaeostomocystis sphaerica* with outer envelope with tail, U1357B-1H-2W 40–42 cm, slide 1, E.F.: U23.3, lower focus on envelope. **(17)** *Palaeostomocystis sphaerica* with outer envelope with tail, U1357B-1H-2W 40–42 cm, slide 1, E.F.: U23.3, lower focus on tail. **(18)** Type AB-27f, falcate, U1357B-1H-2W 40–42 cm, slide 1, E.F.: L27.1, LIB image.
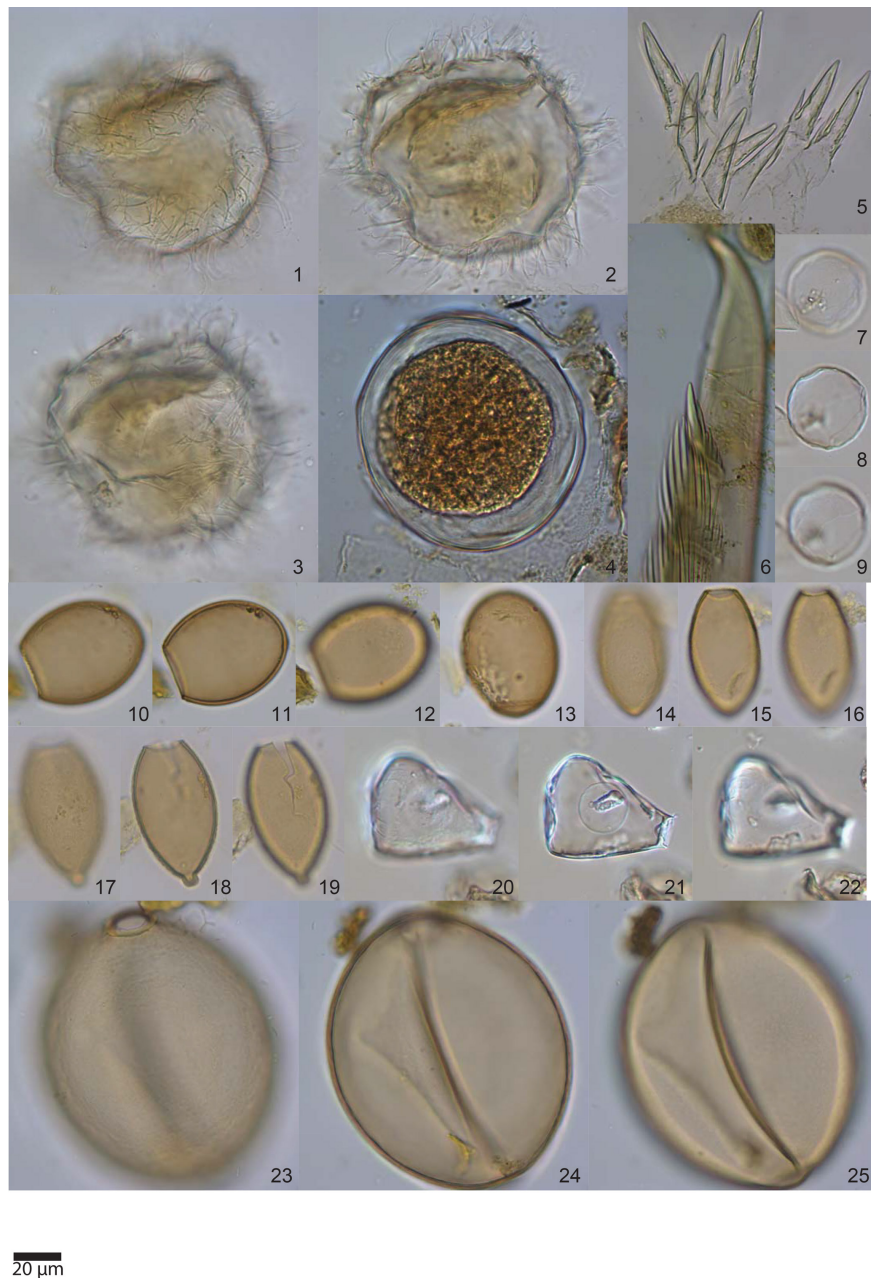
20 µm

Plate 5. (1) Copepod egg, U1357B-2H-6W 6–8 cm, slide 1, E.F.: F28.2, upper focus. **(2)** Copepod egg, U1357B-2H-6W 6–8 cm, slide 1, E.F.: F28.2, mid focus. **(3)** Copepod egg, U1357B-2H-6W 6–8 cm, slide 1, E.F.: F28.2, lower focus. **(4)** Copepod endites, U1357B-2H-6W 6–8 cm, slide 1, E.F.: J36.3, LIB image. **(5)** *Leiosphaeridia* sp. 3, U1357B-8H-3W 54–56 cm, slide 1, E.F.: H19.2, mid focus. **(6)** Detail of the right copepod seta of Plate 4, fig. 13, U1357B-8H-3W 54–56 cm, slide 1, E.F.: T30.1. **(7)** *Leiosphaeridia* sp. 2, U1357B-18H-2W 114–116 cm, slide 1, E.F.: G26.3, upper focus. **(8)** *Leiosphaeridia* sp. 2, U1357B-18H-2W 114–116 cm, slide 1, E.F.: G26.3, upper focus. **(9)** *Leiosphaeridia* sp. 2, an opening with sharp edges is visible, U1357B-18H-2W 114–116 cm, slide 1, E.F.: G26.3, upper focus. **(10)** *Palaeostomocystis* cf. *fritilla*, U1357B-6H-6W 123–125 cm, slide 1, E.F.: K24.1, upper focus. **(11)** *Palaeostomocystis* cf. *fritilla*, U1357B-6H-6W 123–125 cm, slide 1, E.F.: K24.1, mid focus. **(12)** *Palaeostomocystis* cf. *fritilla*, U1357B-6H-6W 123–125 cm, slide 1, E.F.: K24.1, lower focus. **(13)** *Palaeostomocystis* cf. *fritilla* with operculum attached, U1357B-6H-4W 86–88 cm, slide 1, E.F.: K33.3, upper focus. **(14)** *Palaeostomocystis* cf. *reticulata*, U1357B-6H-6W 123–125 cm, slide 1, E.F.: L14.4, upper focus. **(15)** *Palaeostomocystis* cf. *reticulata*, U1357B-6H-6W 123–125 cm, slide 1, E.F.: L14.4, mid focus. **(16)** *Palaeostomocystis* cf. *reticulata*, U1357B-6H-6W 123–125 cm, slide 1, E.F.: L14.4, lower focus. **(17)** *Palaeostomocystis* sp. C, U1357B-3H-3W 8–10 cm, slide 1, E.F.: U28.3, upper focus. **(18)** *Palaeostomocystis* sp. C, U1357B-3H-3W 8–10 cm, slide 1, E.F.: U28.3, mid focus. **(19)** *Palaeostomocystis* sp. C, U1357B-3H-3W 8–10 cm, slide 1, E.F.: U28.3, lower focus. **(20)** *Palaeostomocystis sphaerica*, U1357B-1H-1W 11–13 cm, slide 1, E.F.: L30.3, upper focus. **(21)** *Palaeostomocystis sphaerica*, U1357B-1H-1W 11–13 cm, slide 1, E.F.: L30.3, mid focus. **(22)** *Palaeostomocystis sphaerica*, U1357B-1H-1W 11–13 cm, slide 1, E.F.: L30.3, lower focus.

C. convallaria without an apical horn and *Cymatocylis affinis* Laackmann 1910 and its four formae with an apical horn were in fact the same (Boltovskoy et al., 1990). Therefore the species name *Cymatocylis convallaria–affinis* was proposed (Boltovskoy et al., 1990). A recent genetic study has confirmed that species with much larger lorica and apical horns, *Convallaria drygalski* (Laackmann 1907) Laackmann 1910 and *Cymatocylis calyciformis* (Laackmann 1907) Laackmann 1910 (including their formae described by Laackmann (1910), e.g. forma *subrotundata* and *cylindrica*), are also in fact *C. convallaria–affinis* (Kim et al., 2013). Consequently, these former species and formae have been called *C. affinis–convallaria* forma *calyciformis*, forma *drygalskii*, forma *subrotunda*, and forma *cylindrica* by Dolan et al. (2013). We refer to *C. affinis–convallaria* and all its synonyms as *Cymatocylis convallaria* following Petz et al. (1995) and Petz (2005).

Dimensions: The smaller *C. convallaria* sensu stricto and *C. convallaria* formae *affinis* are $112 \pm 16 \, \mu m$ ($n = 3$) and the larger formae that were found intact show a range in length between 290 and 415 μm ($n = 4$).

Geographic distribution: *C. convallaria* is endemic to the Southern Ocean, but in contrast to *Laackmanniella*, *C. convallaria* is also regularly found in areas outside the winter sea-ice edge (Dolan et al., 2012). Still, *C. convallaria* was already reported off the coast of Adélie Land in the 1950s as *C. affinis* (Balech, 1958a).

The fossil record: No fossil record of *C. convallaria* exists, as even published records of relatively young sedimentary core material containing tintinnid remains do not distinguish between individual species (see e.g. Roncaglia, 2004b; Cromer et al., 2005).

Ecological preferences and environmental interpretation: A temperature range was given by Petz et al. (1995) of -1.2 to $-0.5 \, °C$. With respect to the other Antarctic endemic species the lorica of *Cymatocylis* has a much larger oral diameter, which suggests that these tintinnids feed on larger prey (Dolan and Pierce, 2013). It has been shown that there is a relation between the size of the loricas of *C. convallaria* and the environmental conditions in the surface waters, with higher amounts of the smaller *C. convallaria* forma *affinis* present in food-rich surface waters, both spatially (Boltovskoy et al., 1990) and seasonally (during summer) (Wasik, 1998). It is, however, unknown whether there is any relation between all the other formae of *C. convallaria* and the environmental conditions.

Family uncertain

The *coxliella* form (Plate 3, figs. 3–4)

Morphology and identification: This is a hyaline lorica with a pointed tip and a wall structure resembling a spiraling ribbon. This type of lorica is known as the *coxliella* form.

Biological taxon: *Coxliella* is considered an artificial genus as it is a phenotype of other tintinnid taxa (Agatha and Strüder-Kypke, 2012, 2013; Agatha et al., 2013). Various species of *Coxliella* have, however, been described from around Antarctica (Laackman, 1907; Balech, 1958a, b, 1973).

Dimensions: This particular specimen is 55 μm long.

Geographic distribution: *Coxliella* forms are often abundant in both Arctic and Antarctic assemblages (Dolan et al., 2012).

The fossil record: No fossil record of *coxliella* form loricae exists, as even published records of relatively young sedimentary core material containing tintinnid remains do not distinguish between individual species (see e.g. Roncaglia, 2004b; Cromer et al., 2005).

Ecological preferences and environmental interpretation: It is possible that this type of morphology is characteristic of a rapidly growing population (Dolan et al., 2012).

Palynomorph: Lorica (possibly) type 1 (Plate 3, figs. 13–14)

Morphology and identification: This palynomorph is a bottle-shaped, transparent vesicle with a narrow oral opening and a broad, flat posterior end. There are no scars present of formerly agglutinated (biogenic) material. It does resemble some of the hyaline tintinnid loricae without an apical horn, but the narrow oral opening is atypical. We believe this is the lorica of a tintinnid, but we have not been able to identify the genus.

Biological taxon: Unknown because we have not been able to ascribe the lorica to a genus.

Dimensions: The length of the lorica is $63 \pm 3 \, \mu m$ ($n = 3$).

Geographic distribution: Unknown because we have not been able to ascribe the lorica to a genus.

The fossil record: No similar forms have been found in other published palynological records.

Ecological preferences and environmental interpretation: Unknown because we have not been able to ascribe the lorica to a genus.

5.3 Foraminifer linings

Infrakingdom RHIZARIA Cavalier-Smith 2002

Phylum FORAMINIFERA d'Orbigny 1826

Palynomorph: Foraminifer linings of benthic foraminifera (Plate 3, figs. 5–6; Plate 4, figs. 4, 8)

Morphology and identification: Within Hole U1357B we find trochospiral (Plate 3, fig. 5), triserial (Plate 3, fig. 6), and uniserial foraminifer linings (Plate 4, fig. 4, 8). Triserial and uniserial forms are usually more transparent than the trochospiral forms. Only a few specimens were found completely intact within the samples of U1357B. However, even the damaged specimens can often still be distinguished by the darker-coloured central chamber lining (the proloculum,; see also Wrenn et al., 1998).

Biological taxon: The biological calcareous or arenaceous taxa corresponding to the linings cannot be determined. To be able to do so, the original calcareous and arenaceous shells should be picked before palynological treatment.

Dimensions: These vary strongly between specimens and the original size cannot usually be determined because the specimens are broken.

Geographic distribution: Although benthic foraminifera are common around Antarctica and can be quite diverse (Mikhalevich, 2004), they are often not preserved because the Antarctic shelf waters are highly undersaturated with respect to calcite (Expedition 318 Scientists, 2011), and the remineralization of organic matter causes acidic pore waters which dissolve the foraminifera post-depositional. The inner linings of benthic foraminifera within palynomorph assemblages are found more commonly at sites along the Antarctic coast (Wrenn et al., 1998; Warny et al., 2006; Warny, 2009). However, because around Antarctica tilted Palaeogene and Neogene strata are exposed due to glacial erosion, such foraminifer linings could also be reworked (Warny, 2009).

The fossil record: Foraminiferal linings have been found in fossil assemblages obtained from marine cores as well as continental outcrops around Antarctica with ages ranging between the Cretaceous and the Quaternary. An extensive overview of Antarctic records of fossil foraminiferal linings is given by Concheyro et al. (2014).

Ecological preferences and environmental interpretation: Considering that the majority of palynological remains from Hole U1357B are deposited in situ and the preservation potential of foraminifera in these sediments is far better than those of the Eocene sediments in the region (Expedition 318 Scientists, 2011), the benthic foraminiferal linings are probably in situ. In general, the presence or absence of benthic foraminiferal linings in palynological records is associated with well-ventilated or anoxic bottom waters, respectively (Sluijs et al., 2006, 2008; Frieling et al., 2018). High abundances of benthic foraminifera (and their linings) could also reflect high surface-water productivity as benthic fauna is directly dependent of the organic carbon flux from the surface waters (Jorissen et al., 1995; Thomas et al., 1995; Costello and Bauch, 1997). The ratio between infaunal versus epifaunal species is used as a palaeoproductivity proxy, as infaunal species tend to increase during sustained periods of high productivity, while epifaunal species are more dominant when surface-water productivity occurs in pulses (Thomas et al., 1995; Costello and Bauch, 1997). Because trochospiral (more commonly epifaunal), triserial, and uniserial (more commonly infaunal) foraminifer linings have been found within Hole U1357B, they could potentially be used to qualitatively reconstruct surface-water productivity changes and/or changes in bottom-water oxygenation (Corliss, 1991).

5.4 Prasinophyte phycomata

Kingdom PLANTAE Haeckel 1866

Phylum CHLOROPHYTA Pascher 1914

"Prasinophytes" (paraphyletic taxon; see Nakayama et al., 1998; Guillou et al., 2004)

Order PYRAMIMONADALES Chadefaud 1950

Family HALOSPHAERACEAE Haeckel 1894

Genus *Pterosperma* Pouchet 1894

Phycoma of *Pterosperma cristatum* Schiller 1925 (Plate 2, figs. 29–34 and possibly figs. 41–43)

Morphology and identification: Specimens from Hole U1357B closely resemble the phycoma of *P. cristatum* as depicted by Bérard-Therriault et al. (1999). These specimens possess straight alae (ridges) that form square or pentagonal compartments. *P. cristatum* is very similar to *Pterosperma polygonum*, but in contrast to *P. polygonum* *P. cristatum* does not possess pores on its central body (see Inouye et al., 1990, fig. 3). Because we cannot distinguish any pores on our specimens and because of the strong similarity with the specimens depicted by Bérard-Therriault et al. (1999), we have identified most of our specimens as *P. cristatum*. However, it has been shown that in early developmental stages of *P. polygonum* the pores cannot be resolved (Parke et al., 1978). Even the large central pore of *Pterosperma marginatum* is not visible in non-fully developed specimens, while the alae are present (Parke et al., 1978). It is therefore possible that we have identified some non-fully developed specimens of *P. polygonum* and *P. marginatum* as *P. cristatum*. Light microscope photographs of *P. polygonum* and *P. cristatum* by Bérard-Therriault et al. (1999) show that *P. polygonum* has relatively

higher alae. On the other hand, the alae on *P. polygonum* of Parke et al. (1978) and *P.* cf. *polygonum* of Marchant (2005) are relatively low.

Biological taxon: *Pterosperma cristatum*.

Dimensions: The specimens within Hole U1357B are 13 to 21 µm in diameter (average: 15 µm, $n = 6$).

Geographic distribution: The full geographic distribution of *P. cristatum* in the surface waters is unclear, but it has been reported from around the world: Gulf of Saint Laurent in Canada (Bérard-Therriault et al., 1999), in coastal bays of Japan (Inouye et al., 1990; Kawachi, 2017), off the coast of Portugal (Moita and Vilarinho, 1999), the Baltic Sea area (Hällfors, 2004), the German Wadden Sea (Scholz and Liebezeit, 2012), freshwaters in the Russian Far East (Medvedeva and Nikulina, 2014), the Denube River Basin in Romania and the Black Sea (Cărăuş, 2017), and in Norwegian fjords (Hoem, 2018).

The fossil record: Mudie et al. (2010) noticed the remarkable similarity between the fossil specimens of *Cymatiosphaera globulosa* from the Black Sea (Wall et al., 1973) and the phycoma stage of *P. cristatum*. Originally, *C. globulosa* was described from Oligocene strata in Japan (Takahashi, 1964) and later from Upper Cretaceous strata in Japan (Takahashi, 1967). Similar-looking *Cymatiosphaera* (*Cymatiosphaera* sp. 1, diameter 11 µm) have been recorded in a Miocene record from Prydz Bay, Antarctica (Hannah, 2006), as well as in Quaternary, Miocene, and Oligocene sections from the Ross Sea (Hannah et al., 1998, 2000). It is, however, uncertain whether these old prasinophyte phycomata belong to the same biological species *P. cristatum* with similar environmental preferences as today. On the other hand, Holocene records of *C. globulosa* likely originate from *P. cristatum* in the surface waters. For example, *C. globulosa* is known from several Quaternary records from the Black Sea area where it first appeared in the deeper waters around 9600 cal. yr BP (Atanassova, 2005; Filipova-Marinova, 2007; Filipova-Marinova et al., 2013).

Ecological preferences and environmental interpretation: Although *Pterosperma* is considered a fully marine genus (Parke et al., 1978), the geographic distribution of *P. cristatum* suggests that it is also tolerant to more brackish environments and/or coastal areas influenced by freshwater input. Notably, *C. globulosa* is considered a euryhaline species and therefore able to tolerate large salinity fluctuations (Wall et al., 1973; Atanassova, 2005; Filipova-Marinova, 2007; Filipova-Marinova et al., 2013). In the fossil records from the Black Sea increases in *C. globulosa* together with other euryhaline dinoflagellate species mark the transition from a freshwater lake to increased marine (more saline) conditions (Wall et al., 1973; Atanassova,

2005; Filipova-Marinova, 2007; Filipova-Marinova et al., 2013). Increased amounts of *Cymatiosphaera* in the Miocene record from Prydz Bay are associated with increased freshwater and stratified oceanic waters resulting from increased warming during the Mid-Miocene Climatic Optimum (Hannah, 2006).

> Phycoma of *Pterosperma marginatum* Gaarder 1954 (Plate 2, figs. 38–40 and possibly figs. 41–43)

Morphology and identification: The phycoma of *Pterosperma marginatum*, like *P. ristatum*, possesses alae that form polygonal compartments. However, *P. marginatum* typically possesses a large pore placed centrally within each compartment (Throndsen, 1997; Bérard-Therriault et al., 1999). The alae of this specimen are undulate, which is different from e.g. the specimen depicted by Parke et al. (1978, pl. 1, fig. F) with more straight alae. Specimens with similar undulating ridges have been found lacking these pores (Plate 2, figs. 41–43). Since the central pores are absent in non-fully developed phycomata, it is possible that these are also *P. marginatum*.

Biological taxon: *Pterosperma marginatum*.

Dimensions: Specimens of *P. marginatum* are 14 ± 1 µm ($n = 2$).

Geographic distribution: As with the other *Pterosperma* species, it has a global but patchy distribution. It has been recorded off the coast of Portugal (Moita and Vilarinho, 1999), in the Gulf of Saint Laurent in Canada (Bërard-Therriault et al., 1999), the Norwegian Sea, and the Arctic Ocean (Ocean Biogeographic Information System, 2018)

The fossil record: *P. marginatum* is not known from the fossil record.

Ecological preferences and environmental interpretation: *Pterosperma* is considered a fully marine genus (Parke et al., 1978). Considering it has been found together with *P. polygonum* (Moita and Vilarinho, 1999; Bérard-Therriault et al., 1999) it likely prefers a similar habitat.

> Phycoma of *Pterosperma parallelum* Gaarder 1938 (Plate 2, figs. 24–26, 44–52)

Morphology and identification: The phycoma of *Pterosperma parallelum* possesses low, curved, parallel alae (Throndsen, 1997; Marchant, 2005). In the samples of Hole U1357B there is some variation in the appearance of the alae. The thickness, smoothness, and straightness vary between specimens. Some specimens have relatively thick

and/or undulate alae (Plate 2, figs. 47–52).

Biological taxon: *P. parallelum*.

Dimensions: Phycomata of *P. parallelum* in Hole U1357B range in size between 14 and 25 µm (average: 22 µm, $n = 7$), which compares well with reported sizes of 9–20 µm (Throndsen, 1997; Marchant, 2005).

Geographic distribution: Southern Ocean, near the Polar Front (Marchant, 2005; Australian Antarctic Data Center, 2017), and in inland waters of the Netherlands (Veen et al., 2015).

The fossil record: *P. parallelum* is not known from the fossil record.

Ecological preferences and environmental interpretation: Although *Pterosperma* is considered a fully marine genus (Parke et al., 1978), the multiple recordings of *P. parallelum* in the sea-ice-influenced waters of the Southern Ocean suggest some tolerance to fluctuating surface-water salinities.

Phycoma of *Pterosperma* cf. *parallelum* (Plate 2, fig. 27–28, 53–55)

Morphology and identification: This palynomorph resembles *P. parallelum* as described by Throndsen (1997) and Marchant (2005), but the alae are not simple straight ridges. Instead, this phycoma possesses parallel rows of small, flat, square protuberances. The phycoma wall is thinner than *P. parallelum*.

Biological taxon: It is uncertain whether these phycomata belong to an unknown species of *Pterosperma* or whether they represent an early developmental stage of *P. parallelum*. However, considering that phycomata grow in size during asexual reproduction (Colbath and Grenfell, 1995) and the fact that we find both smaller and larger specimens of *P.* cf. *parallelum* as well as smaller *P. parallelum* within our samples, the latter is less probable.

Dimensions: The size of *P.* cf. *parallelum* ranges between 19 and 26 µm ($n = 3$), comparable to *P. parallelum*.

Geographic distribution: Unknown because no previous record of this species exists.

The fossil record: Unknown because this species has not been recorded in palynological studies before.

Ecological preferences and environmental interpretation: Unknown because no previous record of this species exists.

Phycoma of *Pterosperma polygonum* Ostenfeld in in Ostenfeld & Schmidt 1902 (Plate 2, figs. 35–37)

Morphology and identification: This species is very similar to *Pterosperma cristatum*. As mentioned above, what distinguishes the phycomata of *P. polygonum* from *P. cristatum* is the presence of small pores covering the central body (Throndsen et al., 1997; Bérard-Therriault et al., 1999). However, these are lacking in earlier developmental stages of the phycoma (Parke et al., 1978). In addition, pores can be easily overlooked underneath the light microscope, which is why some specimens of *P. polygonum* can be misidentified as *P. cristatum*. Although originally *Pterosperma polygonum* was described as being twice as large (40 µm) in comparison to our specimens (Ostenfeld and Schmidt, 1902), it is known that phycomata vary in size depending on the stage of asexual reproduction within a phycoma (Colbath and Grenfell, 1995). Notably, smaller phycomata resembling *P. polygonum* have been described (*Pterosperma* cf. *polygonum* in Marchant, 2005). Scanning electron microscope images of *P.* cf. *polygonum* of Marchant (2005) also show the presence of pores.

Biological taxon: *Pterosperma polygonum*.

Dimensions: The specimens in Hole U1357B are 17 ± 1 µm ($n = 2$).

Geographic distribution: Documentation of *P. polygonum* is rather patchy with reports from the Red Sea and the Gulf of Aden (Ostenfeld and Schmidt, 1902), the Gulf of Saint Laurent in Canada (Bérard-Therriault et al., 1999), off the coast of Brittany (France) in the western English Channel (Guilloux et al., 2013), freshwaters of the Russian Far East (Medvedeva and Nikulina, 2014), inland waters of the Netherlands (Veen et al., 2015), the North Sea (Marine Biology Laboratory, 2018), off the coast of Japan (Ocean Biogeographic Information Center, accessed in 2018), the White Sea (Russia) and the Arctic Ocean (Hopcroft, 2016), the Southern Ocean (Davies and Watts, 2017), and *P.* cf. *polygonum* from Davis Station, East Antarctica (Marchant, 2005).

The fossil record: *P. polygonum* is not known from the fossil record.

Ecological preferences and environmental interpretation: *Pterosperma* is considered a fully marine genus (Parke et al., 1978), but like *P. cristatum* the geographic distribution of *P. polygonum* suggests some tolerance to lower salinities.

Phycoma of *Pterosperma* aff. *reticulatum* Ostenfeld in Ostenfeld and Schmidt (1902) (Plate 2, figs. 56–58)

Morphology and identification: The original description of *Pterosperma reticulatum* in Ostenfeld and Schmidt (1902) is based on a specimen of about 80 μm with lamellae (alae) forming a finely reticulated surface. We follow Thorrington-Smith (1970) in assigning similar-looking phycomata but with a much smaller size to *Pterosperma* aff. *reticulatum*. The specimens encountered in Hole U1357B are ornamented with numerous low alae that form a reticulate surface of irregular polygonal fields. The size and wall ornamentation of the specimens from Hole U1357B therefore also resemble *Pterosperma parvareopunctatum* Thorrington-Smith 1970, but they lack the central pores that are present in each of the irregular polygonal fields.

Biological taxon: It is unknown whether the specimens described by Thorrington-Smith (1970) are biologically the same as those described by Ostenfeld and Schmidt (1902), although phycomata are known to grow in size during asexual reproduction (Colbath and Grenfell, 1995).

Dimensions: The specimens encountered in Hole U1357B are 17 ± 1 μm (*n* = 2).

Geographic distribution: Originally, *P. reticulatum* was described from the Red Sea and the Gulf of Aden (Ostenfeld and Schmidt, 1902). For the smaller *P.* aff. *reticulatum* no other record exists apart from its description from the surface waters in the western Indian Ocean (Thorrington-Smith, 1970).

The fossil record: This species is not known from the fossil record.

Ecological preferences and environmental interpretation: Unknown due to the scarce information about its geographic distribution.

Cymatiosphaera sp. 1 (Plate 2, figs. 59–64)

Morphology and identification: This is a transparent sphere with alae forming irregularly shaped polygonal fields. The alae are so high (about 5 μm) and transparent compared to the vesicle diameter that it seems as if bifurcating processes extend to the point at which some of the alae intersect. In some more degraded specimens, bifurcating processes are what is left of the alae (Plate 2, figs. 62–64).

Biological taxon: Unknown, but the size, transparency, and wall ornamentation are very similar to the phycomata of prasinophytes.

Dimensions: The diameter of *Cymatiosphaera* sp. 1 is

17 ± 1 μm (*n* = 4).

Geographic distribution: To our knowledge this species has not been recorded from the surface waters or modern-day surface sediments before.

The fossil record: Although *Cymatiosphaera* is a common genus in fossil records, we have not been able to assign the specimens from Hole U1357B to a specific species. *Cymatiosphaera* sp. 1 differs distinctly from most other *Cymatiosphaera* species found in fossil records close to the Antarctic margin (Hannah et al., 1998, 2000; Wrenn et al., 1998; Hannah, 2006; Warny et al., 2006; Clowes et al., 2016) by the irregular polygonal fields formed by its high septa. *Cymatiosphaera* sp. 2 recorded by Hannah (2006) in a Miocene record from Prydz Bay, Antarctica, also seems to possess such irregular polygonal fields, but its septa are lower. Also, the specimen depicted by Hannah (2006) is larger (32 μm in diameter) than *Cymatiosphaera* sp. 1 recorded in Hole U1357B.

Ecological preferences and environmental interpretation: Unknown because to our knowledge this species has not been recorded from the surface waters or modern-day surface sediments before. Species of *Cymatiosphaera* (including *Cymatiosphaera* sp. 2 of Hannah, 2006) close to the Antarctic margin have, however, been associated with increased freshwater release and stratified oceanic waters during the Mid-Miocene Climatic Optimum (Hannah, 2006).

5.5 Eggs, spermatophores, teeth, and other animal remains

Kingdom ANIMALIA Linnaeus 1758

Phylum ANNELIDA Lamarck 1809

Class POLYCHAETA Grube 1850

Order EUNICIDA Fauchald 1977

Family Dorvilleidae Chamberlin 1919

Genus *Ophryotrocha* Claparède & Mecznikow 1869

Palynomorph: P-type maxillary apparatus of *Ophryotrocha orensanzi* Taboada et al. 2013 (Plate 3, figs. 12, 20)

Morphology and identification: Within the samples of Hole U1357B we find a variety of serrated dark red palynomorphs of various sizes. Some of these have a jaw-like shape, being serrated at one side of an elongated sclerotized part. Notably, the most distal tooth of the serrated side of the "jaw" is the largest. Regularly, longitudinal series are found consisting of multiple jaw-like forms attached together. We have identified these as the P-type maxillary apparatus of the polychaete worm *Ophryotrocha*. Of all the Southern Ocean

species of *Ophryotrocha*, *O. orensanzi* possesses maxillary pieces within its P-type mandibular apparatus that have a very prominent distal tooth similar to the specimens found in Hole U1357B (Taboada et al., 2013; Paxton et al., 2017). This distal tooth is especially prominent on the forceps of the maxillary apparatus and is formally described as a "lateral fang" on the P-type forceps in the emended diagnosis of *O. orensanzi* by Paxton et al. (2017).

Biological taxon: We believe these are the remains of *Ophryotrocha orensanzi*. It could be, however, that these maxillary apparatuses belong to *Ophryotrocha claparedii*, for which the jaw apparatus is poorly known (Szaniawski and Wrona, 1987), or to an unknown species of *Ophryotrocha*, considering that the fauna around the Antarctic coast is poorly explored and the amount of new *Ophryotrocha* species that have been discovered away from the Antarctic coast has increased enormously in recent years (Paxton and Åkesson, 2007; Paxton and Davey, 2010; Taboada et al., 2013; Ravara et al., 2015; Paxton et al., 2017). Species of the dorvilleid *Ophryotrocha* possess a P-type maxillary apparatus when they are young or female (Paxton and Åkesson, 2007). Once they become a sexually mature male or change from female to male (hermaphrodites) this P-type jaw gets replaced by a K-type jaw, which has greatly enlarged basal parts (forceps; Paxton and Åkesson, 2007; Paxton et al., 2017).

Dimensions: The largest specimens are about 160 μm long and the smallest specimens about 16 μm long (average: 38 μm, $n = 9$).

Geographical distribution: Four species of *Ophryotrocha* are known from shallow-water Southern Ocean sites. The species *Ophryotrocha claparedii* has been reported from the Ross Sea (Gambi et al., 1994; Morehead et al., 2008). Recently discovered new species include *Ophryotrocha orensanzi* and *Ophryotrocha clava* discovered on experimentally deployed whale bones off the coast of Deception Island (Taboada et al., 2013) and *Ophryotrocha shieldsi* from underneath a fish farm in Tasmania (Paxton and Davey, 2010). Recently, *O. orensanzi* has also been reported from near Casey Station, East Antarctica (Paxton et al., 2017), which is not too far from Hole U1357B.

The fossil record: Scolecodonts of several *Ophryotrocha* species have been described from the Cape Melville Formation (Lower Miocene) of King George Island (Szaniawski and Wrona, 1987).

Ecological preferences and environmental interpretation: Although *Ophryotrocha* species are generally associated with high-nutrient littoral conditions, whale falls, and hydrothermal vents (Taboada et al., 2013; Paxton et al., 2017), the recent find of *O. orensanzi* near Casey Station

in clean, unpolluted waters has led to the suggestion that *Ophryotrocha* are not specialists of organically enriched substrates, but rather unspecialized opportunists that rapidly increase their population size in nutrient-rich environments (Paxton et al., 2017).

> Palynomorph: Basal part (forceps) of a K-type maxillary apparatus of *Ophryotrocha* (Plate 3, figs. 22–23)

Morphology and identification: These are falcate, dark red sclerotized parts. We have identified these as the basal parts of the K-type maxillary apparatus of *Ophryotrocha*.

Biological taxon: Likely they belong to the same species as the P-type maxillary apparatus, *O. orensanzi*, or an unknown Antarctic species. They belong to male individuals or formerly male individuals, as hermaphrodite *Ophryotrocha* retain their K-type maxillary apparatus once they change from the male to the female sex (Paxton and Åkesson, 2007). The length of the K-type forceps is, however, half the size of the specimen of *O. orensanzi* drawn by Paxton et al. (2017). It is unclear what the size range of the K-type forceps of *O. orensanzi* can be and thus whether the specimens found in Hole U1357B truly belong to this species.

Dimensions: These palynomorphs are 76 ± 3 μm in length ($n = 2$).

Geographic distribution: For this information, see the P-type maxillary apparatus of *Ophryotrocha orensanzi* above.

The fossil record: For this information, see the P-type maxillary apparatus of *Ophryotrocha orensanzi* above.

Ecological preferences and environmental interpretation: For this information, see the P-type maxillary apparatus of *Ophryotrocha orensanzi* above.

> Palynomorph: Anterior denticles of the maxillary apparatus of *Ophryotrocha* (Plate 3, figs. 15–16)

Morphology and identification: These are ovate or lobe-shaped, dark red serrated sclerotized parts. The serration is symmetrical with respect to the central axis of the lobe-shaped part and only present at the distal end. We have identified these exoskeleton parts as the anterior denticles of either a P-type or a K-type mandibular apparatus of the dorvilleid *Ophryotrocha*. The shapes of anterior denticles of *Ophryotrocha* range from ovate to subtriangular (Paxton and Åkesson, 2007; Paxton and Davey, 2010; Taboada et al., 2013; Ravara et al., 2015; Paxton et al., 2017).

Biological taxon: Considering the presence of P-type mandibular apparatuses of *O. orensanzi* (or possibly an

unknown species of *Ophryotrocha*), these anterior denticles likely belong to the same species.

Dimensions: They are $56 \pm 3\,\mu m$ in length ($n = 2$).

Geographic distribution: For this information, see the P-type maxillary apparatus of *Ophryotrocha orensanzi* above.

The fossil record: For this information, see the P-type maxillary apparatus of *Ophryotrocha orensanzi* above.

Ecological preferences and environmental interpretation: For this information, see the P-type maxillary apparatus of *Ophryotrocha orensanzi* above.

Phylum ARTHROPODA von Siebold 1848

Subphylum CRUSTACEA Brünnich 1772

Class MAXILLOPODA Dahl 1956

Subclass COPEPODA Milne-Edwards 1840

Copepod spermatophores

Palynomorph: Copepod spermatophore Type AB-33 (Plate 3, figs. 24–28)

Morphology and identification: Among the palynological remains in Hole U1357B, club-shaped, transparent vesicles have also been found, which are most likely copepod spermatophores. Copepod spermatophores are generally club-shaped or flask-shaped and taper towards the proximal end into a tube-like neck (Subramoniam, 2017).

Biological taxon: It is unknown to which copepod species this spermatophore belongs. Like most crustaceans, copepods produce a spermatophore to aid sperm transfer and avoid loss of sperm (Subramoniam, 2017). The spermatophore is attached to the female genital orifice with some adhesive material around the neck, after which sperm is released through the tube-like neck (Subramoniam, 2017).

Dimensions: The spermatophore is $37 \pm 5\,\mu m$ in length ($n = 2$) when the tube-like neck is not included.

The fossil record: Similar-looking forms have been recovered from a peat section in Tierra del Fuego (Borromei et al., 2010).

Palynomorph: Copepod (possibly) spermatophore Type AB-22 (Plate 4, figs. 6–7)

Morphology and identification: Type AB-22 large, orangish brown tetrahedral casing. The three angles at the "base" of the tetrahedron have rounded edges, while the "top" acuminates into an extended tube-like neck. Due to flattening on the microscope slide the tetrahedral shape can appear more triangular with one of the base angles folded. The tetrahedron casing and tube-like neck show a resemblance to the spermatophores of some crustaceans, copepods in particular (Subramoniam, 2017). If that is the case, Type AB-22 is 4 times larger than Type AB-33, suggesting it is produced by a larger copepod species than the species that produced Type AB-33.

Biological taxon: Possibly a larger copepod species. Larger copepods can produce spermatophores that exceed a length of $100\,\mu m$ (e.g. Hopkins, 1978; Defaye et al., 2000), but the tetrahedron shape of Type AB-22 is different from the typical elongated club-shaped copepod spermatophores (Hopkins, 1978; Defaye et al., 2000; Subramoniam, 2017). We can therefore not be certain that this is indeed a copepod spermatophore. Alternatively, it is produced by another order of small crustaceans that we have not been able to identify.

Dimensions: The width of the casing ranges between 124 and $141\,\mu m$ and the tube-like neck is $115 \pm 20\,\mu m$ long ($n = 4$).

Geographic distribution: Identical specimens derived from surface sediment samples from Prydz Bay have been depicted as an "egg case" by Storkey (2006, pl. 12, figs. 7–10).

Copepod eggs

Palynomorph: Copepod egg (Plate 4, fig. 9; Plate 5, figs. 1–3)

Morphology and identification: A transparent sphere, which is densely covered in spines. The thickness of the egg envelopes in diapause eggs can be several micrometres thick (Santella and Ianora, 1990; Berasategui et al., 2012). Therefore, these eggs are likely quiescence subitaneous eggs because their walls appear relatively thin.

Biological taxon: Considering that *Paralabidocera antarctica* is the most common copepod species at the Adélie coast (Loots et al., 2009) and that *P. antarctica* produces similar-sized eggs (Swadling, 1998), it is possible that these belong to *P. antarctica*. The morphology of subitaneous (and diapause) eggs of *P. antarctica* is, however, unknown to us.

Dimensions: The egg diameter is $115 \pm 15\,\mu m$ ($n = 3$) and the spines have a length of $16 \pm 3\,\mu m$ ($n = 11$).

Copepod mandibular gnathobases

Palynomorph: Copepod mandibular gnathobase 1 (Plate 3, fig. 21)

Morphology and identification: This mandibular gnathobase is rectangular with a toothed edge at one

side consisting of nine triangular teeth, which decrease in size towards one side. It somewhat resembles the mandibular gnathobase of the local copepod *Stephos longipes*. However, this species has a large separation between the ventral (largest) tooth and the first central tooth (Razouls et al., 2005–2017), which is not the case in this specimen. Instead, it is more similar to the mandibular gnathobase of *Centropages hamatus* (Michels and Gorb, 2015), but this is not a Southern Ocean species.

Biological taxon: Although we have not been able to assign it to any specific copepod species, such robust gnathobases with compact relatively short teeth at the distal ends typically belong to species that feed on phytoplankton (i.e. diatoms) (Michels and Gorb, 2015).

Dimensions: It is $68 \pm 5 \,\mu$m wide and $30 \pm 3 \,\mu$m high ($n = 2$).

Palynomorph: Copepod mandibular gnathobase 2 (Plate 3, fig. 17)

Morphology and identification: Compared to mandibular gnathobase 1, this specimen is more square-shaped. It possesses five triangular teeth (chitinous tooth sockets). The ventral tooth is smaller than the two teeth (first and second central tooth) adjacent to it. Both the square-shaped dimensions and the number of teeth strongly resemble the mandibular gnathobase of *Rhincalanus gigas* (Michels and Gorb, 2015). Also, confocal laser scanning micrographs show that the ventral tooth socket is indeed smaller than the first central tooth (Michels and Gorb, 2015).

Biological taxon: Probably *Rhincalanus gigas*.

Dimensions: It has a width of $35 \,\mu$m and height of $50 \,\mu$m ($n = 1$).

Geographic distribution: *R. gigas* is a Southern-Ocean-wide species, but is most common in the Antarctic Circumpolar Current (Atkinson, 1998).

Ecological preferences and environmental interpretation: Being one of the most herbivorous species (feeding mostly on phytoplankton) of the Southern Ocean, *R. gigas* feeds predominantly on diatoms (Atkinson, 1998; Atkinson et al., 2012). Populations of *R. gigas* descend to deeper waters in winter when they do not feed (diapause), although some populations have been found feeding in open surface waters during winter (Atkinson, 1998).

Exoskeleton parts

Palynomorph: Copopod thoracopod (Plate 3, fig. 29)

Morphology and identification: This is a segmented exoskeleton part. Towards the distal end the segments become smaller stepwise. We have identified this as the distal part of a thoracopod (swimming leg) of a copepod.

Biological taxon: Considering its size it probably belonged to a small copepod species.

Dimensions: It is 92 µm long ($n = 1$).

Palynomorph: Copepod endites (Plate 5, fig. 4)

Morphology and identification: Within the samples of Hole U1357B groups transparent conical palynomorphs are encountered, which are attached together at their base by a thin transparent surface. In some cases spines protrude from the base of an individual transparent cone. Although we cannot be certain, we believe that these could be the endites of a copepod maxilla.

Biological taxon: These are probably copepod mandible remains.

Dimensions: The transparent cones are typically $42 \pm 12 \,\mu$m long ($n = 9$).

Palynomorph: Copepod setae (Plate 5, fig. 6; Plate 6, fig. 5)

Morphology and identification: The most frequently encountered remains of copepods in the samples of U1357B are the setae of copepod thoracopods. Fans of bristles are positioned on one side of the seta at constant intervals.

Biological taxon: Such specimens likely belong to the larger copepod species such as *Rhincalanus gigas* (Razouls et al., 2005–2017), of which mandibular gnathobases were also found (see above).

Dimensions: The setae are often fragmented, but the largest specimen that was measured is 527 µm long.

Phylum TARDIGRADA Spallanzani 1776

Class EUTARDIGRADA Marcus 1927

Order PARACHELA Schuster et al. 1980

Superfamily MACROBIOTOIDEA Thulin 1928 in Marley et al. 2011

Palynomorph: Macrobiotoid tardigrade egg (Plate 2, figs. 17–20)

Morphology and identification: The eutardigrade superfamily Macrobiotoidea (Marley et al., 2011) comprises several genera of tardigrades that produce eggs with an ornamentation consisting of tapered, conical projections with or without distal bifurcations or dishes (Bertolani and

Plate 6. (1) *Cymatocylis convallaria* forma *calyciformis*, U1357B-8H-3W 54–56 cm, slide 1, E.F.: K20.2. **(2)** *Cymatocylis convallaria* forma *cylindrica*, U1357B-5H-5W 12–14 cm, slide 1, E.F.: S17.2, LIB image. **(3)** *Cymatocylis convallaria* forma *cylindrica*, U1357B-8H-3W 54–56 cm, slide 1, E.F.: F17.3. **(4)** *Cymatocylis convallaria* forma *cylindrica*, U1357B-6H-6W 123–125 cm, slide 1, E.F.: K24.1, LIB image. **(5)** Copepod setae: a large seta on the right and a smaller seta on the left (anterior ends of *Cymatocylis convallaria* are also present on the left side), U1357B-8H-3W 54–56 cm, slide 1, E.F.: T30.1. **(6)** Type AB-27e, triangular with acute tip, U1357B-5H-7W 5–7 cm, slide 1, E.F.: H27.1, LIB image. **(7)** Type AB-27a, dome-shaped with broad base, U1357B-8H-3W 54–56 cm, slide 1, E.F.: Q31.3, LIB image. **(8)** Type AB-27b, dome-shaped, U1357B-17H-1W 117–119 cm, slide 1, E.F.: G17.3, LIB image. **(9)** Type AB-27d, triangular, U1357B-5H-7W 5–7 cm, slide 1, E.F.: D32.4, LIB image. **(10)** Type AB-29, U1357B-5H-7W 5–7 cm, slide 1, E.F.: E34.4, LIB image. **(11)** Type AB-28, U1357B-10H-1W 58–60 cm, slide 1, E.F.: L23.2, LIB image. **(12)** Type AB-30, U1357B-15H-2W 75–76 cm, slide 1, E.F.: F22.2, LIB image. **(13)** Type AB-32, U1357B-2H-2W 114–116 cm, slide 1, E.F.: N32.3, upper focus. **(14)** Type AB-32, U1357B-2H-2W 114–116 cm, slide 1, E.F.: N32.3, lower focus. **(15)** Type AB-31, top view, U1357B-6H-6W 123–125 cm, slide 1, E.F.: J26.3, upper focus. **(16)** Type AB-31, top view, U1357B-6H-6W 123–125 cm, slide 1, E.F.: J26.3, lower focus. **(17)** Type AB-31, lateral view, U1357B-17H-5W 97–99 cm, slide 1, E.F.: O28.4, upper focus. **(18)** Type AB-31, lateral view, U1357B-17H-5W 97–99 cm, slide 1, E.F.: O28.4, lower focus.

Rebecchi, 1993; Pilato et al., 2004; Gibson and Zale, 2006; Bartels et al., 2009; Altiero et al., 2010; Zawierucha et al., 2016). Within the samples of Hole U1357B we encountered one palynomorph that strongly resembles a macrobiotoid tardigrade egg. This palynomorph is transparent and smooth-walled with transparent, hollow, conical processes (about 20 are visible on one side of the egg). Each conical projection is about 4 μm high and possesses a thread-like extension at its tips, which can be as long as the conical projection itself.

Biological taxon: The egg found in Hole U1357B resembles the eggs of *Macrobiotus krynauwi* (Dastych and Harris, 1995) or *Macrobiotus blocki* (see Gibson et al., 2007), although it is much smaller in size and has longer thread-like extensions at its processes. The exact macrobiotoid tardigrade species to which this egg belongs remains unknown.

Dimensions: Without its processes the egg is 19 μm in diameter ($n = 1$).

Geographic distribution: Macrobiotoid eutardigrades are found worldwide in freshwater and semiterrestrial environments (Bertolani et al., 1996). Also on Antarctica, tardigrade eggs have been found in freshwater and slightly brackish lake sediments (Gibson and Zale, 2006; Gibson et al., 2007; Cromer et al., 2008) as well as on sparsely vegetated and ice-free areas (Dastych and Harris, 1995; Convey and McInnes, 2005; Convey et al., 2008).

The fossil record: The eggs of tardigrades are also known to be preserved in sediments (Gibson and Zale, 2006; Gibson et al., 2007; Cromer et al., 2008; Borromei et al., 2010; Mudie et al., 2011). However, species-specific environmental reconstructions are scarce. Recently, multiple Holocene tardigrade egg records from Antarctic lakes were generated that give insight into Holocene tardigrade dispersal and how they are affected by regional climate change (Gibson and Zale, 2006; Gibson et al., 2007).

Ecological preferences and environmental interpretation: Notably, only eutardigrades, which comprise the freshwater and semiterrestrial tardigrades, produce ornamented eggs in contrast to the marine heterotardigrades, which produce smooth-walled eggs (Bertolani et al., 1996). Within sedimentary records increased amounts of such ornamented tardigrade eggs have been associated with restricted freshwater conditions, such as lakes or ponds (Gibson and Zale, 2006; Gibson et al., 2007; Cromer et al., 2008; Borromei et al., 2010; Mudie et al., 2011). The presence of tardigrade eggs in samples of Hole U1357B is therefore a surprise given the marine conditions as indicated by the other plankton groups. Since we have only found one and because tardigrades are also common on sparsely vegetated and ice-free areas of the Antarctic continent

(Dastych and Harris, 1995; Convey and McInnes, 2005; Convey et al., 2008), it is likely that it has been transported (through icebergs or wind) from the Antarctic mainland.

5.6 Acritarchs

Group *incertae sedis* ACRITARCHA Evitt 1963

Subgroup SPHAEROMORPHITAE Downie, Evitt & Sarjeant 1963

Genus *Leiosphaeridia* Eisenack 1958

Leiosphaeridia sp. 1–3 (Plate 3, figs. 30–34; Plate 5, figs. 5, 7–9; Plate 7, figs. 1–3)

Morphology and identification: The genus *Leiosphaeridia* includes all simple, smooth, spherical palynomorphs, which may or may not exhibit dehiscence through partial rupture (Colbath and Grenfell, 1995). Within Hole U1357B we can distinguish three morphotypes: *Leiosphaeridia* sp. 1 (Plate 7, figs. 1–3), *Leiosphaeridia* sp. 2 (Plate 3, figs. 30–34; Plate 5, figs. 7–9), and *Leiosphaeridia* sp. 3 (Plate 5, fig. 5). All three species are transparent spheres, but *Leiosphaeridia* sp. 2 can be more yellow. Also, some specimens of *Leiosphaeridia* sp. 2 appear to be covered by a second membrane (Plate 3, figs. 32–34) or have a hole (Plate 5, fig. 9).

Biological taxon: The genus *Leiosphaeridia* has been the subject of considerable taxonomic debate, in part due to its uncertain biological affinities (Martin, 1993; Colbath and Grenfell, 1995). An affinity with green algae, such as *Chlorella* Beijerinck 1890 and the prasinophyte *Halosphaera* Schmitz 1879, has been suggested for some *Leiosphaeridia* species, but the genus could very well be polyphyletic (Martin, 1993; Colbath and Grenfell, 1995). Because of its uncertain taxonomic position, we retain it under Acritarcha.

Dimensions: *Leiosphaeridia* sp. 1 is 70 ± 30 μm in diameter ($n = 3$) and has a relatively thin wall, which is sometimes difficult to distinguish and easily ruptured. *Leiosphaeridia* sp. 2 is 30 ± 2 μm in diameter ($n = 6$) and has a relatively thicker wall. *Leiosphaeridia* sp. 3 is only 16 ± 1 μm in diameter ($n = 2$).

Geographic distribution: Smooth-walled transparent spheres can be found in marine sediments worldwide. In the Southern Ocean, *Leiosphaeridia* have been reported from modern-day surface sediments of the Prydz Bay area (Storkey, 2006) and the Ross Sea (Wrenn et al., 1998).

The fossil record: Different sizes of *Leiosphaeridia* spp. have been common near the Antarctic margin since at least the late Eocene (Kemp, 1975; Wrenn et al., 1998; Hannah et al., 2000, 2001; Troedson and Riding, 2002; Hannah, 2006; Warny et al., 2006, 2009, 2016). It is therefore
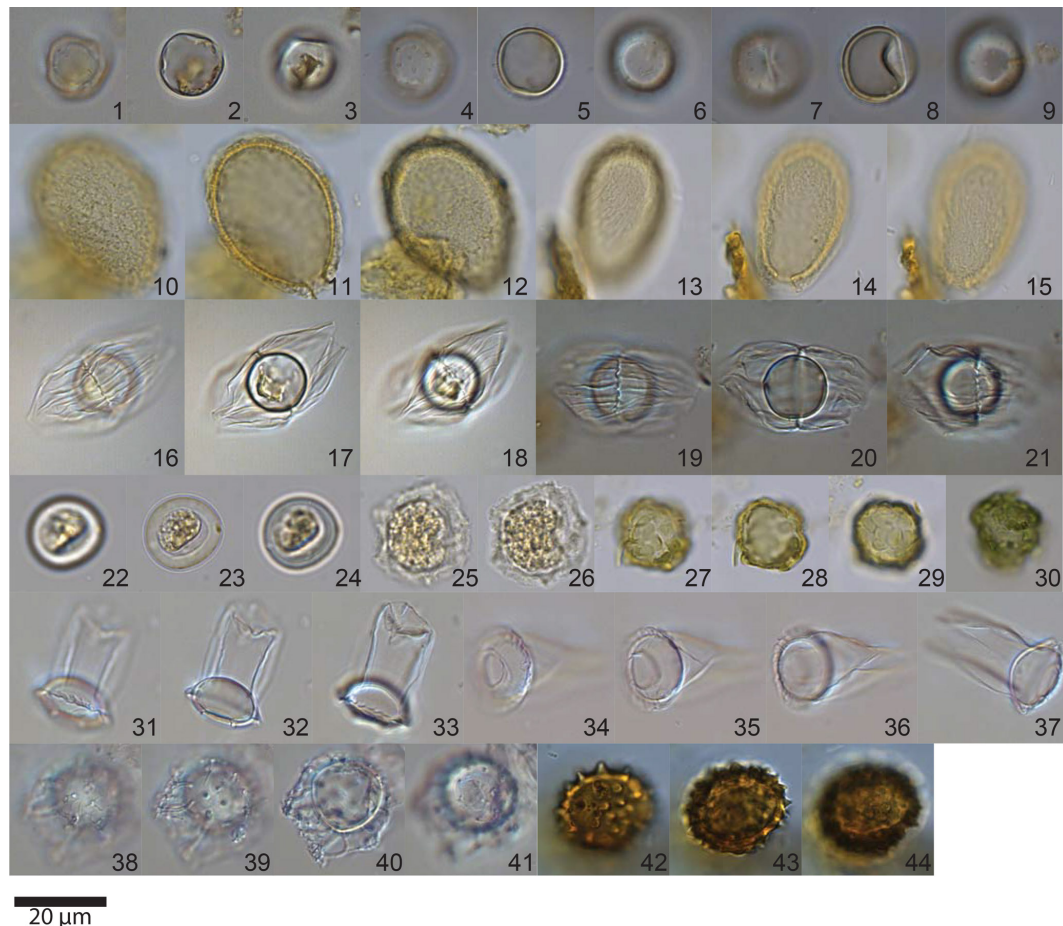
20 µm

Plate 7. (1) *Leiosphaeridia* sp. 1, U1357B-17H-5W 97–99 cm, slide 1, E.F.: L33.4, upper focus. **(2)** *Leiosphaeridia* sp. 1, U1357B-17H-5W 97–99 cm, slide 1, E.F.: L33.4, mid focus. **(3)** *Leiosphaeridia* sp. 1, U1357B-17H-5W 97–99 cm, slide 1, E.F.: L33.4, lower focus. **(4)** *Mecsekia* cf. *Mecsekia* sp. A of Schrank (2003), U1357B-18H-4W 2–3 cm, slide 1, E.F.: D23.3, upper focus. **(5)** *Mecsekia* cf. *Mecsekia* sp. A of Schrank (2003), U1357B-18H-4W 2–3 cm, slide 1, E.F.: D23.3, mid focus. **(6)** *Mecsekia* cf. *Mecsekia* sp. A of Schrank (2003), U1357B-18H-4W 2–3 cm, slide 1, E.F.: D23.3, lower focus. **(7)** *Mecsekia* cf. *Mecsekia* sp. A of Schrank (2003) with dent, U1357B-18H-4W 2–3 cm, slide 1, E.F.: H30.3, upper focus. **(8)** *Mecsekia* cf. *Mecsekia* sp. A of Schrank (2003) with dent, U1357B-18H-4W 2–3 cm, slide 1, E.F.: H30.3, mid focus. **(9)** *Mecsekia* cf. *Mecsekia* sp. A of Schrank (2003) with dent, U1357B-18H-4W 2–3 cm, slide 1, E.F.: H30.3, lower focus. **(10)** *Palaeostomocystis* sp. B, U1357B-6H-6W 123–125 cm, slide 1, E.F.: E30.3, upper focus. **(11)** *Palaeostomocystis* sp. B, U1357B-6H-6W 123–125 cm, slide 1, E.F.: E30.3, mid focus. **(12)** *Palaeostomocystis* sp. B, U1357B-6H-6W 123–125 cm, slide 1, E.F.: E30.3, lower focus. **(13)** *Palaeostomocystis* sp. B, U1357B-3H-7W 10–12 cm, slide 1, E.F.: O19.1, upper focus. **(13)** *Palaeostomocystis* sp. B, U1357B-3H-7W 10–12 cm, slide 1, E.F.: O19.1, mid focus. **(13)** *Palaeostomocystis* sp. B, U1357B-3H-7W 10–12 cm, slide 1, E.F.: O19.1, lower focus. **(16)** Type AB-13, U1357B-17H-1W 117–119 cm, slide 1, E.F.: D25.4, upper focus. **(17)** Type AB-13, U1357B-17H-1W 117–119 cm, slide 1, E.F.: D25.4, mid focus. **(18)** Type AB-13, U1357B-17H-1W 117–119 cm, slide 1, E.F.: D25.4, lower focus. **(19)** Type AB-13, U1357B-18H-4W 2–3 cm, slide 1, E.F.: F21.2, upper focus. **(20)** Type AB-13, U1357B-18H-4W 2–3 cm, slide 1, E.F.: F21.2, mid focus. **(21)** Type AB-13, U1357B-18H-4W 2–3 cm, slide 1, E.F.: F21.2, lower focus. **(22)** Type AB-2, U1357B-18H-2W 114–116 cm, slide 1, E.F.: H28.1, upper focus. **(23)** Type AB-2, U1357B-18H-2W 114–116 cm, slide 1, E.F.: H28.1, mid focus. **(24)** Type AB-2, U1357B-18H-2W 114–116 cm, slide 1, E.F.: H28.1, lower focus. **(25)** Type AB-5, U1357B-1H-1W 11–13 cm, slide 1, E.F.: E22.3, upper focus. **(26)** Type AB-5, U1357B-1H-1W 11–13 cm, slide 1, E.F.: E22.3, mid focus. **(27)** Type AB-19, U1357B-5H-5W 12–14 cm, slide 1, E.F.: F32.1, upper focus. **(28)** Type AB-19, U1357B-5H-5W 12–14 cm, slide 1, E.F.: F32.1, mid focus. **(29)** Type AB-19, U1357B-5H-5W 12–14 cm, slide 1, E.F.: F32.1, lower focus. **(30)** Type AB-19, U1357B-7H-5W 4–6 cm, slide 1, E.F.: V21.4, upper focus. **(31)** Type AB-3, U1357B-1H-1W 11–13 cm, slide 1, E.F.: G23.1, upper focus. **(32)** Type AB-3, U1357B-1H-1W 11–13 cm, slide 1, E.F.: G23.1, mid focus. **(33)** Type AB-3, U1357B-1H-1W 11–13 cm, slide 1, E.F.: G23.1, lower focus. **(34)** Type AB-3, U1357B-3H-7W 10–12 cm, slide 1, E.F.: O22.3, upper focus. **(35)** Type AB-3, U1357B-3H-7W 10–12 cm, slide 1, E.F.: O22.3, mid focus. **(36)** Type AB-3, U1357B-3H-7W 10–12 cm, slide 1, E.F.: O22.3, lower focus. **(37)** Type AB-3, U1357B-3H-7W 10–12 cm, slide 1, E.F.: G29.2, mid focus. **(38)** Type AB-4, U1357B-1H-2W 40–42 cm, slide 1, E.F.: H33.1, upper focus on dendritic distal process endings. **(39)** Type AB-4, U1357B-1H-2W 40–42 cm, slide 1, E.F.: H33.1, upper focus on central body. **(40)** Type AB-4, U1357B-1H-2W 40–42 cm, slide 1, E.F.: H33.1, mid focus. **(41)** Type AB-4, U1357B-1H-2W 40–42 cm, slide 1, E.F.: H33.1, lower focus. **(42)** Type AB-21, U1357B-5H-7W 5–7 cm, slide 1, E.F.: E32.2, upper focus. **(43)** Type AB-21, U1357B-5H-7W 5–7 cm, slide 1, E.F.: E32.2, mid focus. **(44)** Type AB-21, U1357B-5H-7W 5–7 cm, slide 1, E.F.: E32.2, lower focus.

possible that the more yellow specimens are reworked.

Ecological preferences and environmental interpretation: In the Arctic high abundances of *Leiosphaeridia* have been found in the low-salinity surface meltwater within disintegrating pack ice during the spring thaw (Mudie, 1992; Mudie and Harland, 1996). Mudie (1992) has shown that in the Arctic increased abundances of *Leiosphaeridia* are associated with the presence of a fixed ice margin. Therefore, increased abundances of *Leiosphaeridia* have been associated with glacial retreat and freshwater discharge in palaeoreconstructions at the Antarctic margin (Hannah, 2006; Warny et al., 2006, 2016). It is uncertain whether the different sizes of *Leiosphaeridia* are related to environmental conditions, produced by different organisms, or represent different growth stages similar to prasinophyte phycomata during internal cell division.

Subgroup UNCERTAIN

Genus *Mecsekia* Hajós 1966 emend. Schrank 2003

Mecsekia cf. *Mecsekia* sp. A of Schrank (2003)
(Plate 7, figs. 4–9)

Morphology and identification: Within Hole U1357B, transparent spheres ornamented with about 50 pillar-like, subtriangular spines have been found. These spines are evenly distributed and the distance between them is at least 3 times the diameter of the spines. Such acritarchs belong to the genus *Mecsekia*. The genus *Mecsekia* comprises small spherical or ovoidal vesicles with numerous subtriangular spines (Schrank, 2003). The spines are solid apart from a thin central canal (Schrank, 2003). Generally no excystment structure is present (Schrank, 2003). The different species of *Mecsekia* are generally distinguished from each other based on the distribution and space between the spines and the wall structure between the spines (Schrank, 2003). Also in the specimens from Hole U1357B, the thin central canal within the spines can be distinguished. Based on the distance between the spines, the specimens from the samples of Hole U1357B resemble *Mecsekia* sp. A of Schrank (2003). However, the spines of *Mecsekia* sp. A of Schrank (2003) are more unevenly distributed than the specimens from Hole U1357B. Palynomorph Type 115 of Pals et al. (1980), described from a Holocene peat section of the Klokkeweel bog (the Netherlands), is likely also a species of *Mecsekia* and shows resemblance to the specimens from Hole U1357B. However, Type 115 of Pals et al. (1980) also has relatively more processes.

Biological taxon: The biological affinity of this species is unknown.

Dimensions: Specimens are $15 \pm 2\,\mu m$ in diameter ($n = 3$).

Geographic distribution: To our knowledge this particular *Mecsekia* species is not known from modern-day sediments. However, other species of *Mecsekia* have been recovered from sediments underlying brackish water, such as the Black Sea (as *Micrhystridium* cf. *ariakense* in Mudie et al., 2011), and more dynamic coastal marine waters, such as the shallow marine Great Bahama Bank (as Varia-1 type in Traverse and Ginsburg, 1966).

The fossil record: The *Mecsekia* sp. A of Schrank (2003) was described from Maastrichtian deposits in Egypt.

Ecological preferences and environmental interpretation: Based on the distribution pattern of the various *Mecsekia* species, Schrank (2003) infers that *Mecsekia* prefers a shallow marine environment. Notably, Type 115 of Pals et al. (1980) was also only found in the marine clay deposits underlying the lake deposits of this peat section (Pals et al., 1980). However, the fact that *Mecsekia* has also been associated with more restricted brackish water settings today (Mudie et al., 2011) suggests some tolerance to lower salinities. A tolerance to lower salinities is also suggested by fossil accounts of *Mecsekia*, such as the Miocene restriction of the Pannonian Lake and the associated stratification (Magyar et al., 1999; Sütő and Szegő, 2008; Sütőné Szentai, 2012).

Genus *Palaeostomocystis* Deflandre 1937

Palaeostomocystis cf. *fritilla* (Bujak 1984) Roncaglia 2004 (Plate 5, figs. 10–13)

Morphology and identification: Ovoidal, yellow, smooth, thick-walled vesicles with a single polar pylome (opening) with an undulate margin have been found within the samples of U1357B. These belong to the genus *Palaeostomocystis*, which comprises all single-walled vesicles with a large pylome. They resemble *Palaeostomocystis fritilla* in particular, but lack a faveolated wall, resembling a fine-meshed reticulate network of muri (Bujak, 1984; Roncaglia, 2004b; Warny, 2009).

Biological taxon: The biological affinity of *P. fritilla* is unknown (Warny, 2009) and it is uncertain whether *Palaeostomocystis* cf. *fritilla* is produced by a different biological species than the species producing *P. fritilla*. Alternatively, *Palaeostomocystis* cf. *fritilla* are diagenetically altered forms of *P. fritilla*. *P. fritilla* shows some similarity to the egg capsules (oocytes) produced by Turbullaria (Platyhelminthes), which are ovoidal capsules with an single operculum (Harmsworth, 1968). Such oocytes are known to be preserved (Harmsworth, 1968; Borromei et al., 2010; Mudie et al., 2011). For example, larger but similar-looking oocytes with a smooth pylome margin have

been reported from a peat core derived from a mire in Tierra del Fuego (Borromei et al., 2010). Nevertheless, different Turbullaria species produce different shapes and sizes of oocytes. Turbullaria are known to live in Antarctic sea ice and release their eggs upon ice melt (Janssen and Gradinger, 1999; Kramer et al., 2011). However, the studied species by Janssen and Gradinger (1999) do not seem to produce egg capsules and release globular-shaped eggs of 30–90 µm directly into the surface waters.

Dimensions: Specimens of *Palaeostomocystis* cf. *fritilla* are 49 ± 5 µm long and 41 ± 3 µm wide ($n = 5$).

Geographic distribution: *Palaeostomocystis* species in general have been associated with a (sub)polar environment (Warny, 2009). *P. fritilla* has also been reported from surface sediments of the Weddell Sea, Antarctica, although it is possible that these are reworked from older Pleistocene sediments (Yi et al., 2005; Warny, 2009; Pieńkowski et al., 2013b). *P. fritilla* has also been reported from surface sediments in the Prydz Bay area (Storkey, 2006), the (Canadian) Arctic (Pieńkowski et al., 2011), Disko Bay, west Greenland (Roncaglia, 2004b; Seidenkrantz et al., 2008), and the Faroe Islands (Roncaglia, 2004a). Notably, it has also been reported from surface sediments in the more temperate semi-marine environment of the Marmara Sea, although rare in abundance (Mudie et al., 2011).

The fossil record: Originally *P. fritilla* was described from Pleistocene sediments in cores derived from the northern North Pacific and the Bering Sea (Bujak, 1984). Other reports of *P. fritilla* come from middle and late Holocene core sections obtained in Tierra del Fuego, Argentina (Candel et al., 2013), Disko Bay, west Greenland (Roncaglia, 2004b; Seidenkrantz et al., 2008; Ribeiro et al., 2012a), the Faroe Islands (Roncaglia, 2004a), and the Canadian Arctic (Pieńkowski et al., 2011, 2013a, 2014). In addition, Pieńkowski et al. (2014) reports smooth-walled varieties of *P. fritilla*, referred to as *Palaeostomocystis* sp. A, from mid-Holocene deposits of the Canadian Arctic.

Ecological preferences and environmental interpretation: In palaeoenvironmental records increased abundances of *P. fritilla* have been associated with the proximity of the sea-ice margin, the establishment of a seasonal sea-ice environment (Roncaglia, 2004a; Pieńkowski et al., 2013a, 2014), and glacial freshwater discharge and/or stratification (Seidenkrantz et al., 2008). In the Canadian Arctic Archipelago the highest abundances are associated with the modern-day 9–10 months per year of sea-ice cover (Pieńkowski et al., 2013a, 2014).

Palaeostomocystis cf. *reticulata* (Plate 5, fig. 14–16)

Morphology and identification: This species of *Palaeostomocystis* is ovoidal, but more slender than *Palaeostomocystis* cf. *fritilla*, and has reticulate surface-wall ornamentation. It has a yellow thick wall, but the reticulate surface-wall structure is thin, barely visible, and colourless. At one pole a large pylome is present that is almost half the diameter of the vesicle. Because of these characteristics it strongly resembles the *Palaeostomocystis reticulata* of Deflandre (1937), which has been described from Cretaceous flint pebbles in the Paris Basin. However, the specimens of *P.* cf. *reticulata* in Hole U1357B possess a conical antapex often with a (prominent) knob that is lacking in *P. reticulata*.

Biological taxon: The biological affinity of this taxon is unknown.

Dimensions: Specimens of *Palaeostomocystis* cf. *reticulata* are 57 ± 4 µm long and 31 ± 2 µm wide ($n = 5$).

Geographic distribution: These palynomorphs have not been reported from modern-day surface sediments.

The fossil record: This is the first account of *Palaeostomocystis* cf. *reticulata* in the fossil record. However, *P. reticulata* has been reported from Upper Eocene to Pliocene reworked surface sediments around the Antarctic Peninsula (Warny, 2009) apart from its original description from the Paris Basin (Deflandre, 1937).

Ecological preferences and environmental interpretation: Because the biological affinity is unknown, the ecological preferences are unknown for this palynomorph. However, *Palaeostomocystis* have been associated with (sub)polar environments in general (Warny, 2009).

Palaeostomocystis sphaerica Deflandre 1937 sensu Warny 2009 (Plate 4, figs. 10–12, 13–17; Plate 5, figs. 20–22)

Morphology and identification: These acritarchs are yellow-brown, thick-walled, granulated spheres with a single collared pylome in the middle of a frustoconical collar (Deflandre, 1937). They strongly resemble the specimens of *P. sphaerica* depicted by Warny (2009). However, some specimens encountered in Hole U1357B are found with an additional transparent envelope with a long transparent tail (Plate 4, figs. 13–17). This is similar to the specimens depicted as *Zooplankton* spp. from Prydz Bay (Storkey, 2006, pl. 8, figs. 7–12 and pl. 9, figs. 1–9). However, this envelope is generally not present and probably lost due to the process of lithification.

Biological taxon: The original description of Deflandre (1937) for *Palaeostomocystis sphaerica* was based on a single specimen derived from a Cretaceous flint pebble from the Paris Basin. Although the original specimen of Deflandre (1937) was just 20 µm, Warny (2009) also included specimens sampled from Upper Eocene to Pliocene reworked material around the Antarctic Peninsula, which ranged in size between 40 and 120 µm. Although different in size, these specimens are very similar in shape and wall ornamentation (Warny, 2009: pl. 1, fig. 9; Deflandre, 1937: pl. XII, fig. 6).

Dimensions: The spheres in Hole U1357B range between 123 and 167 µm in diameter (average: 138 µm, $n = 7$).

Geographic distribution: Specimens of *P. sphaerica* identical to those of Hole U1357B and similar to the large specimen depicted by Warny (2009) have also been found in surface samples in Prydz Bay (Storkey, 2006, pl. 8, figs. 7–12 and pl. 9, figs. 1–9). The specimens described by Warny (2009) from surface sediments of the Weddell Sea are considered reworked.

The fossil record: *P. sphaerica* has not been described from prehistoric deposits apart from the original description from the Paris Basin (Deflandre, 1937). *P. sphaerica* sensu Warny (2009) is not known from the fossil record, although the specimens from the Weddell Sea are considered reworked from older strata (Warny, 2009).

Ecological preferences and environmental interpretation: In contrast to the specimens of Warny (2009), the occasional occurrence of this transparent envelope and the presence of cell content in some specimens of Hole U1357B could suggest that these specimens are not reworked from older sediments. Like *P. fritilla*, it has been suggested that *P. sphaerica* is also indicative of a (sub)polar environment and that the older species such as *P. sphaerica* might have evolved a preference for colder surface waters since the Cretaceous (Warny, 2009). However, this assumes that the different *Palaeostomocystis* species are phylogenetically related despite the fact that their biological affinity is uncertain (Warny, 2009). Instead, there is a possibility that the different *Palaeostomocystis* species are biologically unrelated. It is even very possible that the smaller *P. sphaerica* described by Deflandre (1937) from the Cretaceous was produced by a very different species than the specimens encountered in modern surface sediments. Today, similar spherical cysts with a single collared pylome are produced by both parasitic perkinsozoans (Leander and Hoppenrath, 2008; Choi and Park, 2010; Mangot et al., 2011) and spirotrich ciliates (Reid and John, 1983; Reid, 1987; Müller and Wünsch, 1999; Kamiyama, 2013). Resting cysts of the tintinnid ciliates encountered in Hole U1357B (i.e. *Codonellopsis*, *Laackmanniella*, *Cymatocylis*) are, however, unknown and

cannot be compared to *P. sphaerica*. The manner in which some of the specimens found in Hole U1357B and in Prydz Bay are enveloped by a tailed transparent sac does, in fact, resemble a host organism (e.g. dinoflagellate) with a parasitic perkinsozoan cyst that has penetrated the host's cell wall with its germ tube (i.e. pylome) to release its newly formed zoospores (see Leander and Hoppenrath, 2008). On the other hand, it is unlikely that the cell wall of the host organism would be preserved. The biological affinity and ecological preferences of *P. sphaerica* sensu Warny (2009) therefore remain uncertain.

Palaeostomocystis sp. B (Plate 7, figs. 10–13)

Morphology and identification: This is a yellowish, ovoidal vesicle with one polar pylome. The surface of the wall is covered by a yellowish to colourless reticulate network of membranes. In this respect it is very similar to the *Palaeostomocystis reticulata* of Deflandre (1937) found in Cretaceous flint pebbles in the Paris Basin. However, the width of the pylome of *P. reticulata* is almost half the diameter of the vesicle and possesses no collar, while the specimens from Hole U1357B have a relatively small pylome with an outward-extending collar more similar to the smooth-walled *Palaeostomocystis* sp. 1 of Warny (2009). In addition, the reticulate network appears to be denser than the original drawings of *P. reticulata* of Deflandre (1937).

Biological taxon: Like the *P. sphaerica* specimens of Hole U1357B, *Palaeostomocystis* sp. B resembles some of the cysts produced by spirotrich ciliates (Reid and John, 1983; Reid, 1987; Müller and Wünsch, 1999; Kamiyama, 2013), which are known to also produce various kinds of surface-wall ornamentation (Foissner et al., 2007).

Dimensions: These palynomorphs are 33 ± 5 µm long and 22 ± 5 µm wide ($n = 4$).

Geographic distribution: *Palaeostomocystis* sp. B is not known from modern-day surface sediments.

The fossil record: *Palaeostomocystis* sp. B is not known from other fossil records.

Ecological preferences and environmental interpretation: Because the biological affinity is unknown, the ecological preferences are unknown for this palynomorph. However, *Palaeostomocystis* have been associated with (sub)polar environments in general (Warny, 2009).

Palaeostomocystis sp. C (Plate 5, figs. 17–19)

Morphology and identification: A transparent globular vesicle with one polar collared pylome. The rounded shape of this vesicle is somewhat flattened at the opposite side of the pylome.

Biological taxon: Smooth spherical cysts with a single collared pylome are produced by both parasitic perkinsozoans (Leander and Hoppenrath, 2008; Choi and Park, 2010; Mangot et al., 2011) and spirotrich ciliates (Reid and John, 1983; Reid, 1987; Müller and Wünsch, 1999; Kamiyama, 2013). As mentioned above, cysts of the Antarctic spirotrich tintinnids are unknown, so it is uncertain whether *Palaeostomocystis* sp. C belongs to any of these tintinnids.

Dimensions: These palynomorphs are $50 \pm 5\,\mu m$ long and $50 \pm 5\,\mu m$ wide ($n = 3$).

Geographic distribution: *Palaeostomocystis* sp. C is not known from modern-day surface sediments.

The fossil record: *Palaeostomocystis* sp. C is not known from other fossil records.

Ecological preferences and environmental interpretation: Because the biological affinity is unknown, the ecological preferences are unknown for this palynomorph. However, *Palaeostomocystis* have been associated with (sub)polar environments in general (Warny, 2009).

5.7 Palynomorphs of unknown affinity

Palynomorph Type AB-2 (Plate 7, figs. 22–24)

This is a $17 \pm 1\,\mu m$ sized sphere ($n = 3$) with a very thick wall and can appear relatively flat under the light microscope. The wall thickness is about one-fifth of the sphere's diameter. It is transparent without any wall ornamentation. It could therefore be considered as a leiosphere, but because there are also 10 μm sized *Leiosphaeridia* without such a distinct thick wall, we treat Type AB-2 separately.

Palynomorph Type AB-3 (Plate 7, figs. 31–37)

Type AB-3 consists of a flattened spherical "body", such that the cross section is ovoidal, and a "tail" shaped like an open cylinder positioned on one of the flattened surfaces. The membrane forming the cylindrical tail expands around one-half of the body and forms a crenulated crest that decorates the equator of the body. The distal end of the cylindrical membrane is slightly tapered. On the flattened surface of the body across from the tail, a single pylome is present without any collar. The diameter of the pylome is about half the size of the diameter of the flattened surface of the body, which has a diameter of $18 \pm 1\,\mu m$ ($n = 4$). The length of body and tail together is $28 \pm 1\,\mu m$.

Palynomorph Type AB-4 (Plate 7, figs. 38–41)

Type AB-4 is a transparent sphere of about $18 \pm 2\,\mu m$ in diameter ($n = 3$) that is ornamented with 35 to 50 solid processes with a length of about 10 μm. At their distal ends the processes are dendritic, showing multiple bifurcations in a tree-like fashion. These distal "branches" do not seem to interconnect between processes.

Palynomorph Type AB-5 (Plate 7, figs. 25–26)

This palynomorph has a fuzzy appearance, but seems to consist of an inner body with cellular content and an outer spongy layer. Although the cellular content in Type AB-5 is contained in a spherical body, the spongy outer layer of the palynomorph seems to be a polyhedron (edges can be distinguished in the outline). Its size is 23 μm in diameter ($n = 1$).

Palynomorph Type AB-13 (Plate 7, figs. 16–21)

This palynomorph consists of a transparent sphere with a diameter of $11 \pm 2\,\mu m$ ($n = 3$). From this sphere an equatorial, undulating crest extends from which a transparent membrane extends towards both poles. This membrane is striated and/or folded longitudinally and is open at the polar ends. Including the membrane the total length of the palynomorph is $34 \pm 1\,\mu m$ ($n = 3$). The presence of an equatorial membrane is similar to the equatorial alae of some phycomata of prasinophyte algae (Parke et al., 1978).

Palynomorph Type AB-19 (Plate 7, figs. 27–29)

A green or yellowish green subspherical body that is covered with wart-like protrusions. Type AB-19 is about $17 \pm 2\,\mu m$ in diameter ($n = 4$). The wart-like protrusions are solid, circular, or ovoid thickenings of the wall surface about 2–3 μm in diameter.

Palynomorph Type AB-21 (Plate 7, figs. 42–44)

Type AB-21 is thick-walled, slightly ovoidal, and ornamented with solid triangular short spines, which are distributed irregularly at some parts of the wall surface. It has a dark yellow colour and is 22 μm in diameter ($n = 1$). The spines resemble those of a tardigrade egg, but tardigrade eggs are transparent and do not possess such a thick wall. Alternatively, it could be an ornamented pollen grain.

Palynomorph: Type AB-27a–f (Plate 4, figs. 12, 18; Plate 6, figs. 6–9)

Within the samples of Hole U1357B there is a variety of thick-walled domes and cones that all share a characteristic semicircular to subtriangular cavity at the base. Their sizes range from 52 to 243 μm long (average: 124 μm, $n = 8$). Some shapes resemble the lorica of a tintinnid ciliate, but tintinnid loricae have a much thinner hyaline wall. Also, all specimens have a thick-walled base and therefore cannot house a single-celled organism. Instead, the cavity is open laterally. If these are in fact parts of a crustacean exoskeleton, it is unknown to which part they belong. We distinguish six different morphotypes: (a) dome-shaped with a broad base, (b) dome-shaped with height and width being equal, (c) bullet-shaped, (d) triangular, (e) triangular with long acute tip, and (f) falcate.

Palynomorph: Type AB-28 (Plate 6, fig. 11)

This is a flat, circular palynomorph, but at one side of the palynomorph two rounded indents interrupt the circular outline. Its diameter is about 117 µm ($n = 1$). It is possible that this is part of an arthropod exoskeleton.

Palynomorph: Type AB-29 (Plate 6, fig. 10)

Sickle-shaped exoskeleton parts extending from a broad base. The sickles are about 44 ± 4 µm long ($n = 2$).

Palynomorph: Type AB-30 (Plate 6, fig. 12)

These are long, yellow, curved blades that are hollow inside. They are generally longer than 100 µm. The lack of distinct characteristics makes it difficult to assign these types of palynomorphs to a particular organism. As discussed above, such forms can be parts of crustacean mandibles or the jaw apparatus of eunicid annelids, although the remains of the latter have a distinct dark red colour in the samples of U1357B. Alternatively they could be the grasping spines positioned on the posterolateral sides of the heads of chaetognaths, which they use for capturing prey (Ball and Miller, 2006). These grasping spines are also hollow and can be longer than 100 µm (for detailed SEM images see Szaniawski, 2002). Chaetognaths are the second most abundant zooplankton group in the Southern Ocean after the copepods, on which they prey (Froneman and Pakhomov, 1998; Terazaki et al., 2013). Also in the Southern Ocean north of the Adélie Coast, chaetognaths, particularly *Eukrohnia hamata* and *Sagitta gazellae*, have been recorded, although their abundance decreases towards higher latitudes due to the scarcity of larger copepod species (Terazaki et al., 2013). However, the number of the deeper-dwelling *E. hamata* particularly increases when the sea ice disappears in spring–summer (Terazaki et al., 2013). It is thus very possible that their grasping spines end up in the sediments of the Adélie Basin.

Palynomorph: Type AB-31 (Plate 6, figs. 15–18)

This palynomorph resembles a hollow thorn. It is similar to Type AB-30, but much shorter: 25 ± 1 µm ($n = 2$). In addition, the bottom aperture, which is about 10 µm, has an outward-extending rim a few micrometres wide. As with Type AB-30, it is unclear to what organism this palynomorph belongs due to the lack of characteristic features. However, the size of Type AB-31 makes it too small to be the remains of chaetognath grasping spines. Alternatively, we found that the circular rim around the aperture is the same size as the pylome of *Palaeostomocystis sphaerica*, which means that Type AB-31 could be the plugs of *P. sphaerica*. These plugs would detach when the content of *P. sphaerica* would have been released, similar to the way the cysts of spirotrich ciliates release an operculum to allow the ciliate to escape (Reid

and John, 1983; Reid, 1987; Müller and Wünsch, 1999). However, spirotrich cysts with a pointy operculum are not known to us.

Palynomorph: Type AB-32 (Plate 6, fig. 13–14)

This is a tooth-like palynomorph with a semicircular outline, one central posterior (proximal) cone, and eight symmetrically arranged anterior (distal) cones. Of the anterior cones the second cone from the centre of the tooth is the largest. The tooth is 82 µm high and 61 µm wide ($n = 1$). It shows resemblance to some conodont teeth, although conodont teeth are generally somewhat larger and conodonts are long extinct (Ulrich and Bassler, 1926). More likely this is a mandible part, the tooth of a eunicid annelid, or a chaetognath unknown to us.

5.8   Reworked palynomorphs

5.8.1   Dinoflagellate cysts

Order GONYAULACALES Taylor 1980

Suborder GONYAULACINEAE (autonym)

Family AREOLIGERACEAE Evitt 1963

Genus *Enneadocysta* Stover & Williams 1995 emend. Fensome et al. 2006

Enneadocysta dictyostila (Menéndez 1965) Stover & Williams 1995 emend. Sarjeant 1981 (Plate 1, figs. 25–26)

Morphology and identification: The species *Enneadocysta dictyostila* has been the subject of substantial taxonomic debate (Sarjeant, 1981; Fensome et al., 2006). It can be recognized by its large apical archaeopyle and ragged clypeate processes (processes possessing a distal perforate quadrate or polygonal platform with broken margins) (Fensome et al., 2006). Clypeate processes and an apical archaeopyle are also present in the species *Areosphaeridium diktyoplokum* (Klumpp 1953) Eaton 1971 emend. Stover & Williams 1995; however, *A. diktyoplokum* possesses only one process on its antapical plate, while *E. dictyostila* possesses two (Fensome et al., 2006). Also, the margins of the distal perforate platforms are mostly continuous (entirely clypeate) in *A. diktyoplokum* (Fensome et al., 2006).

Biological taxon: Irrelevant because this species is part of the reworked microfossil assemblage.

Dimensions: The diameter of the cyst not including its processes ranges between 44 and 81 µm (average: 65 µm, $n = 5$).

Geographic distribution: This species has no modern-day distribution.

The fossil record: In the Southern Ocean *E. dictyostila* ranges from the mid-Eocene to just past the Eocene–Oligocene boundary (Bijl et al., 2013). In younger sediments it is a common species in the reworked assemblage (as *Enneadocysta partridgei* in Hannah, 2006; Warny et al., 2006).

Order PERIDINIALES Haeckel 1894

Suborder PERIDINIINEAE Fensome et al. 1993

Family PERIDINIACEAE Ehrenberg 1831

Subfamily DEFLANDREOIDEAE Bujak & Davies 1983

Genus *Spinidinium* Cookson & Eisenack 1962 emend. Sluijs et al. 2009

Spinidinium colemanii Wrenn & Hart 1988 (Plate 1, figs. 10–12)

Morphology and identification: This circumcavate dinoflagellate cyst is characterized by penitabular capitate spines, an apical horn, and a posteriorly attached (adnate) operculum consisting of one intercalary plate (Wrenn and Hart, 1988; Sluijs et al., 2009). In terms of ornamentation, it is therefore quite similar to *Vozzhennikovia stickleyae*.

Biological taxon: Irrelevant because this species is part of the reworked microfossil assemblage.

Dimensions: Its length including the apical horn is $57 \pm 5\,\mu\text{m}$ ($n = 3$).

Geographic distribution: This species has no modern-day geographic distribution.

The fossil record: The stratigraphic range of *S. colemanii* is from the late Palaeocene to Eocene (Sluijs et al., 2003).

Genus *Vozzhennikovia* Lentin & Williams 1976

Vozzhennikovia apertura (Wilson 1967) Lentin & Williams 1976 (Plate 1, fig. 9)

Morphology and identification: This is a horned, transparent cornucavate dinoflagellate cyst, which can be easily distinguished by its archaeopyle formed through the loss of three intercalary plates and its ornamentation of pointed or flat-tipped short spines (as *Spinidinium aperturum* in Wilson, 1967).

Biological taxon: Unknown because this is the cyst of an extinct dinoflagellate.

Dimensions: Its length including the apical horn is about $41 \pm 1\,\mu\text{m}$ ($n = 2$).

Geographic distribution: This species has no modern-day geographic distribution.

The fossil record: *V. apertura* has a stratigraphic range in the Southern Ocean of Palaeocene to Eocene (Bijl et al., 2013). Despite the fact that its stratigraphic range is restricted to the Palaeogene, it is a commonly found species since the Oligocene in other cores drilled near the Antarctic coast, where it is considered part of the reworked assemblage (Hannah et al., 2000; Hannah and Fielding, 2001; Yi et al., 2005; Hannah, 2006; Warny et al., 2006, 2009; Bijl et al., 2018), because Eocene strata dip up to the surface on the Wilkes Land margin (Truswell, 1982; Expedition 318 Scientists, 2011)

Vozzhennikovia netrona Levy & Harwood 2000 emend. Sluijs et al. 2009 (Plate 1, figs. 22–24)

Morphology and identification: This species has short capitate spines similar to *Vozzhennikovia apertura*, but has in addition to the apical horn a very distinctive antapical horn (Sluijs et al., 2009).

Biological taxon: Irrelevant because this species is part of the reworked microfossil assemblage.

Dimensions: Its length including the apical and antapical horn is $66\,\mu\text{m}$ ($n = 1$).

Geographic distribution: This species has no modern-day geographic distribution.

The fossil record: The stratigraphic range of *V. netrona* is from the middle to late Eocene (Sluijs et al., 2003, 2009).

5.8.2 Pollen and spores

Phylum TRACHEOPHYTA Sinnot ex Cavalier-Smith 1998

Palynomorphs: pollen and spores (Plate 3, figs. 18–19)

Morphology and identification: Remains of vascular plants are scarce within Hole U1357B and consist mainly of pollen and spores. The most common pollen grains belong to the genera *Nothofagidites* (Plate 3, fig. 18) and *Podocarpidites* (Plate 3, fig. 19). The *Nothofagidites* pollen grains are transparent, flattened spheres with a scabrate wall ornamentation and possess seven colpi. The *Podocarpidites* pollen grains are brown-coloured bisaccate pollen grains with a reticulate wall structure on the sacci. We have not identified other pollen and spores down to the species level.

Biological taxon: *Nothofagidites* and *Podocarpidites* are pollen grains of *Nothofagus* trees and Podocarpaceae, respectively.

Dimensions: Most pollen and spores found in Hole U1357B are between 20 and 40 μm.

Geographic distribution: Pollen assemblages dominated by *Nothofagidites* and *Podocarpidites* have been associated with the modern-day (sub)alpine, cold, or temperate rainforests of southern South America, Tasmania, Australia, New Caledonia, New Guinea, and New Zealand (Kennett and Barker, 1990; Roberts et al., 2003; Pross et al., 2012)

The fossil record: Pollen grains of *Nothofagus* and podocarps are found in situ since the Late Cretaceous ranging possibly into the Pliocene and are the dominant vegetation of the Antarctic tundra during the Oligocene and Miocene (Hill and Scriven, 1995; Askin and Raine, 2000; Troedson and Riding, 2002; Prebble et al., 2006; Warny et al., 2006; Pross et al., 2012; Sangiorgi et al., 2018).

6   Conclusions

We describe a total of 74 palynomorphs, which are discussed based on an extensive literature survey to resolve their biological origin and what they represent ecologically. This review serves as a resource for future studies along the Antarctic margin. All the palynomorphs of Hole U1357B represent at least 40 different in situ species. Such diversity illustrates the species richness of a polynya-controlled environment at the Antarctic coast and further highlights the importance of finding well-preserved strata to reconstruct biotic response to past climate or oceanographic changes.

Particularly among the dinoflagellates and tintinnids there is a high degree of Southern Ocean endemism, which reflects the influence of the seasonal sea-ice system. Some of these species have been linked directly to an Antarctic coastal setting (e.g. *Nucicla umbiliphora*; Hartman et al., 2018) and the formation of sea ice and brine release (e.g. *Polarella glacialis*; Thomson et al., 2006). Among the other palynological remains, particularly prasinophytes, leiospheres, and *Palaeostomocystis* have also been linked to a sea-ice-controlled environment (Mudie, 1992; Daugbjerg, 2000; Moro et al., 2002; Warny, 2009). On the other hand, we find the remains of more cosmopolitan species, such as the dinoflagellate *Gymnodinium microreticulatum* and the tintinnid *Codonellopsis pusilla*.

In addition to the richness of the assemblage, the state of preservation in Hole U1357B is truly exceptional. This is evident from the findings of easily degradable species such as cysts of *Polarella glacialis* (Montresor et al., 1999) also

in the lower parts of the sedimentary sequence (Hartman, 2018c), while in general the preservation of organic carbon and palynomorphs at the Antarctic margin and on the Antarctic shelves is very poor (Sackett, 1986; Kvenvolden et al., 1987; Venkatesan and Kaplan, 1987; Wrenn et al., 1998) due to intensive oxygen delivery, strong ocean currents, and therefore the effective remineralization of organic matter (De Vernal and Marret, 2007; Zonneveld et al., 2010).

The palynomorph record of Hole U1357B is an important source for reconstructing Holocene Antarctic climate variability for future work (Hartman et al., 2018c). This extensive review of organic microfossil associations provides the basis to implement an additional tool, next to diatoms, to reconstruct palaeoenvironmental and palaeoceanographic changes in sites close to the Antarctic margin, while considering a wider portion of the ecosystem (primary and secondary producers). This will be presented in another study.

References

Agatha, S.: A Light and Scanning Electron Microscopic Study of the Closing Apparatus in Tintinnid Ciliates (Ciliophora, Spirotricha, Tintinnida): A Forgotten Synapomorphy, J. Eukaryot. Microbiol., 57, 297–307, https://doi.org/10.1111/j.1550-7408.2010.00490.x, 2010.

Agatha, S. and Simon, P.: On the Nature of Tintinnid Loricae (Ciliophora: Spirotricha: Tintinnina): a Histochemical, Enzymatic,

EDX, and High-resolution TEM Study, Acta Protozool., 51, 1–19, https://doi.org/10.4467/16890027AP.12.001.0384, 2012.

Agatha, S. and Strüder-Kypke, M. C.: Reconciling Cladistic and Genetic Analyses in Choreotrichid Ciliates (Ciliophora, Spirotricha, Oligotrichea), J. Eukaryot. Microbiol., 59, 325–350, https://doi.org/10.1111/j.1550-7408.2012.00623.x, 2012.

Agatha, S. and Strüder-Kypke, M. C.: Systematics and Evolution of Tintinnid Ciliates, in: The Biology and Ecology of Tintinnid Ciliates: Models for Marine Plankton, edited by: Dolan, J. R., Montagnes, D. J. S., Agatha, S., Coats, D. W., and Stoecker, D. K., 42–84, Wiley-Blackwell, Hoboken, New Jersey, USA, 2013.

Agatha, S., Laval-Peuto, M., and Simon, P.: The Tintinnid Lorica, in: The Biology and Ecology of Tintinnid Ciliates: Models for Marine Plankton, edited by: Dolan, J. R., Montagnes, D. J. S., Agatha, S., Coats, D. W., and Stoecker, D. K., 17–41, Wiley-Blackwell, Hoboken, New Jersey, USA, 2013.

Alder, V. A.: Tintinnoinea, in: South Atlantic zooplankton, Vol. 1, edited by: Boltovskoy, D., 321–384, Backhuys Publishers, Leiden, the Netherlands, 1999.

Alder, V. A. and Boltovskoy, D.: Microplanktonic distributional patterns west of the Antarctic Peninsula, with special emphasis on the Tintinnids, Polar Biol., 11, 103–112, 1991.

Altiero, T., Bertolani, R., and Rebecchi, L.: Hatching phenology and resting eggs in tardigrades, J. Zool., 280, 290–296, https://doi.org/10.1111/j.1469-7998.2009.00664.x, 2010.

Amenábar, C. R., Candel, M. S., and Guerstein, G. R.: Small Antarctic Late Cretaceous Chorate Dinoflagellate Cysts?: Biological and Palaeoenvironmental Affinities, Palynology, 38, 303–323, 2014.

Amorim, A., Dale, B., Godinho, R., and Brotas, V.: *Gymnodinium catenatum*-like cysts (Dinophyceae) in recent sediments from the coast of Portugal, Phycologia, 40, 572–582, https://doi.org/10.2216/i0031-8884-40-6-572.1, 2001.

Anderson, D. M., Jacobson, D. M., Bravo, I., and Wrenn, J. H.: The unique, microreticulate cyst of the naked dinoflagellate Gymnodinium catenatum, J. Phycol., 24, 255–262, 1988.

Andreoli, C., Tolomio, C., Moro, I., Radice, M., Moschin, E., and Bellato, S.: Diatoms and dinoflagellates in Terra Nova Bay (Ross Sea-Antarctica) during austral summer 1990, Polar Biol., 15, 465–475, https://doi.org/10.1007/BF00237460, 1995.

Andreoli, C., Moro, I., La Rocca, N., Valle, L. D., Masiero, L., Rascio, N., and Vecchia, F. D.: Ecological, physiological, and biomolecular surveys on microalgae from Ross Sea (Antarctica), Ital. J. Zool., 67, 147–156, https://doi.org/10.1080/11250000009356370, 2000.

Apstein, C.: Die Pyrocysteen der Plankton-Expedition, in: Ergebnisse der Plankton-Expedition der Humboldt-Stiftung, Bd. IV M.c., Lipsius and Tischer, Kiel and Leipzig, 1–27, 1909.

Arai, M. and Koutsoukos, E. A. M.: Palynoforaminifera (Foraminiferal Organic Linings and Allied Material: a New Tool for Petroleum Exploration, Am. Assoc. Petr. Geol. AAPG Int. Conf. Exhib. Ext. Abstr. Vol., 82, 584–585, 1998.

Armbrecht, L. H., Eriksen, R., Leventer, A., and Armand, L. K.: First observations of living sea-ice diatom agglomeration to tintinnid loricae in East Antarctica, J. Plankton Res., 39, 795–802, https://doi.org/10.1093/plankt/fbx036, 2017.

Arrigo, K. R. and van Dijken, G. L.: Phytoplankton dynamics within 37 Antarctic coastal polynya systems, J. Geophys. Res., 108, 3271, https://doi.org/10.1029/2002JC001739, 2003.

Arrigo, K. R., Weiss, A. M., and Smith, W. O. J.: Physical forcing of phytoplankton dynamics in the southwestern Ross Sea, J. Geophys. Res., 103, 1007–1021, 1998.

Askin, R. A. and Raine, J. I.: Oligocene and Early Miocene Terrestrial Palynology of the Cape Roberts Drillhole CRP-2/2a, Victoria Land Basin, Antarctica, Terra Ant., 7, 493–501, 2000.

Assmy, P., Cisewski, B., Henjes, J., Klaas, C., Montresor, M., and Smetacek, V.: Response of the protozooplankton assemblage during the European Iron Fertilization Experiment (EIFEX) in the Antarctic circumpolar current, J. Plankton Res., 36, 1175–1189, https://doi.org/10.1093/plankt/fbu068, 2014.

Atanassova, J.: Palaeoecological setting of the western Black Sea area during the last 15 000 years, Holocene, 15, 576–584, 2005.

Atkinson, A.: Life cycle strategies of epipelagic copepods in the Southern Ocean, J. Marine Syst., 15, 289–311, 1998.

Atkinson, A., Hunt, B. P. V., Pakhomov, E. A., and Hosie, G. W.: Overview of Southern Ocean Zooplankton data: Abundance, Biomass, Feeding and Funtional Relationships, CCAMLR Sci., 19, 171–218, 2012.

Attaran-Fariman, G., de Salas, M. F., Negri, A. P., and Bolch, C. J. S.: Morphology and phylogeny of *Gymnodinium trapeziforme* sp. nov. (Dinophyceae): a new dinoflagellate from the southeast coast of Iran that forms microreticulate resting cysts, Phycologia, 46, 644–656, https://doi.org/10.2216/07-05.1, 2007.

Australian Antarctic Data Center: Electron Micrograph Database – Marine Specimens, Occurrence Dataset, https://doi.org/10.15468/5ubdem (last access: 8 February 2018), 2017.

Balech, E.: Dinoflagellés et Tintinnides de la Terre Adélie (Secteur Français Antarctique), Vie Milieu, 8, 382–408, 1958a.

Balech, E.: Plancton de la Campaña Antárctica Argentina, Physis, 21, 75–108, 1958b.

Balech, E.: Segunda contribucion al conocimiento del microplancton del mar de Bellingshausen, Contrib. del Inst. Antart. Argentino, 107, 1–63, 1973.

Ball, E. E. and Miller, D. J.: Phylogeny?: The Continuing Classificatory Conundrum of Chaetognaths, Curr. Biol., 16, R593–R596, https://doi.org/10.1016/j.cub.2006.07.005, 2006.

Bartels, P. J., Pilato, G., Lisi, O., and Nelson, D. R.: Macrobiotus (Eutardigrada, Macrobiotidae) from the Great Smoky Mountains National Park, Tennessee/North Carolina, USA (North America): two new species and six new records, Zootaxa, 2022, 45–57, https://doi.org/10.5281/zenodo.186100, 2009.

Beijerinck, M. W.: Culturversuche mit Zoochlorellen, Lichenengonidien und anderen niederen Algen, Botanische Zeitung, 48, 725–739, 741–754, 757–768, 781–785, 1890.

Bell, E. M. and Laybourn-Parry, J.: Mixotrophy in the Antarctic phytoflagellate, *Pyramimonas gelidicola* (Chlorophyta: Prasinophyceae), J. Phycol., 39, 644–649, 2003.

Belmonte, G.: Diapause egg production in *Acartia (Paracartia) latisetosa* (Crustacea, Copepoda, Calanoida), B. Zool., 59, 363–366, https://doi.org/10.1080/11250009209386694, 1992.

Belmonte, G.: The egg morphology of 7 Acartiidae species?: a preliminary survey of the ootaxonomy of calanoids, J. Marine Syst., 15, 35–39, 1998.

Benedek, P. N.: Phytoplanktonen aus dem Mittel- und Oberoligozän von Tönisberg (Niederrheingebiet), Palaeontographica, Abt. B, 137, 1–71, 1972.

Bérard-Therriault, L., Poulin, M., and Bossé, L.: Guide d'intification du phytoplancton marin de l'estuaire et du Golfe du Saint-Laurent incluant également certaints protozoaires, Publication spéciale canadienne des sciences haleutiques et aquatiques, 128, p. 387, 1999.

Berasategui, A. A., Hoffmeyer, M. S., Dutto, M. S., and Biancalana, F.: Marine Science, ICES J. Mar. Sci., 69, 380–388, 2012.

Bertolani, R. and Rebecchi, L.: A revision of the *Macrobiotus hufelandi* group (Tardigrada, Macrobiotidae), with some observations on the taxonomic characters of eutardigrades, Zool. Scr., 22, 127–152, https://doi.org/10.1111/j.1463-6409.1993.tb00347.x, 1993.

Bertolani, R., Rebecchi, L., and Claxton, S. K.: Phylogenetic significance of egg shell variation in tardigrades, Zool. J. Linn. Soc.-Lond., 116, 139–148, 1996.

Bijl, P. K., Sluijs, A., and Brinkhuis, H.: A magneto- and chemostratigraphically calibrated dinoflagellate cyst zonation of the early Palaeogene South Pacific Ocean, Earth-Sci. Rev., 124, 1–31, https://doi.org/10.1016/j.earscirev.2013.04.010, 2013.

Bijl, P. K., Houben, A. J. P., Bruls, A., Pross, J., and Sangiorgi, F.: Stratigraphic calibration of Oligocene–Miocene organic-walled dinoflagellate cysts from offshore Wilkes Land, East Antarctica, and a zonation proposal, J. Micropalaeontol., 37, 105–138, https://doi.org/10.5194/jm-37-105-2018, 2018.

Bjørnsen, P. K. and Kuparinen, J.: Growth and herbivory by heterotrophic dinoflagellates in the Southern Ocean, studied by microcosm experiments, Mar. Biol., 109, 397–405, https://doi.org/10.1007/BF01313505, 1991.

Boere, A. C., Abbas, B., Rijpstra, W. I. C., Versteegh, G. J. M., Volkman, J. K., Sinninghe Damsté, J. S., and Coolen, M. J. L.: Late-Holocene succession of dinoflagellates in an Antarctic fjord using a multi-proxy approach: Paleoenvironmental genomics, lipid biomarkers and palynomorphs, Geobiology, 7, 265–281, https://doi.org/10.1111/j.1472-4669.2009.00202.x, 2009.

Bolch, C., Negri, A. P., and Hallegraeff, G. M.: *Gymnodinium microreticulatum* sp. nov. (Dinophyceae): a naked, microreticulate cyst-producing dinoflagellate, distinct from *Gymnodinium catenatum* and *Gymnodinium nolleri*, Phycologia, 38, 301–313, https://doi.org/10.2216/i0031-8884-38-4-301.1, 1999.

Bolch, C. J. S. and Reynolds, M. J.: Species resolution and global distribution of microreticulate dinoflagellate cysts, J. Plankton Res., 24, 565–578, 2002.

Boltovskoy, D., Dinofrio, E. O., and Alder, V. A.: Intraspecific variability in Antarctic tintinnids?: the Cymatocylis affinislconvallaria species group, J. Plankton Res., 12, 403–413, 1990.

Bonnet, S., de Vernal, A., Hillaire-Marcel, C., Radi, T., and Husum, K.: Variability of sea-surface temperature and sea-ice cover in the Fram Strait over the last two millennia, Mar. Micropaleontol., 74, 59–74, https://doi.org/10.1016/j.marmicro.2009.12.001, 2010.

Borromei, A. M., Coronato, A., Franzén, L. G., Ponce, J. F., Sáez, J. A. L., Maidana, N., Rabassa, J., and Candel, M. S.: Multiproxy record of Holocene paleoenvironmental change, Tierra del Fuego, Argentina, Palaeogeogr. Palaeocl., 286, 1–16, https://doi.org/10.1016/j.palaeo.2009.11.033, 2010.

Brinkhuis, H., Munsterman, D. K., Sengers, S., Sluijs, A., Warnaar, J., and Williams, G. L.: Late Eocene-Quaternary dinoflagellate cysts from ODP Site 1168, off Western Tasmania, Proc. ODP, Sci. Results, 189, 1–36, 2003.

Brünnich, M. T.: Zoologiae fundamenta praelectionibus academicis accomodata. Grunde i dyrelaeren, Friderik Christian Pelt, Hafnia et Lipsia, p. 253, 1772.

Buck, K. R., Bolt, P. A., Bentham, W. N., and Garrison, D. L.: A dinoflagellate cyst from Antarctic sea ice, J. Phycol., 28, 15–18, 1992.

Bujak, J. P.: Cenozoic Dinoflagellate Cysts and Acritarchs from the Bering Sea and Northern North Pacific, DSDP Leg 19, Micropaleontology, 30, 180–212, https://doi.org/10.2307/1485717, 1984.

Bujak, J. P. and Davies, E. H.: Modern and fossil Peridiniineae, American Association of Stratigraphic Palynologists, Contribution Series, 13, 202, 1983.

Bujak, J. P. and Davies, E. H.: Protoperidiniaceae fam. nov. – Type: Protoperidinium Bergh, Taxon, 47, 729, 1998.

Bütschli, O.: Dr. H. G. Bronn's Klassen und Ordnungen Thier-Reichs, wissenschaftlich dargestellt in Wort und Bild, C. F. Winter'sche Verlagshandlung, Leipzig and Heidelberg, 1096, 1885.

Candel, M. S., Borromei, A. M., Martínez, M. A., and Bujalesky, G.: Palynofacies analysis of surface sediments from the Beagle Channel and its application as modern analogues for Holocene records of Tierra del Fuego, Argentina, Palynology, 37, 62–76, https://doi.org/10.1080/01916122.2012.718994, 2013.

Cărăuş, I.: Algae of Romania. A distributional checklist of actual algae., Stud. Cercet.-Biologie, 7, 1–1002, 2017.

Castellani, C. and Lucas, I. A. N.: Seasonal variation in egg morphology and hatching success in the calanoid copepods *Temora longicornis*, *Acartia clausi* and *Centropages hamatus*, J. Plankton Res., 25, 527–537, 2003.

Cavalier-Smith, T.: Eukaryote kingdoms: Seven or nine?, BioSystems 14, 461–481, 1981.

Cavalier-Smith, T.: The origin of eukaryotic and archaebacterial cells, Ann. N.Y. Acad. Sci., 503, 17–54, 1987.

Cavalier-Smith, T.: Cell diversification in heterotrophic flagellates, in: The Biology of Free-Living Heterotrophic Flagellates, edited by: Patterson, D. J. and Larsen, J., 113–131, Oxford University Press, Oxford, UK, 1991.

Cavalier-Smith, T.: A revised six-kingdom system of life, Biol. Rev., 73, 203–266, 1998.

Cavalier-Smith, T.: The phagotrophic origin of eukaryotes and phylogenetic classification of Protozoa, Int. J. Syst. Evol. Micr., 52, 297–354, 2002.

Cavalier-Smith, T.: Kingdoms Protozoa and Chromista and the eozoan root of the eukaryotic tree, Biol. Lett., 6, 342–345, 2010.

Chadefaud, M.: Les cellules nageuses des algues dans l'embranchement de Chromophycées, C. R. Acad. Sci. Paris, 231, 788–790, 1950.

Chamberlin, R. V.: The Annelida Polychaeta, Memoirs of the Museum of Comparative Zoölogy at Harvard Collage, 48, 1–514, 1919.

Choi, K.-S. and Park, K.-I.: Review on the Protozoan Parasite Perkinsus olseni (Lester and Davis 1981) Infection in Asian Waters, in: Coastal Environmental and Ecosystem Issues of the East China Sea, edited by: Ishimatsu, A. and Lie, H.-J., 269–281, TERRAPUB and Nagasaki University, Nagasaki, Japan, 2010.

Claparède, E. and Mecznikow, E.: Beiträge zur Kenntniss der Entwickelungsgeschichte der Chaetopoden, Zeitschrift für Wissenschaftliche Zoologie, 19, 163–205, 1869.

Clarke, A. and Leakey, R. J. G.: The seasonal cycle of phytoplankton, macronutrients, and the microbial community in a

nearshore Antarctic marine ecosystem., Limnol. Oceanogr., 41, 1281–1294, 1996.

Cleve, P. T.: Some Atlantic Tintinnodea, Öfversigt af Konglig Vetenskaps-Akademiens Förhandlingar, 10, 969–975, 1899.

Clowes, C. D., Hannah, M. J., Wilson, G. J., and Wrenn, J. H.: Marine Micropaleontology Marine palynostratigraphy and new species from the Cape Roberts drill-holes, Victoria land basin, Antarctica, Mar. Micropaleontol., 126, 65–84, https://doi.org/10.1016/j.marmicro.2016.06.003, 2016.

Colbath, G. K. and Grenfell, H. R.: Review of biological affinities of Paleozoic acid-resistant, organic-walled eukaryotic algal microfossils (including "acritarchs"), Rev. Palaeobot. Palyno., 86, 287–314, 1995.

Concheyro, A., Caramés, A., Amenábar, C. R., and Lescano, M.: Nannofossils, foraminifera and microforaminiferal linings in the Cenozoic diamictites of Cape Lamb, Vega Island, Antarctica, Pol. Polar Res., 35, 1–26, https://doi.org/10.2478/popore-2014-0003, 2014.

Convey, P. and McInnes, S. J.: Exceptional tardigrade-dominated ecosystems in Ellsworth Land, Antarctica, Ecology, 86, 519–527, 2005.

Convey, P., Gibson, J. A. E., Hillenbrand, C.-D., Hodgson, D. A., Pugh, P. J. A., Smellie, J. L., and Stevens, M. I.: Antarctic terrestrial life – challenging the history of the frozen continent?, Biol. Rev., 83, 103–117, https://doi.org/10.1111/j.1469-185X.2008.00034.x, 2008.

Cookson, I. C. and Eisenack, A.: Additional microplankton from the Australian Cretaceous sediments, Micropaleontology, 8, 485–507, 1962.

Corliss, B. H.: Morphology and microhabitat preferences of benthic foraminifera from the northwest Atlantic Ocean, Mar. Micropaleontol., 17, 195–236, https://doi.org/10.1016/0377-8398(91)90014-W, 1991.

Costello, O. P. and Bauch, H. A.: Late Pleistocene-Holocene productivity record of benthic foraminifera from the Iceland Plateau (Core PS 1246-2), in: Contributions of the Micropaleontology and Paleoceanography of the Northern North Atlantic, edited by: Hass, H. C. and Kaminski, M. A., 141–148, Grzybowski Foundation Special Publication, Krakow, 1997.

Cromer, L., Gibson, J. A. E., Swadling, K. M., and Ritz, D. A.: Faunal microfossils?: Indicators of Holocene ecological change in a saline Antarctic lake, Palaeogeogr. Palaeocl., 221, 83–97, https://doi.org/10.1016/j.palaeo.2005.02.005, 2005.

Cromer, L., Gibson, J. A. E., McInnes, S. J., and Agius, J. T.: Tardigrade remains from lake sediments, J. Paleolimnol., 39, 143–150, https://doi.org/10.1007/s10933-007-9102-5, 2008.

Crouch, E. M., Mildenhall, D. C., and Neil, H. L.: Distribution of organic-walled marine and terrestrial palynomorphs in surface sediments, offshore eastern New Zealand, Mar. Geol., 270, 235–256, https://doi.org/10.1016/j.margeo.2009.11.004, 2010.

Dahl, E.: Some crustacean relationships, in: Festschrift für Bertil Hanström: Zoological Papers in Honour of his Sixty-Fifth Birthday, edited by: Wingstrand, K. G., 138–147, Zoological Institute, Lund, 1956.

Dastych, H. and Harris, J. M.: A new species of the genus *Macrobiotus* from inland nunataks in western Dronning Maud Land, continental Antarctica (Tardigrada), Entomol. Mitt. Zool. Mus. Hamburg, 11, 175–182, 1995.

Daugbjerg, N.: Pyramimonas tychotreta, sp. nov. (Prasinophyceae), a new marine species from Antarctica: light and electron microscopy of the motile stage and notes on growth rates, J. Phycol., 36, 160–171, 2000.

Davies, C., Watts, D.: The Australian Phytoplankton Database (1844 onwards), CSIRO Oceans and Atmosphere, Occurrence Dataset, https://doi.org/10.15468/my3fxc (last access: 8 February 2018), 2017.

Defaye, D., Cuoc, C., and Brunet, M.: Genital structures and spermatophore placement in female Paradiaptominae (Copepoda, Calanoida, Diaptomidae), J. Crustacean Biol., 20, 245–261, https://doi.org/10.1651/0278-0372(2000)020[0245:GSASPI]2.0.CO;2, 2000.

Deflandre, G.: Microfossiles des Silex Crétacés. Deuxième partie: Flagellés incertae sedis, Hystrichosphaeridés, Sarconidés, Organismes divers, Ann. Paléontologie, 26, 51–103, 1937.

Deppeler, S. L. and Davidson, A. T.: Southern Ocean Phytoplankton in a Changing Climate, Front. Mar. Sci., 4, 40, https://doi.org/10.3389/fmars.2017.00040, 2017.

De Schepper, S., Fischer, E. I., Groeneveld, J., Head, M. J., and Matthiessen, J.: Deciphering the palaeoecology of Late Pliocene and Early Pleistocene dinoflagellate cysts, Palaeogeogr. Palaeocl., 309, 17–32, https://doi.org/10.1016/j.palaeo.2011.04.020, 2011.

De Vernal, A.: Marine palynology and its use for studying nearshore environments, IOP C. Ser. Earth Env., 5, 1–13, https://doi.org/10.1088/1755-1307/5/1/012002, 2009.

De Vernal, A. and Marret, F.: Chapter Nine Organic-Walled Dinoflagellate Cysts: Tracers of Sea-Surface Conditions, in: Developments in Marine Geology, 1, 371–408, Elsevier B.V., Amsterdam and London, 2007.

De Vernal, A., Goyette, C., and Rodrigues, C. G.: Contribution palynostratigraphique (dinokystes, pollen et spores) à la connaissance de la mer de Champlain: coupe de Saint-Césaire, Québec, Can. J. Earth Sci., 26, 2450–2464, 1989.

De Vernal, A., Rochon, A., Turon, J.-L., and Matthiessen, J.: Organic-walled Dinoflagellate Cysts: Palynol,gial Tracers of Sea-surface Conditions in Middle to High Latitude Marine Environments, Geobios, 30, 905–920, 1997.

De Vernal, A., Henry, M., Matthiessen, J., Mudie, P. J., Rochon, A., Boessenkool, K. P., Eynaud, F., Grøsfjeld, K., Joel, G., Hamel, D., Harland, R., Head, M. J., Kunz-Pirrung, M., Levac, E., Loucheur, V., Peyron, O., Pospelova, V., Radi, T., Turon, J., and Voronina, E.: Dinoflagellate cyst assemblages as tracers of sea-surface conditions in the northern North Atlantic, Arctic and sub-Arctic seas?: the new "$n = 677$" data base and its application for quantitative palaeoceanographic reconstruction, J. Quaternary Sci., 16, 681–698, https://doi.org/10.1002/jqs.659, 2001.

Doflein, F.: Die Protozoen als Parasiten und Krankheitserreger nach biologischen Gesichtspunkten dargestellt, Jena, Gustav Fischer, 274, 1901.

Dolan, J. R. and Pierce, R. W.: Diversity and Distributions of Tintinnids, in: The Biology and Ecology of Tintinnid Ciliates: Models for Marine Plankton, edited by: Dolan, J. R., Montagnes, D. J. S., Agatha, S., Coats, D. W., and Stoecker, D. K., 214–243, Wiley-Blackwell, Hoboken, New Jersey, USA., 2013.

Dolan, J. R., Pierce, R. W., Yang, E. J., and Kim, S. Y.: Southern ocean biogeography of tintinnid ciliates of

the marine plankton, J. Eukaryot. Microbiol., 59, 511–519, https://doi.org/10.1111/j.1550-7408.2012.00646.x, 2012.

Dolan, J. R., Yang, E. J., Lee, S. H., and Kim, S. Y.: Tintinnid ciliates of Amundsen Sea (Antarctica) plankton communities, Polar Res., 32, 19784, https://doi.org/10.3402/polar.v32i0.19784, 2013.

D'Orbigny, M. D.: Tableau méthodique de la classe des Céphalopodes, Ann. Sci. Nat., 7, 245–314, 1826.

Downie, C., Evitt, W. R., and Sarjeant, W. A. S.: Dinoflagellates, hystrichospheres, and the classification of the acritarchs, Stanford Univ. Pubs. Geol. Sci., 7, 16, 1963.

Dumont, H. J., Nandini, S., and Sarma, S. S. S.: Cyst ornamentation in aquatic invertebrates?: a defence against egg-predation, Hydrobiologia, 486, 161–167, 2002.

Eaton, G. L.: A morphogenetic series of dinoflagellate cysts from the Bracklesham Beds of the Isle of Wight, Hampshire, England, in: Proceedings of the Second Planktonic Conference, Rome, 1970, edited by: Farinacci, A., 355–379, Edizioni Tecnoscienza, Rome, 1971.

Ehrenberg, C. G.: Animalia evertebrata, in: Symbolae physicae seu icones et descriptiones naturalium novorum aut minus cognitorum quae ex itineribus Lybiam Aegyptum Nubiam Dongalam Syriam Arabiam et Habessinian. Pars Zoologica, edited by: Hemprich, P. C. and Ehrenberg, C. G., Abhandlungen der deutschen Akademie der Wissenschaften, 1831.

Eisenack, A.: Mikroplankton aus dem norddeutsche Apt nebst einigen Bemerkungen über fossile Dinoflagellaten, Neues Jahrbuch für Geologie und Paläontologie, Abhandlungen, 106, 383–422, 1958.

Ellegaard, M. and Moestrup, Ø.: Fine structure of the flagellar apparatus and morphological details of *Gymnodinium nolleri* sp. nov. (Dinophyceae), an unarmored dinoflagellate producing a microreticulate cyst, Phycologia, 38, 289–300, 1999.

Ellegaard, M., Figueroa, R. L., and Versteegh, G. J. M.: Dinoflagellate life cycles, strategy and diversity: key foci for future research, in: Biological and Geological Perspectives of Dinoflagellates, edited by: Lewis, J. M., Marret, F., and Bradley, L. R., 249–261, The Micropalaeontological Society, Special Publications, London, 2013.

Esper, O. and Zonneveld, K. A. F.: Distribution of organic-walled dinoflagellate cysts in surface sediments of the Southern Ocean (eastern Atlantic sector) between the Subtropical Front and the Weddell Gyre, Mar. Micropaleontol., 46, 177–208, https://doi.org/10.1016/S0377-8398(02)00041-5, 2002.

Esper, O. and Zonneveld, K. A. F.: The potential of organic-walled dinoflagellate cysts for the reconstruction of past sea-surface conditions in the Southern Ocean, Mar. Micropaleontol., 65, 185–212, https://doi.org/10.1016/j.marmicro.2007.07.002, 2007.

Evitt, W. R.: A discussion and proposals concerning fossil dinoflagellates, hystrichospheres and acritarchs, II, P. Natl. Acad. Sci. USA, 49, 298–302, 1963.

Evitt, W. R.: Sporopollenin dinoflagellate cysts. Their morphology and interpretation, American Association of Stratigraphic Palynology Foundation, Austin, Texas, 333, 1985.

Expedition 318 Scientists: Site U1357, in: Proceedings of the Integrated Ocean Drilling Program, vol. 318, edited by: Escutia, C., Brinkhuis, H., Klaus, A., and the Expeditions 318 Scientists, 1–74, Integrated Ocean Drilling Program Management International, Inc., Tokyo, 2011.

Fabiano, M., Chiantore, M., Povero, P., Cattaneo-Vietti, R., Pusceddu, A., Misic, C., and Albertelli, G.: Short-term variations in particulate matter flux in Terra Nova Bay, Ross Sea, Antarct. Sci., 9, 143–149, https://doi.org/10.1017/S0954102097000187, 1997.

Fauchald, K.: The Polychaete Worms. Definitions and Keys to the Orders, Families and Genera, Nat. Hist. Museum Los Angeles Cty. Sci. Ser., 28, 1–188, 1977.

Fensome, R. A., Taylor, F. J. R., Norris, G., Sarjeant, W. A. S., Wharton, D. I., and Williams, G. L.: A classification of fossil and living dinoflagellates, Micropaleontology Press Special Paper, 7, 351, 1993.

Fensome, R. A., Bujak, J., Dale, B., Davies, E. H., Dodge, J. D., Edwards, L. E., Harland, R., Head, M. J., Lentin, J. K., Lewis, J., Matsuoka, K., Norris, G., Sarjeant, W. A. S., Taylor, F. J. R., and Williams, G. L.: Proposal to conserve the name Protoperidiniaceae against Congruentidiaceae, Diplopsalaceae, and Kolkwitziellaceae (Dinophyceae), Taxon, 47, 727–730, 1998.

Fensome, R. A., Guerstein, G. R., and Williams, G. L.: New insights on the Paleogene dinoflagellate cyst genera Enneadocysta and Licracysta gen. nov. based on material from offshore eastern Canada and southern Argentina, Micropaleontology, 52, 385–410, 2006.

Fertouna-Bellakhal, M., Dhib, A., Béjaoui, B., Turki, S., and Aleya, L.: Driving factors behind the distribution of dinocyst composition and abundance in surface sediments in a western Mediterranean coastal lagoon?: Report from a high resolution mapping study, Mar. Pollut. Bull., 84, 347–362, https://doi.org/10.1016/j.marpolbul.2014.04.041, 2014.

Filipova-Marinova, M.: Archaeological and paleontological evidence of climate Dynamics, sea level change, and coastline migration in the Bulgarian sector of the Circum-Pontic Region, in: The Black Sea Flood Question: Changes in Coastline, Climate and Human Settlement, edited by: Yanko-Hombach, V., Gilbert, A. S., Panin, N., and Dolukhanov, P. M., 453–481, Springer, New York, 2007.

Filipova-Marinova, M., Pavlov, D., Vergiev, S., Slavchev, V., and Giosan, L.: Palaeoecology and Geoarchaeology of Varna Lake, Northeastern Bulgaria, Comptes rendus l'Académie Bulg. des Sci., 66, 377–392, 2013.

Fjellså, A. and Nordberg, K.: Toxic dinoflagellate "blooms" in the Kattegat, North Sea, during the Holocene, Palaeogeogr. Palaeocl., 124, 87–105, https://doi.org/10.1016/0031-0182(96)00009-0, 1996.

Foissner, W., Müller, H., and Agatha, S.: A comparative fine structural and phylogenetic analysis of resting cysts in oligotrich and hypotrich Spirotrichea (Ciliophora), Eur. J. Protistol., 43, 295–314, https://doi.org/10.1016/j.ejop.2007.06.001, 2007.

Fonda Umani, S., Monti, M., Bergamasco, A., Cabrini, M., De Vittor, C., Burba, N., and Del Negro, P.: Plankton community structure and dynamics versus physical structure from Terra Nova Bay to Ross Ice Shelf (Antarctica), J. Marine Syst., 55, 31–46, https://doi.org/10.1016/j.jmarsys.2004.05.030, 2005.

Frieling, J., Reichart, G.-J., Middelburg, J. J., Röhl, U., Westerhold, T., Bohaty, S. M., and Sluijs, A.: Tropical Atlantic climate and ecosystem regime shifts during the Paleocene–Eocene Thermal Maximum, Clim. Past, 14, 39–55, https://doi.org/10.5194/cp-14-39-2018, 2018.

Froneman, P. W. and Pakhomov, E. A.: Trophic importance of the chaetognaths *Eukrohnia hamata* and *Sagitta gazellae* in the pelagic system of the Prince Edward Islands (Southern Ocean), Polar Biol., 19, 242–249, 1998.

Fujiwara, A., Hirawake, T., Suzuki, K., Imai, I., and Saitoh, S.-I.: Timing of sea ice retreat can alter phytoplankton community structure in the western Arctic Ocean, Biogeosciences, 11, 1705–1716, https://doi.org/10.5194/bg-11-1705-2014, 2014.

Gaarder, K. R.: Phytoplankton Studies from the Trømso District 1930–31, Trømso Museums Arshefter Naturh. Avd. Nr. 11, 55, 1, 1–159, 1938.

Gaarder, K. R.: Coccolithineae, Silicoflagellatae, Pterospermataceae and other forms from the 'Michael Sars' North Atlantic Deep-Sea Expedition 1910, Report on the Scientific Results of the 'Michael Sars' North Atlantic Deep-Sea Expedition 1910 2, 4, 1–20, 1954.

Gambi, M. C., Lorenti, M., Russo, G. F., and Scipione, M. B.: Benthic associations of the shallow hard bottoms off Terra Nova Bay, Ross Sea: zonation, biomass and population structure, Antarct. Sci., 6, 449–462, 1994.

Garrison, D. L. and Buck, K. R.: Protozooplankton in the Weddell Sea, Antarctica: Abundance and Distribution in the Ice-Edge Zone, Polar Biol., 9, 341–351, 1989.

Garzio, L. M. and Steinberg, D. K.: Microzooplankton community composition along the Western Antarctic Peninsula, Deep-Sea Res. Pt. I, 77, 36–49, https://doi.org/10.1016/j.dsr.2013.03.001, 2013.

Gibson, J. A. E. and Zale, R.: Holocene development of the fauna of Lake Boeckella, northern Antarctic Peninsula, Holocene, 16, 625–634, https://doi.org/10.1191/0959683606hl959rp, 2006.

Gibson, J. A. E., Cromer, L., Agius, J. T., McInnes, S. J., and Marley, N. J.: Tardigrade eggs and exuviae in Antarctic lake sediments: Insights into Holocene dynamics and origins of the fauna, J. Limnol., 66, 65–71, https://doi.org/10.4081/jlimnol.2007.s1.65, 2007.

Gowing, M. M. and Garrison, D. L.: Abundance and feeding ecology of larger protozooplankton in the ice edge zone of the Weddell and Scotia Seas during the austral winter, Deep-Sea Res., 39, 893–919, 1992.

Grube, A. E.: Die Familien der Anneliden, Archiv für Naturgeschichte, 16, Bd. 1, 249–364, 1850.

Guillou, L., Eikrem, W., Chrétiennot-Dinet, M.-J., Le Gall, F., Massana, R., Romari, K., Pedrós-Alió, C., and Vaulot, D.: Diversity of Picoplanktonic Prasinophytes Assessed by Direct Nuclear SSU rDNA Sequencing of Environmental Samples and Novel Isolates Retrieved from Oceanic and Coastal Marine Ecosystems, Protist, 155, 193–214, 2004.

Guilloux, L., Rigaut-Jalabert, F., Jouenne, F., Ristori, S., Viprey, M., Not, F., Vaulot, D., and Simon, N.: An annotated checklist of Marine Phytoplankton taxa at the SOMLIT-Astan time series off Roscoff (Western English Channel, France): data collected from 2000 to 2010, Cah. Biol. Mar., 54, 247–256, 2013.

Haeckel, E.: Generelle Morphologie der Organismen. Allgemeine Grundzüge der organischen Formenwissenschaft, mechanisch begründet durch die von Charles Darwin reformirte Descendenz-Theorie, Bd. 2: Allgemeine Entwickelungsgeschichte der Organismen, Georg Reimer, Berlin, 462, 1866.

Haeckel, E.: Ueber einige neue pelagische Infusorien, Jenaische Zeitschrift für Naturwissenschaft 7 (year 1871), 561–568, 1873.

Haeckel, E.: Systematische Phylogenie. Entwurf eines natürlichen Systems der Organismen auf Grund ihrer Stammegeschichte, Erster Theil: Systematische Phylogenie der Protisten und Pflanzen, Georg Reimer, Berlin, 400, 1894.

Hajós, M.: A mecseki mioc'en diatomaföld rétegek mikroplanktonja. (Das Mikroplankton der Kieselgurschichten im Miozän des Mecsekgebirges), Magyar Állami Földtani Intézet jelentése az 1964. évről., 139–171, 1966.

Hallegraeff, G. M.: Transport of toxic dinoflagellates via ships' ballast water: bioeconomic risk assessment and efficacy of possible ballast water management strategies, Mar. Ecol. Prog. Ser., 168, 297–309, 1998.

Hällfors, G.: Checklist of Baltic Sea phytoplankton species (including some heterotrophic protistan groups), Baltic Sea Environment Proceedings, 95, 1–208, 2004.

Hannah, M. J.: The palynology of ODP site 1165, Prydz Bay, East Antarctica?: A record of Miocene glacial advance and retreat, Palaeogeogr. Palaeocl., 231, 120–133, https://doi.org/10.1016/j.palaeo.2005.07.029, 2006.

Hannah, M. J. and Fielding, C. R.: Chronostratigraphy of the CRP-3 Drillhole, Victoria Land Basin, Antarctica © Terra Antartica Publication, 2001.

Hannah, M. J., Wrenn, J. H., and Wilson, G. J.: Early Miocene and Quaternary Marine Palynomorphs from Cape Roberts Project CRP-1, McMurdo Sound, Antarctica, Terra Ant., 5, 527–538, 1998.

Hannah, M. J., Wilson, G. J., and Wrenn, J. H.: Oligocene and Miocene Marine Palynomorphs from CRP-2/2A, Victoria Land Basin, Antarctica, Terra Ant., 7, 503–511, 2000.

Hannah, M. J., Wrenn, J. H., and Wilson, G. J.: Preliminary Report on Early Oligocene and Latest Eocene Marine Palynomorphs from CRP-3 Drillhole, Victoria Land Basin, Antarctica, Terra Ant., 8, 383–388, 2001.

Hansen, B. W., Drillet, G., Kristensen, R. M., Sørensen, T. F., and Tøttrup, M. T.: Production, hatching success and surface ornamentation of eggs of calanoid copepods during a winter at 57° N, Mar. Biol., 157, 59–68, https://doi.org/10.1007/s00227-009-1295-x, 2010.

Harðardóttir, S., Lundholm, N., Moestrup, Ø., and Nielsen, T. G.: Description of Pyramimonas diskoicola sp. nov. and the importance of the flagellate *Pyramimonas* (Prasinophyceae) in Greenland sea ice during the winter-spring transition, Polar Biol., 37, 1479–1494, https://doi.org/10.1007/s00300-014-1538-2, 2014.

Harland, R. and Pudsey, C. J.: Dinoflagellate cysts from sediment traps deployed in the Bellingshausen, Weddell and Scotia seas, Antarctica, Mar. Micropaleontol., 37, 77–99, https://doi.org/10.1016/S0377-8398(99)00016-X, 1999.

Harland, R., Pudsey, C. J., Howe, J. A., and Fitzpatrick, M. E. J.: Recent dinoflagellate cysts in a transect from the Falkland Trough to the Weddell Sea, Antarctica, Palaeontology, 41, 1131–1998, 1998.

Harland, R., FitzPatrick, M. E. J., and Pudsey, C. J.: Latest Quaternary dinoflagellate cyst climatostratigraphy for three cores from the Falkland Trough, Scotia and Weddell Seas, Southern Ocean, Rev. Palaeobot. Palyno., 107, 265–281, https://doi.org/10.1016/S0034-6667(99)00023-8, 1999.

Harmsworth, R. V.: The Developmental History of Blelham Tarn (England) as Shown by Animal Microfossils, with Special Reference to the Cladocera, Ecol. Monogr., 38, 223–241, 1968.

Harris, R.: Copepods, in: Encyclopedia of Ocean Sciences, edited by: Steele, J. H., Thorpe, S. A., and Turekian, K. K., 640–650, Academic Press, San Diego, 2001.

Hartman, J. D., Sangiorgi, F., Bijl, P. K., and Versteegh, G. J. M.: *Nucicla umbiliphora* gen. et sp. nov.: a Quaternary peridinioid dinoflagellate cyst from the Antarctic margin, Palynology, 1–10, https://doi.org/10.1080/01916122.2018.1430070, 2018a.

Hartman, J. D., Sangiorgi, F., Salabarnada, A., Peterse, F., Houben, A. J. P., Schouten, S., Brinkhuis, H., Escutia, C., and Bijl, P. K.: Paleoceanography and ice sheet variability offshore Wilkes Land, Antarctica – Part 3: Insights from Oligocene–Miocene TEX$_{86}$-based sea surface temperature reconstructions, Clim. Past, 14, 1275–1297, https://doi.org/10.5194/cp-14-1275-2018, 2018b.

Hartman, J. D., Willmott, V., Peterse, F., Bijl, P. K., Sangiorgi, F., and Schouten, S.: A Holocene record of environmental change in the polynya-influenced waters of the Adélie Basin, East Antarctica, in preparation, 2018c.

Hashihama, F., Hirawake, T., Kudoh, S., Kanda, J., Furuya, K., Yamaguchi, Y., and Ishimaru, T.: Size fraction and class composition of phytoplankton in the Antarctic marginal ice zone along the 140° E meridian during February–March 2003, Polar Sci., 2, 109–120, https://doi.org/10.1016/j.polar.2008.05.001, 2008.

Head, M. J.: Dinoflagellate cysts, sporomorphs, and other palynomorphs from the marine uppermost Pliocene St. Erth Beds, Cornwall, southwestern England, The Paleontological Society, Memoir 31 (Suppl. to J. Paleontol. 67, 3), 1–62, 1993.

Head, M.: Modern dinoflagellate cysts and their biological affinities, in: Palynology: principles and applications, edited by: Jansonius, J. and McGregor, D. C., 1197–1248, American Association of Stratigraphic Palynologists Foundation, Salt Lake City, Utah, 1996.

Head, M. J., Harland, R., and Matthiessen, J.: Cold marine indicators of the late Quaternary: The new dinoflagellate cyst genus *Islandinium* and related morphotypes, J. Quaternary Sci., 16, 621–636, https://doi.org/10.1002/jqs.657, 2001.

Head, M. J., Riding, J. B., Eidvin, T., and Chadwick, R. A.: Palynological and foraminiferal biostratigraphy of (Upper Pliocene) Nordland Group mudstones at Sleipner, northern North Sea, Mar. Petrol. Geol., 21, 277–297, https://doi.org/10.1016/j.marpetgeo.2003.12.002, 2004.

Heikkilä, M., Pospelova, V., Hochheim, K. P., Kuzyk, Z. Z. A., Stern, G. A., Barber, D. G., and Macdonald, R. W.: Surface sediment dinoflagellate cysts from the Hudson Bay system and their relation to freshwater and nutrient cycling, Mar. Micropaleontol., 106, 79–109, https://doi.org/10.1016/j.marmicro.2013.12.002, 2014.

Hemleben, C., Bé, A. W. H., Anderson, O. R., and Tuntivate, S.: The morphology, organic layers and chamber formation of the planktonic foraminifer Globorotalia menardii (d'Orbigny), J. Foramin. Res., 7, 1–25, 1977.

Hill, R. S. and Scriven, L. J.: The angiosperm-dominated woody vegetation of Antarctica: A review, Rev. Palaeobot. Palyno., 86, 175–198, https://doi.org/10.1016/0034-6667(94)00149-E, 1995.

Hoem, S. A.: Norwegian Biodiversity Information Centre – Other datasets, Version 31.217, Natural History Museum, University of Oslo, Occurrence Dataset, https://doi.org/10.15468/tm56sc, last access: 8 February 2018.

Hopcroft, R.: Phytoplankton from the White Sea, Barents Sea, Norwegian Sea and Arctic Basin 1993–2003, Conservation of Arctic Flora and Fauna, Occurrence Dataset, https://doi.org/10.15468/tvpmov (last access: 8 February 2018), 2016.

Hopkins, C. C. E.: The male genital system, and spermatophore production and function in *Euchaeta norvegica* Boeck (Copepoda: Calanoida), J. Exp. Mar. Biol. Ecol., 35, 197–231, https://doi.org/10.1016/0022-0981(78)90076-X, 1978.

Houben, A. J. P., Bijl, P. K., Pross, J., Bohaty, S. M., Passchier, S., Stickley, C. E., Röhl, U., Sugisaki, S., Tauxe, L., van de Flierdt, T., Olney, M., Sangiorgi, F., Sluijs, A., Escutia, C., Brinkhuis, H., Dotti, C. E., Klaus, A., Fehr, A., Williams, T., Bendle, J. A. P., Carr, S. A., Dunbar, R. B., Flores, J.-A., Gonzàlez, J. J., Hayden, T. G., Iwai, M., Jimenez-Espejo, F. J., Katsuki, K., Kong, G. S., McKay, R. M., Nakai, M., Pekar, S. F., Riesselman, C., Sakai, T., Salzmann, U., Shrivastava, P. K., Tuo, S., Welsh, K., and Yamane, M.: Reorganization of Southern Ocean plankton ecosystem at the onset of Antarctic glaciation., Science, 340, 341–344, https://doi.org/10.1126/science.1223646, 2013.

Howe, J. A., Harland, R., and Pudsey, C. J.: Dinoflagellate cyst evidence for Quaternary palaeoceanographic change in the northern Scotia Sea, South Atlantic Ocean, Mar. Geol., 191, 55–69, https://doi.org/10.1016/S0025-3227(02)00498-X, 2002.

Ichinomiya, M., Nakamachi, M., Fukuchi, M., and Taniguchi, A.: Resting cells of microorganisms in the 20–100 μm fraction of marine sediments in an Antarctic coastal area, Polar Sci., 2, 27–32, https://doi.org/10.1016/j.polar.2007.12.001, 2008.

Inouye, I., Hori, T., and Chihara, M.: Absolute configuration analysis of the flagellar apparatus of *Pterosperma cristatum* (Prasinophyceae) and consideration of its phylogenetic position, J. Phycol., 26, 329–344, 1990.

Jacobson, D. M.: A brief history of dinoflagellate feeding research, J. Eukaryot. Microbiol., 46, 376–381, 1999.

Janssen, H. H. and Gradinger, R.: Turbellaria (Archoophora: Acoela) from Antarctic sea ice endofauna – examination of their micromorphology, Polar Biol., 21, 410–416, 1999.

Jörgensen, E.: Mediterranean Tintinnidae. Report of the Danish Oceanographical Expeditions 1908–1910 to the Mediterranean and adjacent seas, Vol. 2, Biology, No. 8, J.3 (Thor Expedition), Copenhagen, 109, 1924.

Jorissen, F. J., de Stigter, H. C., and Widmark, J. G. V: A conceptual model explaining benthic foraminiferal microhabitats, Mar. Micropaleontol., 26, 3–15, https://doi.org/10.1016/0377-8398(95)00047-X, 1995.

Kamiyama, T.: Comparative Biology of Tintinnid Cysts, in: The Biology and Ecology of Tintinnid Ciliates: Models for Marine Plankton, edited by: Dolan, J. R., Montagnes, D. J. S., Agatha, S., Coats, D. W., and Stoecker, D. K., 171–185, Wiley-Blackwell, Hoboken, New Jersey, USA, 2013.

Kamykowski, D., Reed, R. E., and Kirkpatrick, G. J.: Comparison of sinking velocity, swimming velocity, rotation and path characteristics among six marine dinoflagellate species, Mar. Biol., 113, 319–328, https://doi.org/10.1007/BF00347287, 1992.

Katajisto, T.: Development of *Acartia bifilosa* (Copepoda?: Calanoida) eggs in the northern Baltic Sea with special reference to dormancy, J. Plankton Res., 25, 357–364, 2003.

Kawachi, M.: Microbial Culture Collection, National Institute for Environmental Studies, Version 5.5, National Institute of Genet-

ics, ROIS, Occurrence Dataset, https://doi.org/10.15468/8rml10 (last access: 8 February 2018), 2017.

Kemp, E. M.: Palynology of Leg 28 drill sites, Deep Sea Drilling Project, Initial Rep. DSDP, 28, 699–623, 1975.

Kennett, J. P. and Barker, P. F.: Latest Cretaceous to Cenozoic Climate and Oceanographic Developments in the Weddell Sea, Antarctica: an Ocean-Drilling Perspective, in: Proceedings of the Ocean Drilling Program, Scientific Results, vol. 113, edited by: Barker, P. F., Kennett, J. P., O'Connell, S., and Pisias, N. G., 937–960, 1990.

Kim, S. Y., Choi, J. K., Dolan, J. R., Shin, H. C., Lee, S., and Yang, E. J.: Morphological and Ribosomal DNA-based Characterization of Six Antarctic Ciliate Morphospecies from the Amundsen Sea with Phylogenetic Analyses, J. Eukaryot. Microbiol., 60, 497–513, https://doi.org/10.1111/jeu.12057, 2013.

Klumpp, B.: Beitrag zur Kenntnis der Mikrofossilien des mittleren und oberen Eozän, Palaeontographica, Abteilung A, 103, 377–406, 1953.

Kofoid, C. A. and Campbell, A. S.: A conspectus of the marine and freshwater ciliata belonging to the suborder Tintinnoinea, with descriptions of new species principally from the Agassiz expedition to the Eastern Tropical Pacific 1904–1905, Univ. Calif. Publ. Zool., 34, 1–403, 1929.

Koga, F.: On the Pelagic Eggs of Copepoda, J. Oceanogr. Soc. Japan, 24, 16–20, 1968.

Kozlowski, W. A., Deutschman, D., Garibotti, I., Trees, C., and Vernet, M.: An evaluation of the application of CHEMTAX to Antarctic coastal pigment data, Deep-Sea Res. Pt. I, 58, 350–364, https://doi.org/10.1016/j.dsr.2011.01.008, 2011.

Kramer, M., Swadling, K. M., Meiners, K. M., Kiko, R., Scheltz, A., Nicolaus, M., and Werner, I.: Antarctic sympagic meiofauna in winter?: Comparing diversity, abundance and biomass between perennially and seasonally ice-covered regions, Deep-Sea Res. Pt. II, 58, 1062–1074, https://doi.org/10.1016/j.dsr2.2010.10.029, 2011.

Kunz-Pirrung, M., Matthiessen, J., and De Vernal, A.: Relationships between dinoflagellate cyst assemblages in surface sediment and hydrographic conditions in the Bering and Chukchi seas, J. Quaternary Sci., 16, 667–680, https://doi.org/10.1002/jqs.652, 2001.

Kvenvolden, K. A., Rapp, J. B., Golan-Bac, M., and Hostettler, F. D.: Multiple sources of alkanes in Quaternary oceanic sediment of Antarctica, Org. Geochem., 11, 291–302, https://doi.org/10.1016/0146-6380(87)90040-4, 1987.

Laackmann, H.: Antarktische Tintinnen, Zool. Anz., 31, 235–239, 1907.

Laackmann, H.: Die Tintinnodeen der Deutschen Südpolar-Expedition 1901–1903, in: Deutsche Südpolar-Expedition, 1901–1903, im Auftrage des Reichsamtes des Innern, Bd. 11, edited by: Von Drygalski, E., 341–496, Georg Reimer, Berlin, 1910.

Lamarck, J. B. P. A.: Philosophie Zoologique ou Exposition des Considérations relatives à l'histoire naturelle des Animaux, Tome Premier, Paris, 428, 1809.

Lankester, E. R.: Protozoa, in: The Encyclopedia Brittanica, 9th edn., 19, 830–866, 1885.

Leander, B. S. and Hoppenrath, M.: Ultrastructure of a novel tube-forming, intracellular parasite of dinoflagellates: *Parvilucifera prorocentri* sp. nov. (Alveolata, Myzozoa), Eur. J. Protistol., 44, 55–70, https://doi.org/10.1016/j.ejop.2007.08.004, 2008.

Lentin, J. K. and Williams, G. L.: A monograph of fossil peridinioid dinoflagellate cysts, Bedford Institute of Oceanography, Report Series BI-R-75-16, 1–237, 1976.

Levy, R. H. and Harwood, D. M.: Tertiary marine palynomorphs from McMurdo Sound erratics, Antarctica, in: Paleobiology and Paleoenvironments of Eocene Rocks, McMurdo Sound, East Antarctica, Antarctic Research Series 76, edited by: Stilwell, J. D. and Feldman, R. M., 183–242, American Geophysical Union, Washington D.C., 2000.

Li, Z., Pospelova, V., Liu, L., Zhou, R., and Song, B.: High-resolution palynological record of Holocene climatic and oceanographic changes in the northern South China Sea, Palaeogeogr. Palaeocl., 483, 94–124, https://doi.org/10.1016/j.palaeo.2017.03.009, 2017.

Lindemann, E.: Abteilung Peridineae (Dinoflagellatae), in: Die Natürlichen Pflanzenfamilien nebst ihren Gattungen und wichtigeren Arten insbesondere den Nutzpflanzen. Zweite stark vermehrte und verbesserte Auflage herausgegeben von A. Engler. Bd. 2, edited by: Engler, A. and Prantl, K., 3–104, Wilhelm Engelmann, Leipzig, 1928.

Linnaeus, C.: Systema Naturae per Regna Tria Naturae, secundum Classes, Ordines, Genera, Species cum characteribus, differentiis, synonymis, locis, Tomus I, 10th edition, Laurentius Salvius, Holmiae, 824, 1758.

Loots, C., Swadling, K. M., and Koubbi, P.: Annual cycle of distribution of three ice-associated copepods along the coast near Dumont d'Urville, Terre Adélie (Antarctica), J. Marine Syst., 78, 599–605, https://doi.org/10.1016/j.jmarsys.2009.01.003, 2009.

Magyar, I., Geary, D. H., and Müller, P.: Paleogeographic evolution of the Late Miocene Lake Pannon in Central Europe, Palaeogeogr. Palaeocl., 147, 151–167, https://doi.org/10.1016/S0031-0182(98)00155-2, 1999.

Malinverno, E., Maffioli, P., and Gariboldi, K.: Latitudinal distribution of extant fossilizable phytoplankton in the Southern Ocean?: Planktonic provinces, hydrographic fronts and palaeoecological perspectives, Mar. Micropaleontol., 123, 41–58, https://doi.org/10.1016/j.marmicro.2016.01.001, 2016.

Mangot, J. F., Debroas, D., and Domaizon, I.: Perkinsozoa, a well-known marine protozoan flagellate parasite group, newly identified in lacustrine systems: A review, Hydrobiologia, 659, 37–48, https://doi.org/10.1007/s10750-010-0268-x, 2011.

Marchant, H. J.: Prasinophytes, in: Antarctic Marine Protists, edited by: Scott, F. and Marchant, H. J., 308–315, Australian Biological Resources Study, Canberra and Australian Antarctic Division, Hobart, 2005.

Marcus, E.: Zur Anatomie und Ökologie mariner Tardigraden, Zoologische Jahrbücher, Abteilung für Systematik, 53, 487–558, 1927.

Marcus, N. H.: Ecological and evolutionary significance of resting eggs in marine copepods?: past, present, and future studies, Hydrobiologia, 320, 141–152, 1996.

Marin, B. and Melkonian, M.: Molecular Phylogeny and Classification of the Mamiellophyceae class. nov. (Chlorophyta) based on Sequence Comparisons of the Nuclear- and Plastid-encoded rRNA Operons, Protist, 161, 304–336, https://doi.org/10.1016/j.protis.2009.10.002, 2010.

Marine Biology Laboratory: MICROBIS database, Occurrence Dataset, https://doi.org/10.15468/wi6v9k, last access: 8 February 2018.

Marley, N. J., McInnes, S. J., and Sands, C. J.: Phylum Tardigrada: A re-evaluation of the Parachela, Zootaxa, 2819, 51–64, 2011.

Marret, F. and De Vernal, A.: Dinoflagellate cyst distribution in surface sediments of the southern Indian Ocean, Mar. Micropaleontol., 29, 367–392, https://doi.org/10.1016/S0377-8398(96)00049-7, 1997.

Marret, F. and Zonneveld, K. A. F.: Atlas of modern organic-walled dinoflagellate cyst distribution, Rev. Palaeobot. Palyno., 125, 1–200, https://doi.org/10.1016/S0034-6667(02)00229-4, 2003.

Marret, F., De Vernal, A., Benderra, F., and Harland, R.: Late quaternary sea-surface conditions at DSDP Hole 594 in the Southwest Pacific Ocean based on dinoflagellate cyst assemblages, J. Quaternary Sci., 16, 739–751, https://doi.org/10.1002/jqs.648, 2001.

Marsland, S. J., Church, J. A., Bindoff, N. L., and Williams, G. D.: Antarctic coastal polynya response to climate change, J. Geophys. Res., 112, C07009, https://doi.org/10.1029/2005JC003291, 2007.

Martin, F.: Acritarchs: a review, Biol. Rev. Camb. Philos., 68, 475–538, 1993.

McMinn, A.: Marine Quaternary dinoflagellate cysts of Australia, Papua-New Guinea, New Zealand and the Southern Ocean?: a review, Alcheringa, 26, 519–530, https://doi.org/10.1080/03115510208619541, 2002.

Medvedeva, L. A. and Nikulina, T. V: Catalogue of freshwater algae of the southern part of the Russian Far East, Dalnauka, Vladivostok, 2014.

Menéndez, C. A.: Microplancton fósil de sedimentos Terciarios y Cretácicos del norte de Tierra del Fuego (Argentina), Ameghiniana 4, 7–18, 1965.

Mertens, K. N., Ribeiro, S., Bouimetarhan, I., Caner, H., Combourieu Nebout, N., Dale, B., De Vernal, A., Ellegaard, M., Filipova, M., Godhe, A., Goubert, E., Grøsfjeld, K., Holzwarth, U., Kotthoff, U., Leroy, S. A. G., Londeix, L., Marret, F., Matsuoka, K., Mudie, P. J., Naudts, L., Peña-Manjarrez, J. L., Persson, A., Popescu, S.-M., Pospelova, V., Sangiorgi, F., van der Meer, M. T. J., Vink, A., Zonneveld, K. A. F., Vercauteren, D., Vlassenbroeck, J., and Louwye, S.: Process length variation in cysts of a dinoflagellate, *Lingulodinium machaerophorum*, in surface sediments?: Investigating its potential as salinity proxy, Mar. Micropaleontol., 70, 54–69, https://doi.org/10.1016/j.marmicro.2008.10.004, 2009.

Michels, J. and Gorb, S. N.: Mandibular gnathobases of marine planktonic copepods – feeding tools with complex micro- and nanoscale composite architectures, Beilstein J. Nanotech., 6, 674–685, https://doi.org/10.3762/bjnano.6.68, 2015.

Mikhalevich, V. I.: Major features of the distribution of Antarctic foraminifera, Micropaleontology, 50, 179–194, 2004.

Milne-Edwards, M.: Histoire naturelle des crustacés, comprenant l'anatomie, la physiologie et la classification de ces animaux, Tome Troisième, Librairie Encyclopedique de Roret, Paris, 638, 1840.

Moestrup, Ø., Inouye, I., and Hori, T.: Ultrastructural studies on *Cymbomonas tetramitiformis* (Prasinophyceae). I. General structure, scale microstructure, and ontogeny, Can. J. Botany, 81, 657–671, https://doi.org/10.1139/B03-055, 2003.

Moita, M. T. and Vilarinho, M. G.: Checklist of phytoplankton species off Portugal: 70 years (1929–1998) of studies, Portugaliae Acta Biol. Ser. B. Sist., 18, 5–50, 1999.

Montagnes, D. J. S.: Ecophysiology and Behaviour of Tintinnids, in: The Biology and Ecology of Tintinnid Ciliates: Models for Marine Plankton, edited by: Dolan, J. R., Montagnes, D. J. S., Agatha, S., Coats, D. W., and Stoecker, D. K., 85–121, Wiley-Blackwell, Hoboken, New Jersey, USA, 2013.

Montresor, M., Procaccini, G., and Stoecker, D. K.: *Polarella glacialis*, Gen. Nov., sp. Nov. (Dinophyceae): Suessiaceae are still alive, J. Phycol., 35, 186–197, 1999.

Montresor, M., Lovejoy, C., Orsini, L., Procaccini, G., and Roy, S.: Bipolar distribution of the cyst-forming dinoflagellate *Polarella glacialis*, Polar Biol., 26, 186–194, https://doi.org/10.1007/s00300-002-0473-9, 2003.

Morales Maqueda, M. A., Willmott, A. J., and Biggs, N. R. T.: Polynya Dynamics: A review of observations and modeling, Rev. Geophys., 42, RG1004, https://doi.org/10.1029/2002RG000116, 2004.

Morehead, S., Montagna, P., and Kennicutt II, M. C.: Comparing fixed-point and probabilistic sampling designs for monitoring the marine ecosystem near McMurdo Station, Ross Sea, Antarctica, Antarct. Sci., 20, 471–484, https://doi.org/10.1017/S0954102008001326, 2008.

Moro, I., La Rocca, N., Valle, L. D., Moschin, E., Negrisolo, E., and Andreoli, C.: Pyramonas australis sp. nov. (Prasinophyceae, Chlorophyta) form Antarctica: fine structure and molecular phylogeny, Eur. J. Phycol., 37, 103–114, 2002.

Mousing, E. A., Ribeiro, S., Chisholm, C., Kuijpers, A., Moros, M. and Ellegaard, M.: Size differences of Arctic marine protists between two climate periods – using the paleoecological record to assess the importance of within-species trait variation, Ecol. Evol., 7, 3–13, https://doi.org/10.1002/ece3.2592, 2017.

Mudie, P. J.: Circum-arctic Quaternary and Neogene marine palynofloras: paleoecology and statistical analysis, in: Neogene and Quaternary dinoflagellate cysts and acritarchs, edited by: Head, M. X. and Wrenn, J. H., 347–390, American Association of Stratigraphic Palynologists Foundation, Dallas, Texas, 1992.

Mudie, P. J. and Harland, R.: Chapter 21. Aquatic Quaternary, in: Palynology: Principles and Applications, edited by: Jansonius, J. and McGregor, D. C., 843–877, American Association of Stratigraphic Palynologists Foundation, Dallas, Texas, 1996.

Mudie, P. J., Marret, F., Rochon, A., and Aksu, A. E.: Non-pollen palynomorphs in the Black Sea corridor, Veg. Hist. Archaeobot., 19, 531–544, https://doi.org/10.1007/s00334-010-0268-9, 2010.

Mudie, P. J., Leroy, S. A. G., Marret, F., Gerasimenko, N. P., Kholeif, S. E. A., Sapelko, T., and Filipova-Marinova, M.: Non-pollen palynomorphs: indicators of salinity and environmental change in the Caspian – Black Sea – Mediterranean corridor, in: Geology and Geoarchaeology of the Black Sea Region: Beyond the Flood Hypothesis, vol. 473, edited by: Buynevich, I. V., Yanko-Hombach, V., Gilbert, A. S., and Martin, R. E., 89–115, The Geological Society of America Special Paper, Boulder, Colorado, 2011.

Müller, H. and Wünsch, C.: Seasonal dynamics of cyst formation of pelagic strombidiid ciliates in a deep prealpine lake, Aquat. Microb. Ecol., 17, 37–47, 1999.

Nakayama, T., Marin, B., Kranz, H. D., Surek, B., Huss, V. A. R., Inouye, I., and Melkonian, M.: The Basal Position of Scaly Green Flagellates among the Green Algae (Chlorophyta) is Revealed by Analyses of Nuclear-Encoded SSU rRNA Sequences, Protist,

149, 367–380, https://doi.org/10.1016/S1434-4610(98)70043-4, 1998.

Ní Fhlaithearta, S., Ernst, S. R., Nierop, K. G. J., de Lange, G. J., and Reichart, G.-J.: Molecular and isotopic composition of foraminiferal organic linings, Mar. Micropaleontol., 102, 69–78, https://doi.org/10.1016/j.marmicro.2013.06.004, 2013.

Ocean Biogeographic Information System: NODC WOD01 Plankton Database, Occurrence Dataset, https://doi.org/10.15468/ahpulo, last access: 8 February 2018.

O'Kelly, C. J.: Origin and Early Evolution of Green Plants, in: Evolution of Primary Producers in the Sea, edited by: Falkowski, P. G. and Knoll, A. H., 287–309, Academic Press, Burlington, 2007.

Orlova, T. Y., Morozova, T. V., Gribble, K. E., Kulis, D. M., and Anderson, D. M.: Dinoflagellate cysts in recent marine sediments from the east coast of Russia, Bot. Mar., 47, 184–201, https://doi.org/10.1515/BOT.2004.019, 2004.

Ostenfeld, C. H. and Schmidt, J.: Plankton fra det Røde Hav og Adenbugten (Plankton from the Red Sea and Gulf of Aden), in: Videnskabilige Meddelelser fra Dansk Naturhistorisk Forening, for Aaret 1901, 141–182, Bianco Lunos, Kjøbenhavn, 1902.

Pals, J. P., van Geel, B., and Delfos, A.: Paleoecoogical studies in the Klokkeweel Bog near Hoogkarspel (Prov. of Noord-Holland), Rev. Palaeobot. Palyno., 30, 371–418, 1980.

Parke, M., Boalch, G. T., Jowett, R., and Harbour, D. S.: The genus *Pterosperma* (Prasinophyceae): species with a single equatorial ala, J. Mar. Biol. Assoc. UK, 58, 239–276, 1978.

Pascher, A.: Über Flagellaten und Algen, Ber. Deut. Bot. Ges., 32, 136–160, 1914.

Pasternak, A. F. and Schnack-Schiel, S. B.: Seasonal feeding patterns of the dominant Antarctic copepods *Calanus propinquus* and *Calanoides acutus* in the Weddell Sea, Polar Biol., 24, 771–784, https://doi.org/10.1007/s003000100283, 2001.

Paxton, H. and Åkesson, B.: Redescription of Ophryotrocha puerilis and O. labronica (Annelida, Dorvilleidae), Mar. Biol. Res., 3, 3–19, https://doi.org/10.1080/17451000601024373, 2007.

Paxton, H. and Davey, A.: A new species of *Ophryotrocha* (Annelida?: Dorvilleidae) associated with fish farming at Macquarie Harbour, Tasmania, Australia, Zootaxa, 2509, 53–61, https://doi.org/10.5281/zenodo.196027, 2010.

Paxton, H., Wiklund, H., Alexander, F., and Taboada, S.: Is the Antarctic Ophryotrocha orensanzi (Annelida?: Dorvilleidae) a circumpolar non-specialized opportunist?, Syst. Biodivers., 15, 105–114, https://doi.org/10.1080/14772000.2016.1218371, 2017.

Petersen, S. V. and Schrag, D. P.: Antarctic ice growth before and after the Eocene-Oligocene Transition: New estimates from clumped isotope paleothermometry, Paleoceanography, 30, 1–13, https://doi.org/10.1002/2014PA002769, 2015.

Petz, W.: Ciliates, in: Antarctic Marine Protists, edited by: Scott, F. and Marchant, H. J., 347–448, Australian Biological Resources Study, Canberra and Australian Antarctic Division, Hobart, 2005.

Petz, W., Song, W., and Wilbert, N.: Taxonomy and ecology of the ciliate fauna (Protozoa, Ciliophora) in the endopagial and pelagial of the Weddell Sea, Antarctica, Stapfia, 40, 1–223, 1995.

Pieńkowski, A. J., Mudie, P. J., England, J. H., Smith, J. N., and Furze, M. F. A.: Late Holocene environmental conditions in Coronation Gulf, southwestern Canadian Arctic

Archipelago: Evidence from dinoflagellate cysts, other non-pollen palynomorphs, and pollen, J. Quaternary Sci., 26, 839–853, https://doi.org/10.1002/jqs.1503, 2011.

Pieńkowski, A. J., England, J. H., Furze, M. F. A., Blasco, S., Mudie, P. J., and MacLean, B.: 11,000 yrs of environmental change in the Northwest Passage: A multiproxy core record from central Parry Channel, Canadian High Arctic, Mar. Geol., 341, 68–85, https://doi.org/10.1016/j.margeo.2013.04.008, 2013a.

Pieńkowski, A. J., Marret, F., Scourse, J. D., and Thomas, D. N.: Organic-walled microfossils from the north-west Weddell Sea, Antarctica: records from surface sediments after the collapse of the Larsen-A and Prince Gustav Channel ice shelves, Antarct. Sci., 25, 565–574, https://doi.org/10.1017/S0954102012001186, 2013b.

Pieńkowski, A. J., England, J. H., Furze, M. F. A., MacLean, B., and Blasco, S.: The late Quaternary environmental evolution of marine Arctic Canada?: Barrow Strait to Lancaster Sound, Quaternary Sci. Rev., 91, 184–203, https://doi.org/10.1016/j.quascirev.2013.09.025, 2014.

Pilato, G., Binda, M. G., and Lisi, O.: Tardigrades of the Seychelles Islands, with the description of three new species, Ital. J. Zool., 71, 171–178, https://doi.org/10.1080/11250000409356569, 2004.

Pouchet, M.: Chapter X. Histoire naturelle, in: Voyage de "La Manche" à l'île Jan-Mayen et au Spitzberg, edited by: Leroux, E., 155–217, Paris, 1894.

Prebble, J. G., Raine, J. I., Barrett, P. J., and Hannah, M. J.: Vegetation and climate from two Oligocene glacioeustatic sedimentary cycles (31 and 24 Ma) cored by the Cape Roberts Project, Victoria Land Basin, Antarctica, Palaeogeogr. Palaeocl., 231, 41–57, https://doi.org/10.1016/j.palaeo.2005.07.025, 2006.

Prebble, J. G., Crouch, E. M., Carter, L., Cortese, G., Bostock, H., and Neil, H.: An expanded modern dinoflagellate cyst dataset for the Southwest Pacific and Southern Hemisphere with environmental associations, Mar. Micropaleontol., 101, 33–48, https://doi.org/10.1016/j.marmicro.2013.04.004, 2013.

Pross, J. and Brinkhuis, H.: Organic-walled dinoflagellate cysts as paleoenvironmental indicators in the Paleogene; a synopsis of concepts, Paläontologische Zeitschrift, 79, 53–59, 2005.

Pross, J., Contreras, L., Bijl, P. K., Greenwood, D. R., Bohaty, S. M., Schouten, S., Bendle, J. a, Röhl, U., Tauxe, L., Raine, J. I., Huck, C. E., van de Flierdt, T., Jamieson, S. S. R., Stickley, C. E., van de Schootbrugge, B., Escutia, C., and Brinkhuis, H.: Persistent near-tropical warmth on the Antarctic continent during the early Eocene epoch, Nature, 488, 73–77, https://doi.org/10.1038/nature11300, 2012.

Radi, T., Bonnet, S., Cormier, M.-A., de Vernal, A., Durantou, L., Faubert, É., Head, M. J., Henry, M., Pospelova, V., Rochon, A., and Van Nieuwenhove, N.: Operational taxonomy and (paleo-)autecology of round, brown, spiny dinoflagellate cysts from the Quaternary of high northern latitudes, Mar. Micropaleontol., 98, 41–57, https://doi.org/10.1016/j.marmicro.2012.11.001, 2013.

Ravara, A., Marçal, A. R., Wiklund, H., and Hilário, A.: First account on the diversity of Ophryotrocha (Annelida, Dorvilleidae) from a mammal-fall in the deep-Atlantic Ocean with the description of three new species, Syst. Biodivers., 13, 555–570, https://doi.org/10.1080/14772000.2015.1047428, 2015.

Razouls, C., de Boyée, F., Kouwenberg, J., and Desreumaux, N.: Diversity and Geographic Distribution of Marine Planktonic Cope-

pods, available at: http://copepodes.obs-bayuls.fr/en (last access: 25 December 2017), 2005–2017.

Reid, P. C.: Mass encystment of a planktonic oligotrich ciliate, Mar. Biol., 95, 221–230, 1987.

Reid, P. C. and John, A. W. G.: Resting Cysts in the Ciliate Class Polyhymenophorea: Phylogenetic Implications, J. Protozool., 30, 710–713, 1983.

Rengefors, K., Laybourn-Parry, J., Logares, R., Marshall, W. A., and Hansen, G.: Marine-Derived Dinoflagellates in Antarctic Saline Lakes: Community Composition and Annual Dynamics, J. Phycol., 44, 592–604, https://doi.org/10.1111/j.1529-8817.2008.00517.x, 2008.

Ribeiro, S., Amorim, A., Andersen, T. J., Abrantes, F., and Ellegaard, M.: Reconstructing the history of an invasion?: the toxic phytoplankton species *Gymnodinium catenatum* in the Northeast Atlantic, Biol. Invasions, 14, 969–985, https://doi.org/10.1007/s10530-011-0132-6, 2012a.

Ribeiro, S., Moros, M., Ellegaard, M., and Kuijpers, A.: Climate variability in West Greenland during the past 1500 years: evidence from a high-resolution marine palynological record from Disko Bay, Boreas, 41, 68–83, https://doi.org/10.1111/j.1502-3885.2011.00216.x, 2012b.

Ribeiro, S., Amorim, A., Abrantes, F., and Ellegaard, M.: Environmental change in the Western Iberia Upwelling Ecosystem since the preindustrial period revealed by dinoflagellate cyst records, Holocene, 26, 874–889, https://doi.org/10.1177/0959683615622548, 2016.

Roberts, A. P., Wilson, G. S., Harwood, D. M., and Verosub, K. L.: Glaciation across the Oligocene-Miocene boundary in southern McMurdo Sound, Antarctica: New chronology from the CIROS-1 drill hole, Palaeogeogr. Palaeocl., 198, 113–130, https://doi.org/10.1016/S0031-0182(03)00399-7, 2003.

Roncaglia, L.: New acritarch species from Holocene sediments in central West Greenland, Grana, 43, 81–88, https://doi.org/10.1080/00173130410018966, 2004a.

Roncaglia, L.: Palynofacies analysis and organic-walled dinoflagellate cysts as indicators of palaeo-hydrographic changes: an example from Holocene sediments in Skálafjord, Faroe Islands, Mar. Micropaleontol., 50, 21–42, https://doi.org/10.1016/S0377-8398(03)00065-3, 2004b.

Rozema, P. D., Venables, H. J., Poll, W. H. Van De, Clarke, A., Meredith, M. P., and Buma, A. G. J.: Interannual variability in phytoplankton biomass and species composition in northern Marguerite Bay (West Antarctic Peninsula) is governed by both winter sea ice cover and summer stratification, Limnol. Oceanogr., 62, 235–252, https://doi.org/10.1002/lno.10391, 2017.

Ruggiero, M. A., Gordon, D. P., Orrell, T. M., Bailly, N., Bourgoin, T., Brusca, R. C., Cavalier-Smith, T., Guiry, M. D., and Kirk, P. M.: A higher level classification of all living organisms, PLoS One, 10, 1–60, https://doi.org/10.1371/journal.pone.0119248, 2015.

Sackett, W. M.: Organic carbon in sediments underlying the Ross Ice Shelf, Org. Geochem., 9, 135–137, https://doi.org/10.1016/0146-6380(86)90103-8, 1986.

Sangiorgi, F. and Donders, T. H.: Reconstructing 150 years of eutrophication in the north-western Adriatic Sea (Italy) using dinoflagellate cysts, pollen and spores, Estuar. Coast. Shelf S., 60, 69–79, https://doi.org/10.1016/j.ecss.2003.12.001, 2004.

Sangiorgi, F., Bijl, P. K., Passchier, S., Salzmann, U., Schouten, S., McKay, R., Cody, R. D., Pross, J., Van De Flierdt, T., Bohaty, S. M., Levy, R., Williams, T., Escutia, C., and Brinkhuis, H.: Southern Ocean warming and Wilkes Land ice sheet retreat during the mid-Miocene, Nat. Commun., 9, 317, https://doi.org/10.1038/s41467-017-02609-7, 2018.

Santella, L. and Ianora, A.: Subitaneous and diapause eggs in Mediterranean populations of *Pontella mediterranea* (Copepoda?: Calanoida): a morphological study, Mar. Biol., 105, 83–90, 1990.

Sarjeant, W. A. S.: A Restudy of some Dinoflagellate Cyst Holotypes in the University of Kiel Collections. II. The Eocene Holotypes of Barbara Klumpp (1953); with a Revision of the Genus Cordosphaeridium Eisenack, 1963, Meyniana, 33, 97–132, 1981.

Schiller, J.: Die planktontischen Vegetationen des adriatischen Meeres. B. Chrysomonadina, Heterokontae, Cryptomonadina, Eugleninae, Volvocales. 1. Systematischer Teil, Arch. Protistenkd., 53, 59–123, 1925.

Schmitz, F.: Halosphaera, eine neue Gattung grüner Algen aus dem Mittelmeer, in: Mitteilungen aus der zoologischen Station zu Neapel, Bd. 1, Wilhelm Engelmann, Leipzig, 1879.

Scholz, B. and Liebezeit, G.: Microphytobenthic dynamics in a Wadden Sea intertidal flat – Part II: Seasonal and spatial variability of non-diatom community components in relation to abiotic parameters, Eur. J. Phycol., 47, 120–137, https://doi.org/10.1080/09670262.2012.665251, 2012.

Schrank, E.: Small acritarchs from the Upper Cretaceous?: taxonomy, biological affinities and palaeoecology, Rev. Palaeobot. Palyno., 123, 199–235, 2003.

Schuster, R. O., Nelson, D. R., Grigarick, A. A., and Christenberry, D.: Systematic criteria of the Eutardigrada, T. Am. Microsc. Soc., 99, 284–303, 1980.

Seidenkrantz, M.-S., Roncaglia, L., Fischel, A., Heilmann-Clausen, C., Kuijpers, A., and Moros, M.: Variable North Atlantic climate seesaw patterns documented by a late Holocene marine record from Disko Bugt, West Greenland, Mar. Micropaleontol., 68, 66–83, https://doi.org/10.1016/j.marmicro.2008.01.006, 2008.

Sluijs, A., Brinkhuis, H., Stickley, C. E., Warnaar, J., Williams, G. L., and Fuller, M.: Dinoflagellate Cysts From the Eocene – Oligocene Transition in the Southern Ocean?: Results From Odp Leg 189, Proc. ODP, Sci. Results, 189, 1–42, 2003.

Sluijs, A., Schouten, S., Pagani, M., Woltering, M., Brinkhuis, H., Sinninghe Damsté, J. S., Dickens, G. R., Huber, M., Reichart, G.-J., Stein, R., Matthiessen, J., Lourens, L. J., Pedentchouk, N., Backman, J., Moran, K., Clemens, S., Cronin, T., Eynaud, F., Gattacceca, J., Jakobsson, M., Jordan, R., Kaminski, M., King, J., Koc, N., Martinez, N. C., McInroy, D., Moore Jr., T. C., O'Regan, M., Onodera, J., Pälike, H., Rea, B., Rio, D., Sakamoto, T., Smith, D. C., St John, K. E. K., Suto, I., Suzuki, N., Takahashi, K., Watanabe, M., and Yamamoto, M.: Subtropical Arctic Ocean temperatures during the Palaeocene/Eocene thermal maximum, Nature, 441, 610–613, https://doi.org/10.1038/nature04668, 2006.

Sluijs, A., Röhl, U., Schouten, S., Brumsack, H.-J., Sangiorgi, F., Sinninghe Damsté, J. S., and Brinkhuis, H.: Arctic late Paleocene – Early Eocene paleoenvironments with special emphasis on the Paleocene-Eocene thermal maximum (Lomonosov Ridge, Integrated Ocean Drilling Program Expedition 302), Paleoceanography, 23, PA1S11, https://doi.org/10.1029/2007PA001495, 2008.

Sluijs, A., Brinkhuis, H., Williams, G. L., and Fensome, R. A.: Taxonomic revision of some Cretaceous-Cenozoic spiny organic-walled peridiniacean dinoflagellate cysts, Rev. Palaeobot. Palyno., 154, 34–53, https://doi.org/10.1016/j.revpalbo.2008.11.006, 2009.

Small, E. B. and Lynn, D. H.: Phylum Ciliophora, in: An Illustrated Guide to the Protozoa, edited by: Lee, J. J., Hunter, S. H., and Bovee, E. C., 393–575, Society of Protozool. Spec. Publ., Lawrence, Kansas, 1985.

Smith Jr., W. O., Shields, A. R., Dreyer, J. C., Peloquin, J. A., and Asper, V.: Interannual variability in vertical export in the Ross Sea: Magnitude, composition, and environmental correlates, Deep-Sea Res. Pt. I, 58, 147–159, https://doi.org/10.1016/j.dsr.2010.11.007, 2011.

Spallanzani, L.: Opuscoli di fisica animale, e vegetabile, Volume Secondo, Presso la Societa Tipografica, 277, 1776.

Stirling, I.: The importance of polynas, ice edges, and leads to marine mammals and birds, J. Marine Syst., 10, 9–21, https://doi.org/10.1016/S0924-7963(96)00054-1, 1997.

Stocchi, P., Escutia, C., Houben, A. J. P., Vermeersen, B. L. A., Bijl, P. K., Brinkhuis, H., DeConto, R. M., Galeotti, S., Passchier, S., Pollard, D., Brinkhuis, H., Escutia, C., Klaus, A., Fehr, A., Williams, T., Bendle, J. A. P., Bijl, P. K., Bohaty, S. M., Carr, S. A., Dunbar, R. B., Flores, J. A., Gonzàlez, J. J., Hayden, T. G., Iwai, M., Jimenez-Espejo, F. J., Katsuki, K., Kong, G. S., McKay, R. M., Nakai, M., Olney, M. P., Passchier, S., Pekar, S. F., Pross, J., Riesselman, C., Röhl, U., Sakai, T., Shrivastava, P. K., Stickley, C. E., Sugisaki, S., Tauxe, L., Tuo, S., van de Flierdt, T., Welsh, K., and Yamane, M.: Relative sea-level rise around East Antarctica during Oligocene glaciation, Nat. Geosci., 6, 380–384, https://doi.org/10.1038/ngeo1783, 2013.

Stoecker, D. K.: Predators of Tintinnids, in: The Biology and Ecology of Tintinnid Ciliates: Models for Marine Plankton, edited by: Dolan, J. R., Montagnes, D. J. S., Agatha, S., Coats, D. W., and Stoecker, D. K., 122–144, Wiley-Blackwell, Hoboken, New Jersey, USA, 2013.

Stoecker, D. K., Gustafson, D. E., Merrell, J. R., Black, M. M. D., and Baier, C. T.: Excystment and growth of chrysophytes and dinoflagellates at low temperatures and high salinities in Antarctic sea-ice, J. Phycol., 33, 585–595, https://doi.org/10.1111/j.0022-3646.1997.00585.x, 1997.

Storkey, C. A.: Distribution of Marine Palynomorphs in Surface Sediments, Prydz Bay, Antarctica, Victoria University of Wellington, 2006.

Stover, L. E. and Evitt, W. R.: Analyses of pre-Pleistocene organic-walled dinoflagellates, Stanford Univ. Publ. Geol. Sci., 15, 1–300, 1978.

Stover, L. E. and Williams, G. L.: A revision of the Paleogene dinoflagellate genera Areosphaeridium Eaton 1971 and Eatonicysta Stover and Evitt 1978, Micropaleontology, 41, 97–141, 1995.

Struck, T. H., Purschke, G. and Halanych, K. M.: Phylogeny of Eunicida (Annelida) and Exploring Data Congruence Using a Partition Addition Bootstrap Alteration (PABA) Approach, Syst. Biol., 55, 1–20, 2006.

Strüder-Kypke, M. C. and Lynn, D. H.: Morphological versus molecular data – Phylogeny of tintinnid ciliates (Ciliophora, Choreotrichia) inferred from small subunit rRNA gene sequences, Denisia, 23, 417–424, 2008.

Subramoniam, T.: Spermatophore and Sperm Transfer Mechanisms, in: Sexual Biology and Reproduction in Crustaceans, edited by: Subramoniam, T., 325–367, Academic Press, Amsterdam, 2017.

Suda, S., Bhuiyan, M. A. H., and Faria, D. G.: Genetic diversity of Pyramimonas From Ryukyu Archipelago, Japan (Chlorophyceae, Pyramimonadales), J. Mar. Sci. Technol., 21, 285–296, https://doi.org/10.6119/JMST-013-1220-16, 2013.

Sütő, Z. and Szegő, É.: Szervesvázú mikroplankton-vizsgálatok az erdélyi-medencei marosorbói (Oarba de Mures) szarmata és pannóniai emelet határsztratotípus rétegeiből, Földtani Közlöny, 138, 279–296, 2008.

Sütőné Szentai, M.: Szervesvázú mikroplankton zónák a szarmata és a pannóniai emeletek határán Magyarországról, Acta Nat. Pannonica, 4, 5–34, 2012.

Swadling, M. K.: Influence of Seasonal Ice Formation on Life Cycle Strategies of Antarctic Copepods, University of Tasmania, Hobart, 1998.

Szaniawski, H.: New evidence for the protoconodont origin of chaetognaths, Acta Palaeontol. Pol., 47, 405–419, 2002.

Szaniawski, H. and Wrona, R.: Polychaete jaws from the Cape Melville Formation (Lower Miocene) of King George Island, West Antarctica, Palaeontologia Polonica, 49, 105–125, 1987.

Taboada, S., Wiklund, H., Glover, A. G., Dahlgren, T. G., and Cristobo, J.: Two new Antarctic Ophryotrocha (Annelida?: Dorvilleidae) described from shallow-water whale bones, Polar Biol., 36, 1031–1045, https://doi.org/10.1007/s00300-013-1326-4, 2013.

Taboada, S., Bas, M., and Avila, C.: A new Parougia species (Annelida, Dorvilleidae) associated with eutrophic marine habitats in Antarctica, Polar Biol., 38, 517–527, https://doi.org/10.1007/s00300-014-1614-7, 2015.

Takahashi, K.: Microplankton from the Asagai Formation in the Joban Coal-Field, Trans. Proc. Paleontol. Soc. Japan N.S., 54, 201–214, 1964.

Takahashi, K.: Upper Cretaceous and Lower Paleogene microfloras of Japan, Rev. Palaeobot. Palyno., 5, 227–234, 1967.

Taylor, F. J. R.: On dinoflagellate evolution, BioSystems, 13, 65–108, 1980.

Terazaki, M., Takahashi, K. T., and Odate, T.: Zonal variations in abundance and body length of chaetognaths in the 140° E seasonal ice zone during the austral summer of 2001/02, Polar Sci., 7, 39–47, https://doi.org/10.1016/j.polar.2013.02.002, 2013.

The Expedition 318 Scientists: Expedition 318 summary, Proc. IODP, 318, 1–59, https://doi.org/10.2204/iodp.proc.318.101.2011, 2011.

Thomas, E., Booth, L., Maslin, M., and Shackleton, N. J.: Northeastern Atlantic benthic foraminifera during the last 45,000 years: Changes in productivity seen from the bottom up, Paleoceanography, 10, 545–562, https://doi.org/10.1029/94PA03056, 1995.

Thomson, P. G., Wright, S. W., Bolch, C. J. S., Nichols, P. D., Skerratt, J. H., and Mcminn, A.: Antarctic distribution, pigment and lipid composition, and molecular identification of the brine dinoflagellate Polarella glacialis (Dinophyceae), J. Phycol., 40, 867–873, https://doi.org/10.1111/j.1529-8817.2004.03169.x, 2004.

Thomson, P. G., McMinn, A., Kiessling, I., Watson, M., and Goldsworthy, P. M.: Composition and succession of di-

noflagellates and chrysophytes in the upper fast ice of Davis Station, East Antarctica, Polar Biol., 29, 337–345, https://doi.org/10.1007/s00300-005-0060-y, 2006.

Thorrington-Smith, M.: Some new and little known phytoplankton forms from the West Indian Ocean, Brit. Phycol. J., 5, 51–56, https://doi.org/10.1080/00071617000650071, 1970.

Thorsen, T. A., Dale, B., and Nordberg, K.: 'Blooms' of the toxic dinoflagellate *Gymnodinium catenatum* as evidence of climatic fluctuations in the late Holocene of southwestern Scandinavia, Holocene, 5, 435–446, 1995.

Throndsen, J.: The planktonic marine flagellates, in: Identifying marine phytoplankton, edited by: Tomas, C. R., 591–730, Academic Press, San Diego, 1997.

Thulin, G.: Über die Phylogenie und das System der Tardigraden, Hereditas, 11, 207–266, 1928.

Tragin, M., Lopes dos Santos, A., Christen, R., and Vaulot, D.: Diversity and ecology of green microalgae in marine systems?: an overview based on 18S rRNA gene sequences, Perspect. Phycol., 3, 141–154, https://doi.org/10.1127/pip/2016/0059, 2016.

Traverse, A. and Ginsburg, R. N.: Palynology of the surface sediments of Great Bahama Bank, as related to water movement and sedimentation, Mar. Geol., 4, 417–459, https://doi.org/10.1016/0025-3227(66)90010-7, 1966.

Troedson, A. L. and Riding, J. B.: Upper Oligocene to Lowermost Miocene Strata of King George Island, South Shetland Islands, Antarctica: Stratigraphy, Facies Analysis, and Implications for the Glacial History of the Antarctic Peninsula, J. Sediment. Res., 72, 510–523, https://doi.org/10.1306/110601720510, 2002.

Truswell, E. M.: Palynology of seafloor samples collected by the 1911–14 Australasian Antarctic Expedition: Implications for the geology of coastal East Antarctica, J. Geol. Soc. Aust., 29, 343–356, https://doi.org/10.1080/00167618208729218, 1982.

Ulrich, E. O. and Bassler, R. S.: A Classification of the toothlike fossils, Conodonts, with descriptions of American Devonian and Mississippian species, Proc. U.S. Natl. Museum, 68, 1–63, 1926.

Van Waveren, I. M.: Morphology of probable planktonic crustacean eggs from the Holocene of the Banda Sea (Indonesia), in: Neogene and Quaternary dinoflagellate cysts and acritarchs, edited by: Head, M. J. and Wrenn, J. H., 89–120, American Association of Stratigraphic Palynologists Foundation, Dallas, 1992.

Varela, M., Fernandez, E., and Serret, P.: Size-fractionated phytoplankton biomass and primary production in the Gerlache and south Bransfield Straits (Antarctic Peninsula) in Austral summer 1995–1996, Deep-Sea Res. Pt. II, 49, 749–768, 2002.

Veen, A., Hof, C. H. J., Kouwets, F. A. C., and Berkhout, T.: Rijkswaterstaat Waterdienst, Informatiehuis Water, available at: http://ipt.nlbif.nl/ipt/resource?r=checklist-twn (last access: 8 February 2018), 2015.

Venkatesan, M. I. and Kaplan, I. R.: The lipid geochemistry of Antarctic marine sediments: Bransfield Strait, Mar. Chem., 21, 347–375, 1987.

Verleye, T. J. and Louwye, S.: Recent geographical distribution of organic-walled dinoflagellate cysts in the southeast Pacific (25–53° S) and their relation to the prevailing hydrographical conditions, Palaeogeogr. Palaeocl., 298, 319–340, https://doi.org/10.1016/j.palaeo.2010.10.006, 2010.

Versteegh, G. J. M. and Zonneveld, K. A. F.: Determination of (palaeo-)ecological preferences of dinoflagellates by applying Detrended and Canonical Correspondence analysis to

Late Pliocene dinoflagellate cyst assemblages of the south Italian Singa section, Rev. Palaeobot. Palyno., 84, 181–199, https://doi.org/10.1016/0034-6667(94)90050-7, 1994.

Von Siebold, C. T.: Lehrbuch der vergleichenden Anatomie der wirbellosen Thiere, in: Lehrbuch der vergleichenden Anatomie, Erster Theil, edited by: Von Siebold, C. T. and Stannius, H., 1–679, Veit and Comp., Berlin, 1848.

Wall, D., Dale, B., and Harada, K.: Description of new fossil dinoflagellates from the Late Quaternary of the Black Sea, Micropaleontology, 19, 18–31, 1973.

Warny, S.: Species of the acritarch genus Palaeostomocystis Deflandre 1937: Potential indicators of neritic subpolar to polar environments in Antarctica during the Cenozoic, Palynology, 33, 43–54, https://doi.org/10.1080/01916122.2009.9989682, 2009.

Warny, S., Wrenn, J. H., Bart, P. J., and Askin, R.: Palynology of the NBP03-01 A Transect in the Northern Basin, Western Ross Sea, Antarctica: a Late Pliocene Record, Palynology, 30, 151–182, 2006.

Warny, S., Askin, R. A., Hannah, M. J., Mohr, B. A. R., Raine, J. I., Harwood, D. M., Florindo, F., and the S. S. Team: Palynomorphs from a sediment core reveal a sudden remarkably warm Antarctica during the middle Miocene, Geology, 37, 955–958, https://doi.org/10.1130/G30139A.1, 2009.

Warny, S., Kymes, C. M., Askin, R. A., Krajewski, K. P., and Bart, P. J.: Remnants of Antarctic vegetation on King George Island during the early Miocene Melville Glaciation, Palynology, 40, 66–82, https://doi.org/10.1080/01916122.2014.999954, 2016.

Wasik, A.: Antarctic Tintinnids: Their Ecology, Morphology, Ultrastructure and Polymorphism, Acta Protozool., 37, 5–15, 1998.

Wasik, A., Mikolajczyk, E., and Ligowski, R.: Agglutinated loricae of some Baltic and Antarctic Tintinnina species (Ciliophora), J. Plankton Res., 18, 1931–1940, 1996.

Williams, G. L., Fensome, R. A., and MacRae, R. A.: The Lentins and Williams Index of Fossil Dinoflagellates 2017 Edition, Am. Assoc. Stratigr. Palynol. Contrib. Ser., 48, 1–1097, 2017.

Wilson, G. J.: Some new species of lower Tertiary Dinoflagellates from McMurdo sound, Antarctica, New Zeal. J. Bot., 5, 57–83, https://doi.org/10.1080/0028825X.1967.10428735, 1967.

Wrenn, J. H. and Hart, G. F.: Paleogene dinoflagellate cyst biostratigraphy of Seymour Island, Antarctica, Geol. Soc. Am. Mem., 169, 321–447, 1988.

Wrenn, J. H., Hannah, M. J., and Raine, J. I.: Diversity and Palaeoenvironmental Significance of Late Cainozoic Marine Palynomorphs from the CRP-1 Core, Ross Sea, Antarctica, Terra Ant., 5, 553–570, 1998.

Yi, S., Batten, D. J., and Joo, S.: Provenance of recycled palynomorph assemblages recovered from surficial glaciomarine sediments in Bransfield Strait, offshore Antarctic Peninsula, Cretaceous Res., 26, 906–919, https://doi.org/10.1016/j.cretres.2005.06.004, 2005.

Zawierucha, K., Kolicka, M., and Kaczmarek, Ł.: Redescription of the Arctic tardigrade Tenuibiotus voronkovi (Tumanov, 2007) (Eutardigrada; Macrobiotidea), with the first molecular data for the genus, Zootaxa, 4196, 498–510, https://doi.org/10.11646/zootaxa.4196.4.2, 2016.

Zevenboom, D., Brinkhuis, H., and Visscher, H.: Dinoflagellate cysts palaeoenvironmental analysis of the Oligocene/Miocene transition in northwest and central Italy, Giorn. Geol., 56, 155–169, 1994.

Zonneveld, K. A. F.: New species of organic walled dinoflagellate cysts from modern sediments of the Arabian Sea (Indian Ocean), Rev. Palaeobot. Palyno., 97, 317–337, 1997.

Zonneveld, K. A. F., Versteegh, G. J. M., Kasten, S., Eglinton, T. I., Emeis, K.-C., Huguet, C., Koch, B. P., de Lange, G. J., de Leeuw, J. W., Middelburg, J. J., Mollenhauer, G., Prahl, F. G., Rethemeyer, J., and Wakeham, S. G.: Selective preservation of organic matter in marine environments; processes and impact on the sedimentary record, Biogeosciences, 7, 483–511, https://doi.org/10.5194/bg-7-483-2010, 2010.

Zonneveld, K. A. F., Marret, F., Versteegh, G. J. M., Bogus, K., Bonnet, S., Bouimetarhan, I., Crouch, E., De Vernal, A., Elshanawany, R., Edwards, L., Esper, O., Forke, S., Grøsfjeld, K., Henry, M., Holzwarth, U., Kielt, J., Kim, S., Ladouceur, S., Ledu, D., Chen, L., Limoges, A., Londeix, L., Lu, S.-H., Mahmoud, M. S., Marino, G., Matsouka, K., Matthiessen, J., Mildenhal, D. C., Mudie, P., Neil, H. L., Pospelova, V., Qi, Y., Richerol, T., Rochon, A., Sangiorgi, F., Solignac, S., Turon, J., Verleye, T., Wang, Y., Wang, Z., and Young, M.: Atlas of modern dinoflagellate cyst distribution based on 2405 data points, Rev. Palaeobot. Palyno., 191, 1–197, https://doi.org/10.1016/j.revpalbo.2012.08.003, 2013.